



International Workshop on Hadron Structure and Spectroscopy 2023

25-28 June 2023, Prague - Czechia

MAPTMD22 : femtography of unpolarized protons and pions at N^3LL accuracy

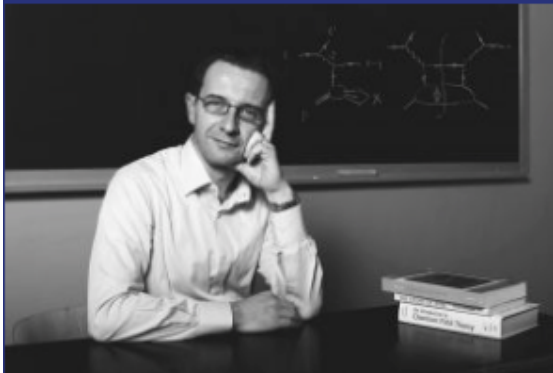
Marco Radici



for the **MAP** Collaboration
(Multi-dimensional Analysis of Partonic distributions)
<https://github.com/MapCollaboration/>

Results with contributions from...

Alessandro Bacchetta



Marco Radici



Matteo Cerutti



Andrea Signori



Valerio Bertone



Chiara Bissolotti



Giuseppe Bozzi



Fulvio Piacenza



Simone Venturini



...and published in...



PUBLISHED FOR SISSA BY SPRINGER

RECEIVED: June 23, 2022
REVISED: September 13, 2022
ACCEPTED: October 10, 2022
PUBLISHED: October 19, 2022

Unpolarized transverse momentum distributions from a global fit of Drell-Yan and semi-inclusive deep-inelastic scattering data

The MAP Collaboration¹

Alessandro Bacchetta^{1,2}, Valerio Bertone^{3,4}, Chiara Bissolotti^{1,2}, Giuseppe Bozzi^{1,5}, Matteo Cerutti^{1,2}, Fulvio Piacenza¹, Marco Radici¹ and Andrea Signori^{1,2}

¹Dipartimento di Fisica, Università di Pavia, via Bassi 6, I-27100 Pavia, Italy

²INFN — Sezione di Pavia, via Bassi 6, I-27100 Pavia, Italy

³IRFU, CEA, Université Paris-Saclay, F-91191 Gif-sur-Yvette, France

⁴HEP Division, Argonne National Laboratory, 9700 S. Cass Avenue, Lemont, IL, 60439 U.S.A.

⁵Dipartimento di Fisica, Università di Cagliari,
Cittadella Universitaria, I-09042 Monserrato (CA), Italy

^fINFN — Sezione di Cagliari, Cittadella Universitaria, I-09042 Monserrato (CA), Italy

E-mail: alessandro.bacchetta@unipv.it, valerio.bertone@cea.fr,
cbissolotti@anl.gov, giuseppe.bozzi@unica.it,
matteo.cerutti@pv.infn.it, fu.piacenza@gmail.com,
marco.radici@pv.infn.it, andrea.signori@unipv.it

arXiv:2206.07598

JHEP10(2022)127

arXiv:2210.01733

PHYSICAL REVIEW D **107**, 014014 (2023)

Extraction of pion transverse momentum distributions from Drell-Yan data

Matteo Cerutti^{1,2,*}, Lorenzo Rossi^{1,2,†}, Simone Venturini^{1,2,‡}, Alessandro Bacchetta^{1,2,§}, Valerio Bertone^{1,||}, Chiara Bissolotti^{1,4,¶} and Marco Radici^{1,2,**}

(MAP Collaboration)^{††}

¹Dipartimento di Fisica, Università di Pavia, via Bassi 6, I-27100 Pavia, Italy

²INFN—Sezione di Pavia, via Bassi 6, I-27100 Pavia, Italy

³IRFU, CEA, Université Paris-Saclay, F-91191 Gif-sur-Yvette, France

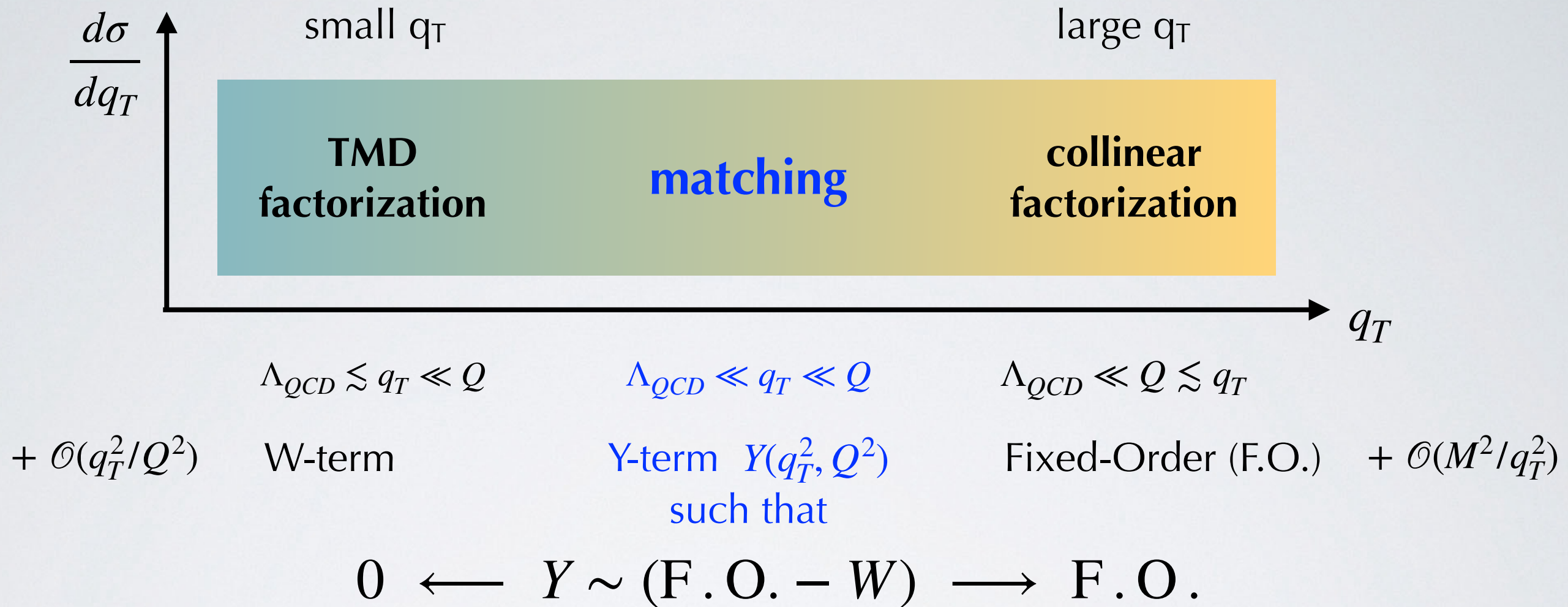
⁴HEP Division, Argonne National Laboratory, 9700 S. Cass Avenue, Lemont, Illinois 60439, USA

(Received 11 October 2022; accepted 21 December 2022; published 11 January 2023)

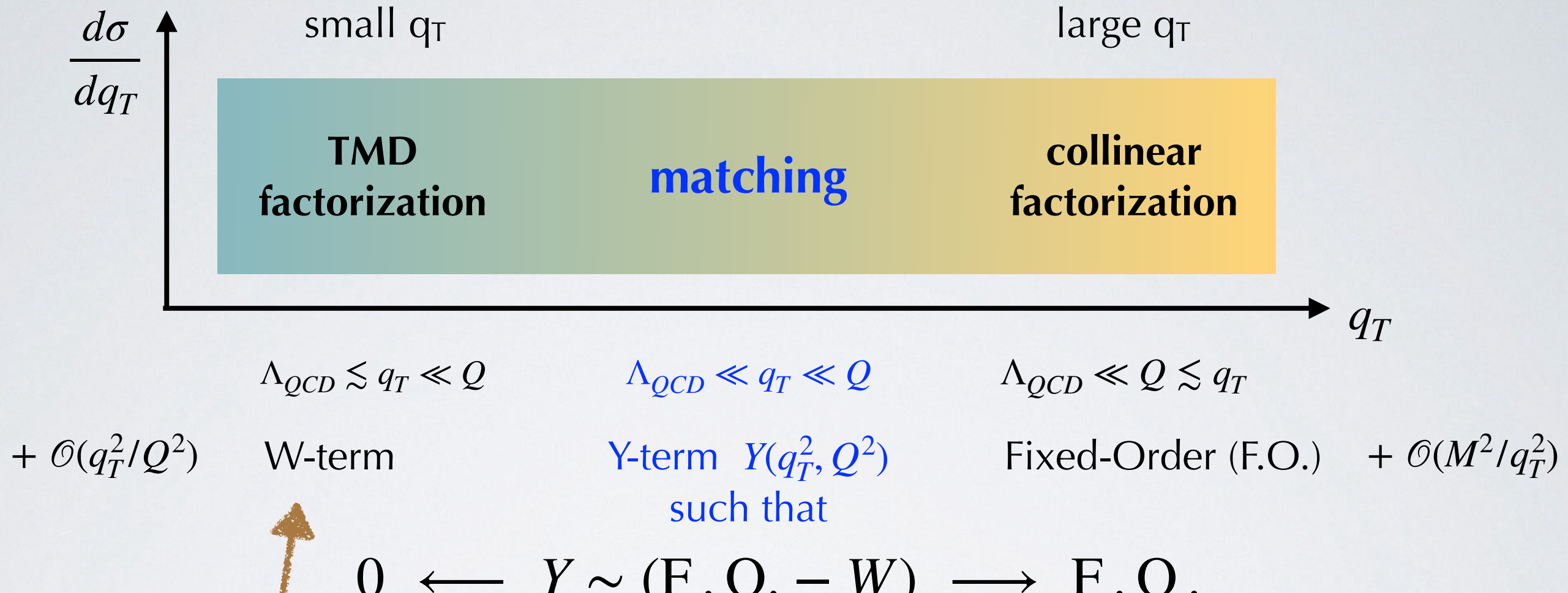
We map the distribution of unpolarized quarks inside a unpolarized pion as a function of the quark's transverse momentum, encoded in unpolarized transverse momentum distributions (TMDs). We extract the pion TMDs from available data of unpolarized pion-nucleus Drell-Yan processes, where the cross section is differential in the lepton-pair transverse momentum. In the cross section, pion TMDs are convoluted with nucleon TMDs that we consistently take from our previous studies. We obtain a fairly good agreement with data. We present also predictions for pion-nucleus scattering that is being measured by the COMPASS Collaboration.

DOI: 10.1103/PhysRevD.107.014014

TMD factorization

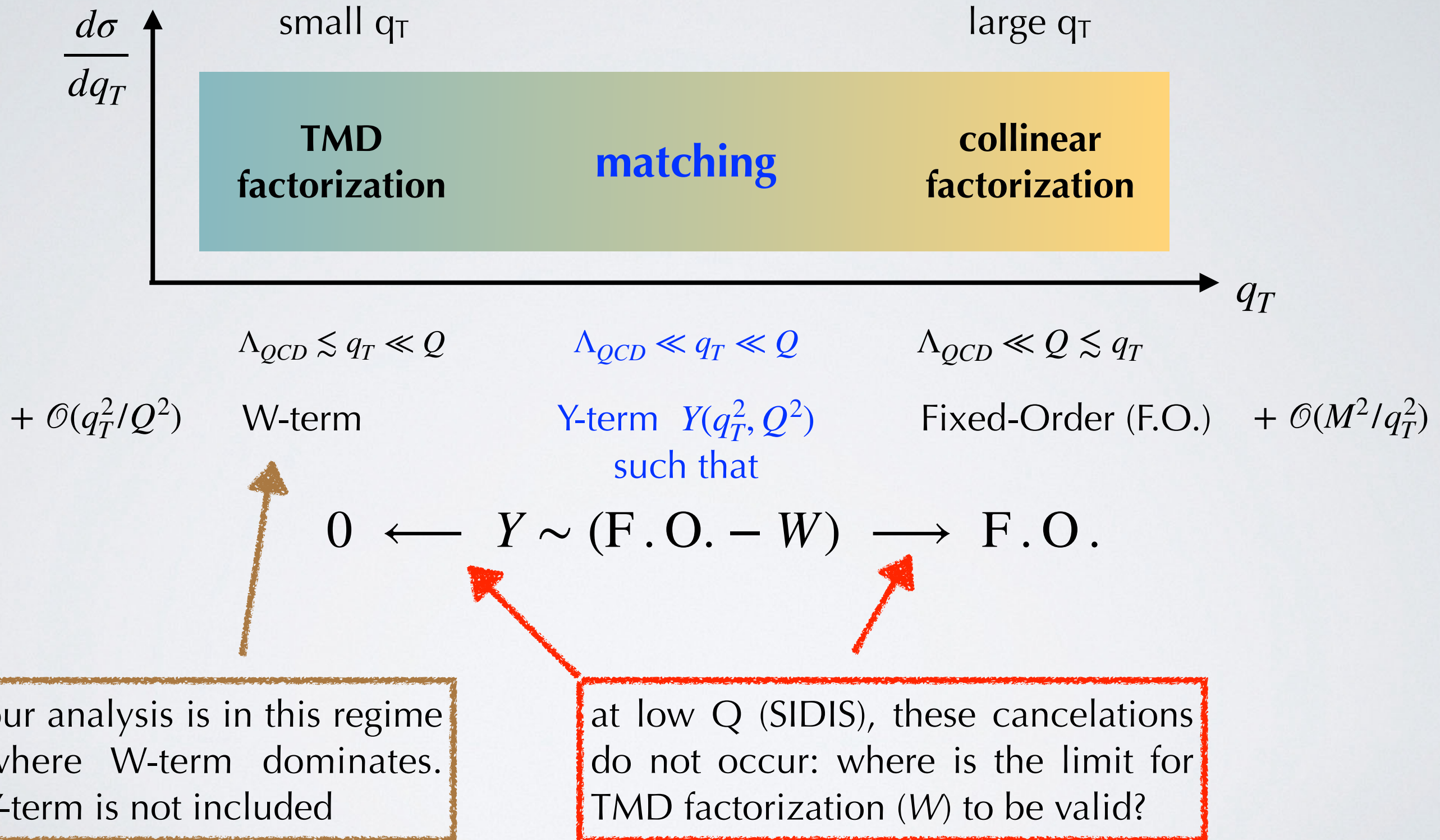


TMD factorization



our analysis is in this regime
where W-term dominates.
Y-term is not included

TMD factorization

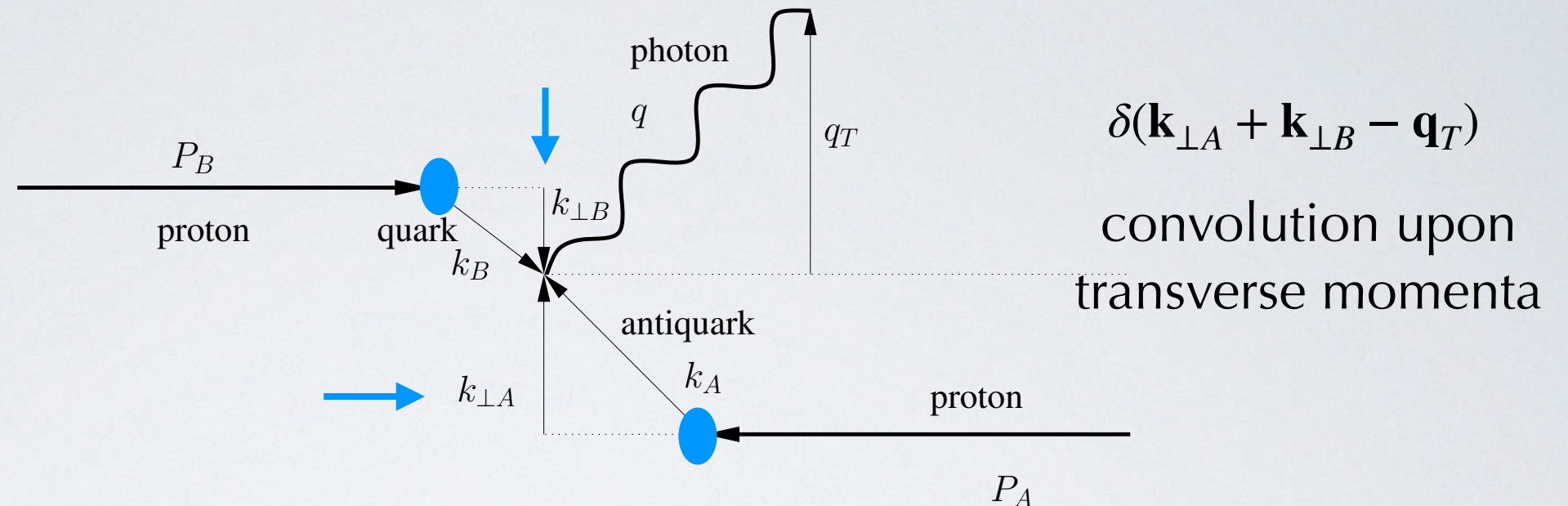


TMD factorization: Drell-Yan

$$M^2 \ll Q^2$$

$$q_T^2 \ll Q^2$$

\mathcal{W} -term dominant



$$\frac{d\sigma}{dq_T dy dQ} \sim W(x_A, x_B, q_T, Q) \sim \mathcal{H}^{\text{DY}}(Q^2) \left[f_1^{\bar{q}}(x_A, \mathbf{k}_{\perp A}^2; Q^2) \otimes f_1^q(x_B, \mathbf{k}_{\perp B}^2; Q^2) \right]$$

hard factor	TMD PDF anti-q	TMD PDF q
-------------	-----------------------	------------------

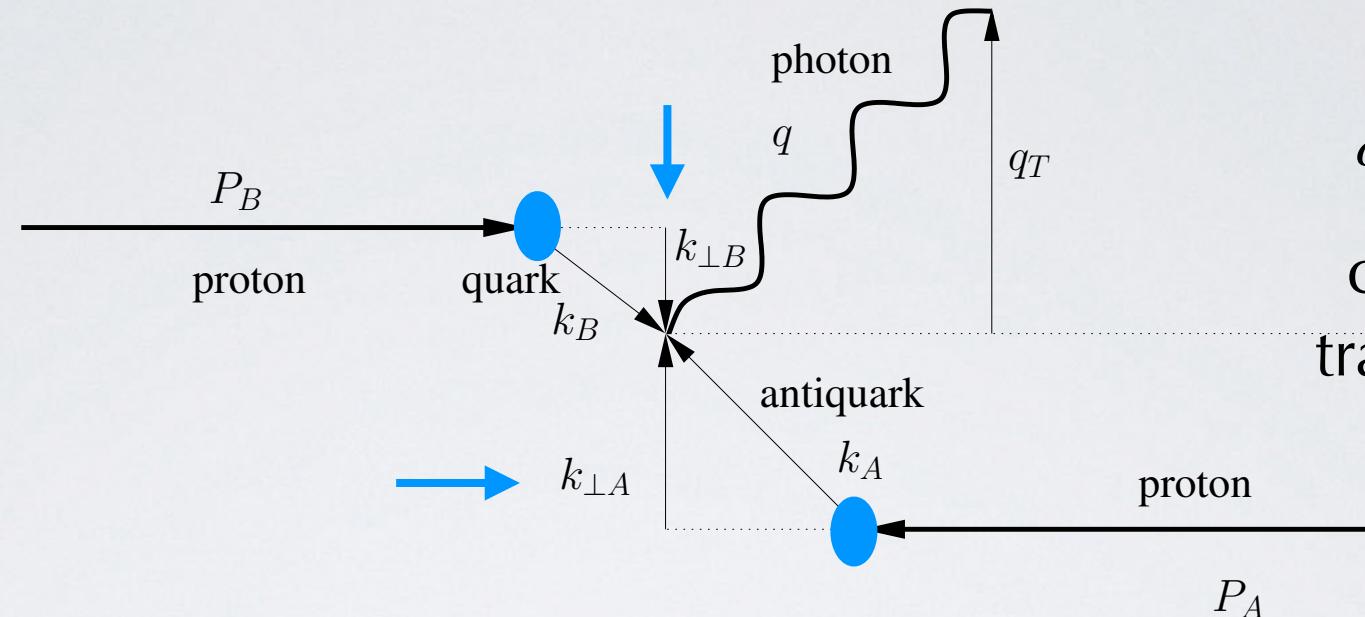
TMDs depend on two scales μ, ζ ; can be chosen as $\zeta = \mu^2 = Q^2$

TMD factorization: Drell-Yan

$$M^2 \ll Q^2$$

$$q_T^2 \ll Q^2$$

\mathcal{W} -term dominant



$\delta(\mathbf{k}_{\perp A} + \mathbf{k}_{\perp B} - \mathbf{q}_T)$
convolution upon
transverse momenta

$$\frac{d\sigma}{dq_T dy dQ} \sim W(x_A, x_B, q_T, Q) \sim \mathcal{H}^{\text{DY}}(Q^2) \left[f_1^{\bar{q}}(x_A, \mathbf{k}_{\perp A}^2; Q^2) \otimes f_1^q(x_B, \mathbf{k}_{\perp B}^2; Q^2) \right]$$

Fourier Transform:
from convolution to
simple product



hard factor

TMD PDF anti-q

TMD PDF q

$$= \mathcal{H}^{\text{DY}}(Q^2) \frac{1}{2\pi} \int_0^\infty db_T b_T J_0(b_T, q_T) \tilde{f}_1^{\bar{q}}(x_A, b_T^2; Q^2) \tilde{f}_1^q(x_B, b_T^2; Q^2)$$

TMDs depend on two scales μ, ζ ; can be chosen as $\zeta = \mu^2 = Q^2$

TMD factorization: SIDIS

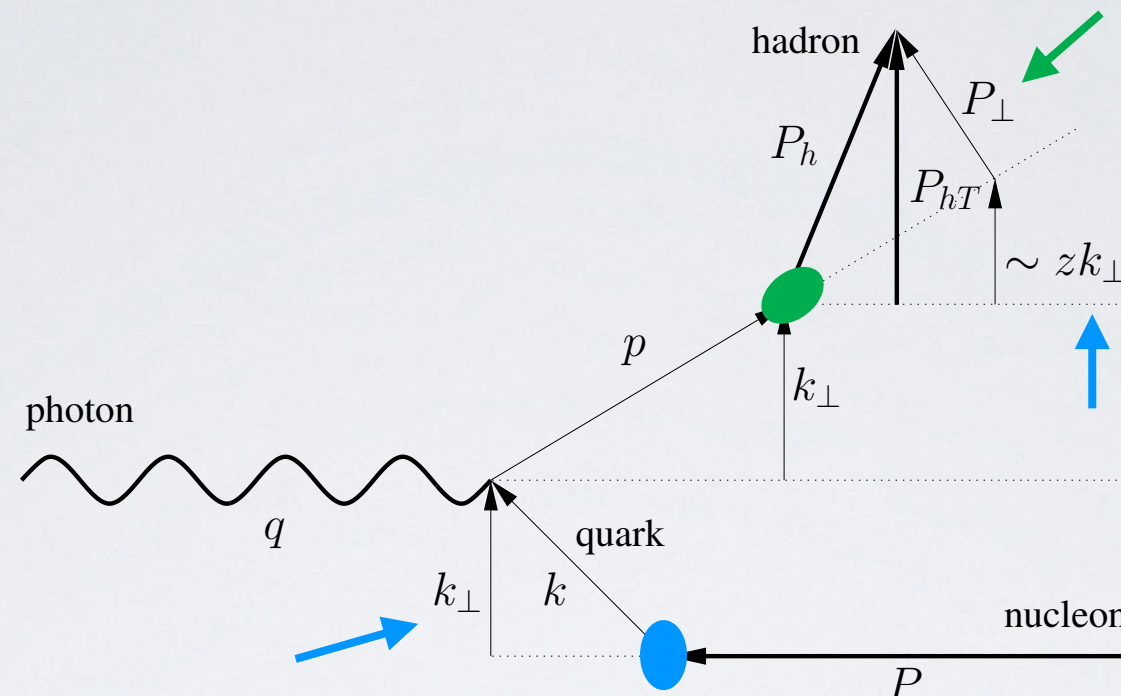
$$M^2 \ll Q^2$$

$$q_T^2 = \frac{P_{hT}^2}{z^2} \ll Q^2$$

W-term dominant

$$\frac{d\sigma}{dxdzdq_TdQ} \sim W(x, z, q_T, Q) \sim \mathcal{H}^{\text{SIDIS}}(Q^2) \left[f_1^q(x, \mathbf{k}_\perp^2; Q^2) \otimes D_1^{q \rightarrow h}(z, \mathbf{P}_\perp^2; Q^2) \right]$$

Fourier Transform:
from convolution to
simple product



$$-z\mathbf{q}_T \approx \mathbf{P}_{hT} = z\mathbf{k}_\perp + \mathbf{P}_\perp$$

— — — — —

$$\delta(\mathbf{k}_\perp + \mathbf{P}_\perp/z + \mathbf{q}_T)$$

convolution upon
transverse momenta

hard factor **TMD PDF**

TMD FF

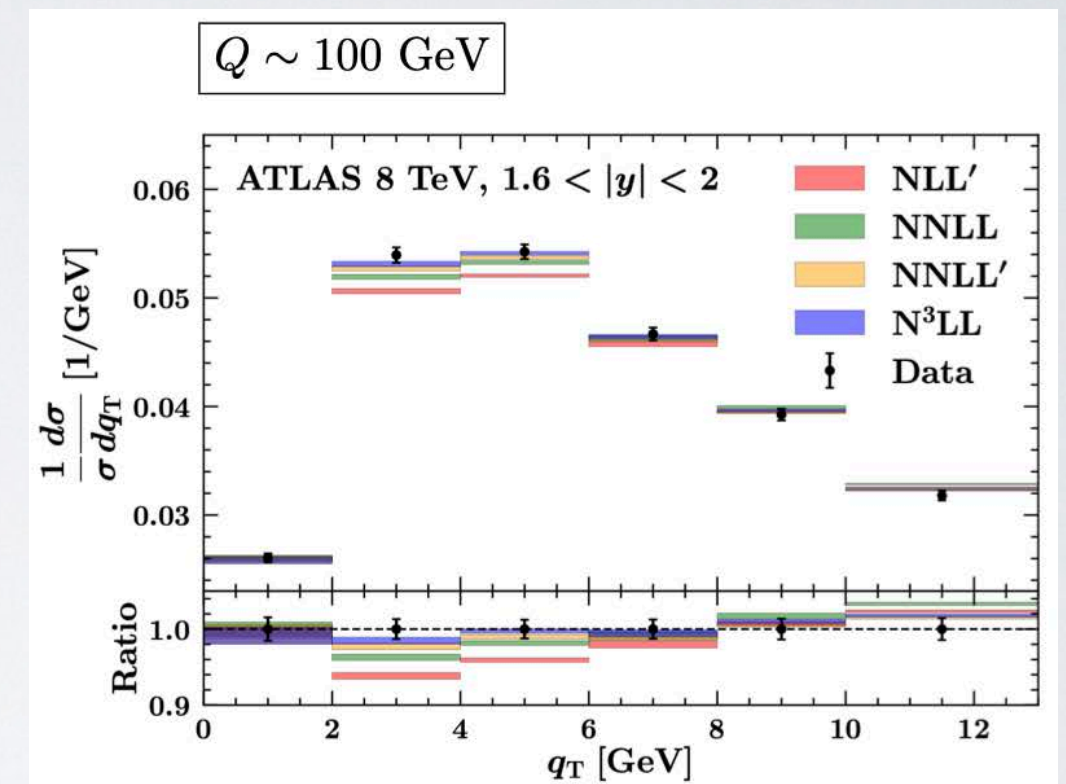
$$= \mathcal{H}^{\text{SIDIS}}(Q^2) \frac{1}{2\pi} \int_0^\infty db_T b_T J_0(b_T, q_T) \tilde{f}_1^q(x, b_T^2; Q^2) \tilde{D}_1^{q \rightarrow h}(z, b_T^2; Q^2)$$

TMDs depend on two scales μ, ζ ; can be chosen as $\zeta = \mu^2 = Q^2$

Normalization problem in SIDIS

increasing perturbative accuracy

increases agreement with Drell-Yan

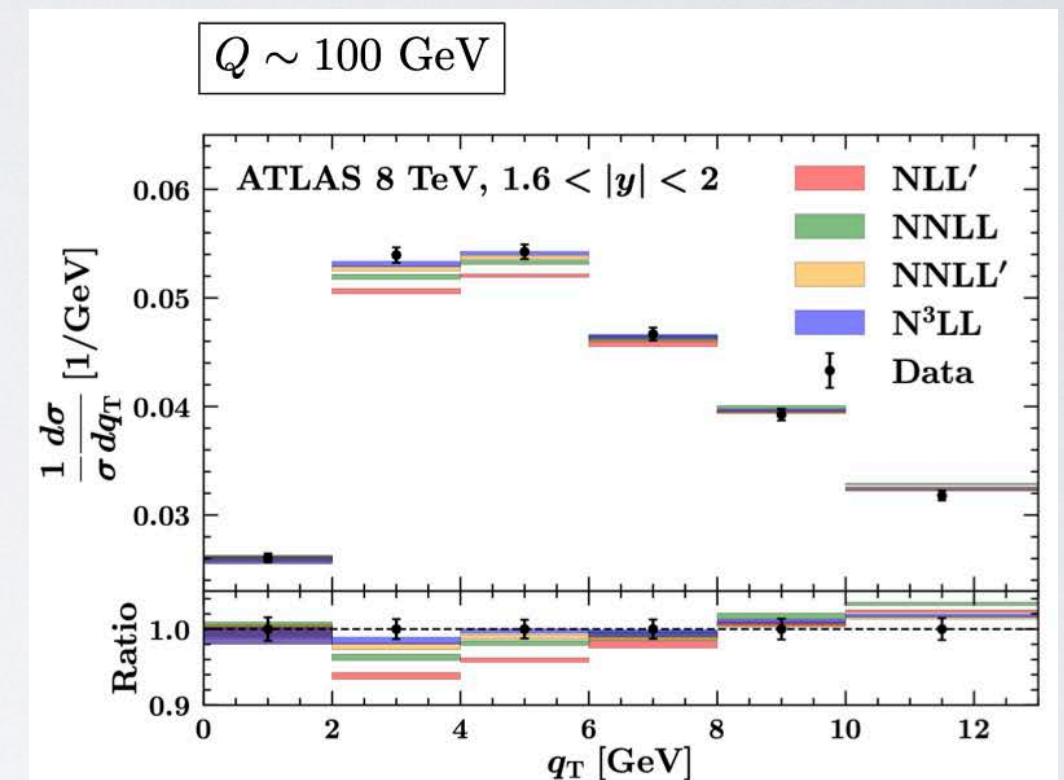
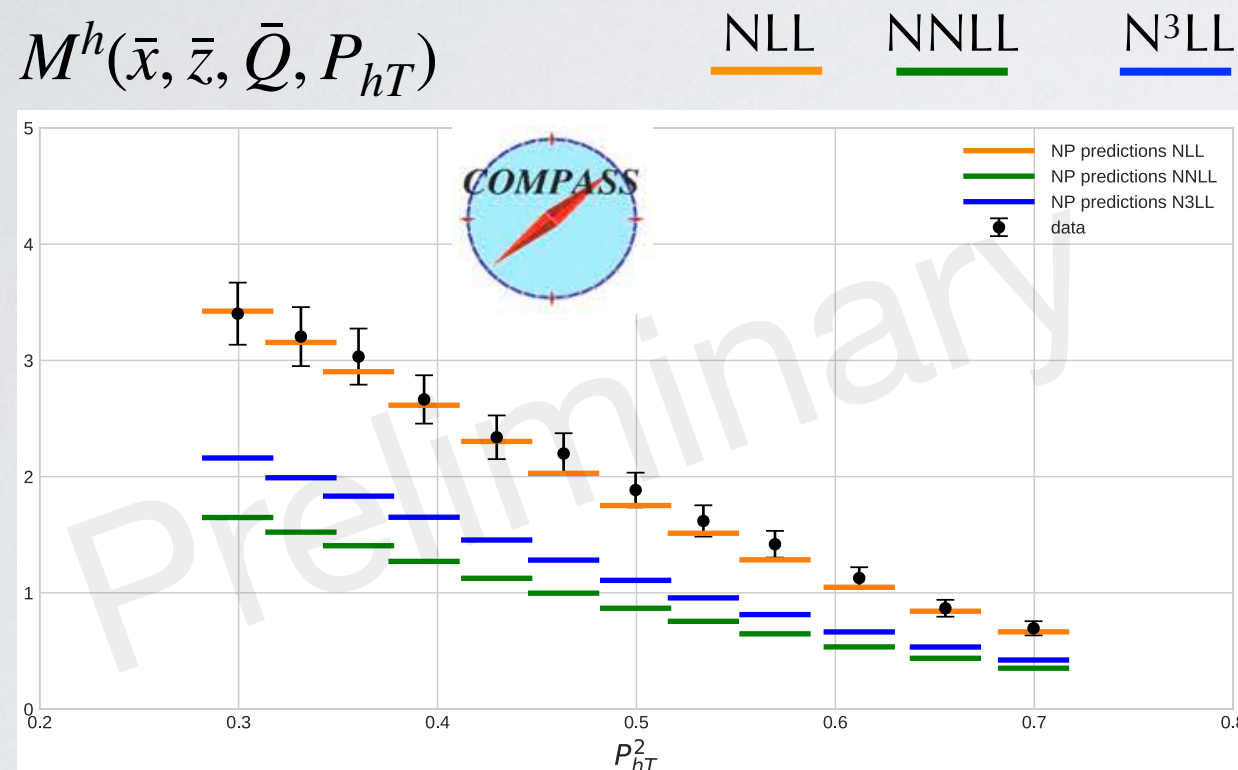


Normalization problem in SIDIS

increasing perturbative accuracy

worsens agreement with SIDIS !

increases agreement with Drell-Yan



discrepancy is P_{hT} -independent:

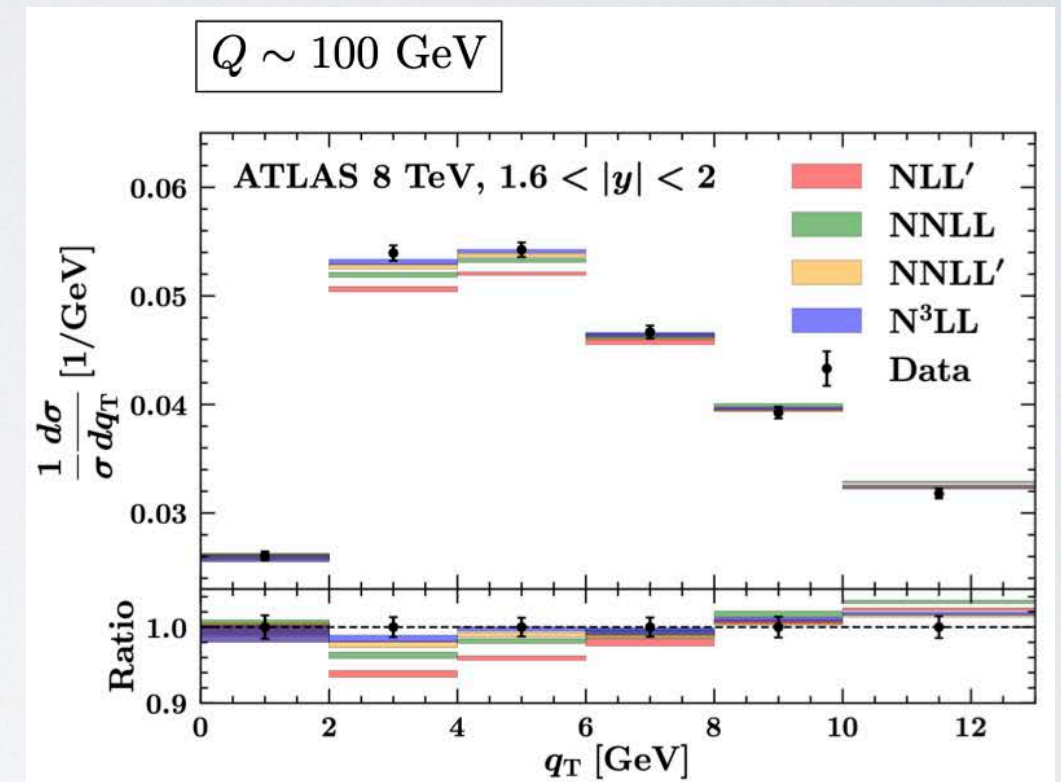
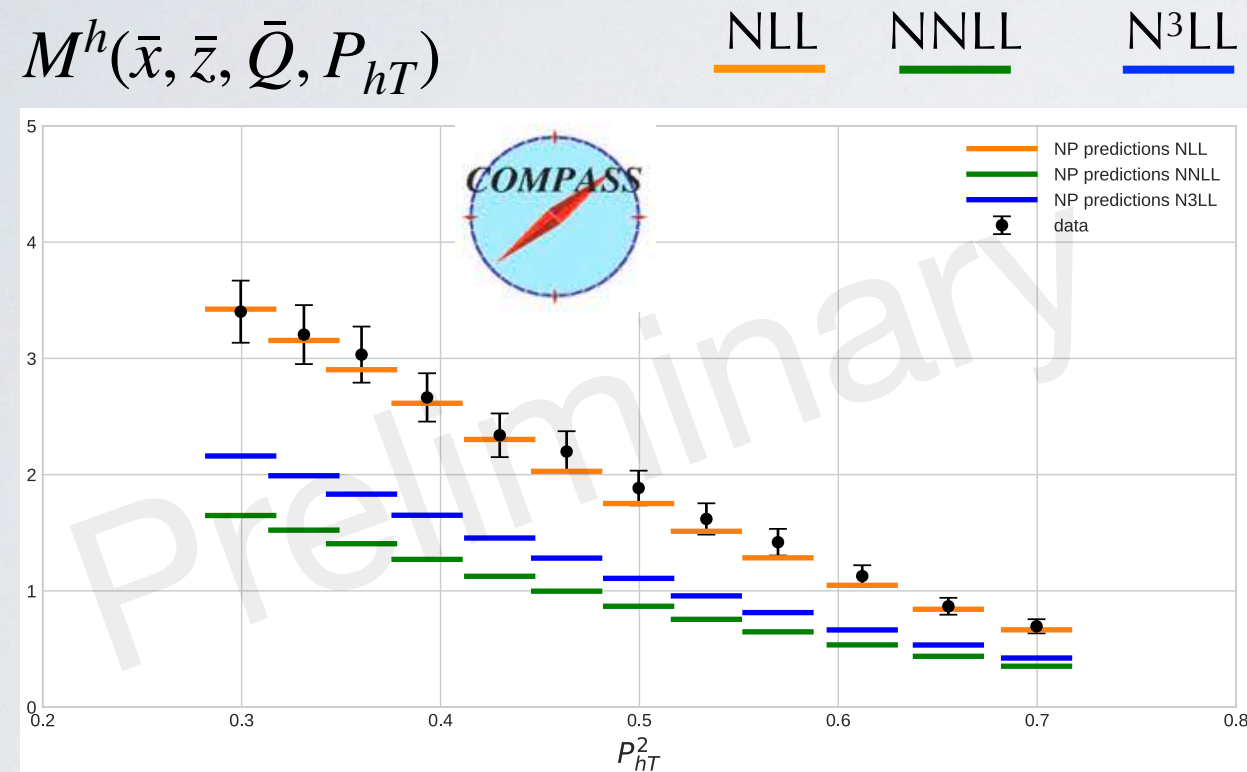
$$M_{\text{NLL}}/M_{\text{NNLL}} \sim 2 \quad M_{\text{NLL}}/M_{N^3\text{LL}} \sim 1.5$$

Normalization problem in SIDIS

increasing perturbative accuracy

worsens agreement with SIDIS !

increases agreement with Drell-Yan



discrepancy is P_{hT} -independent:

$$M_{\text{NLL}}/M_{\text{NNLL}} \sim 2 \quad M_{\text{NLL}}/M_{N^3\text{LL}} \sim 1.5$$

tensions observed also at larger q_T
and also in Drell-Yan at low Q
and also in e+e- annihilations

No normalization problems for
collinear SIDIS $d\sigma/dxdzdQ$:

Gonzalez et al., P.R. D98 (18) 114005

Bacchetta et al., P.R. D100 (19) 014018

Moffat et al., P.R. D100 (19) 094014

but not in SV 2019 fit

Scimemi & Vladimirov,
arXiv:1912.06532

MAPFF1.0 (Map Collaboration)
Abdul Khalek et al., arXiv:2105.08725

Normalization problem in SIDIS

at NLL, $\mathcal{H}^{\text{SIDIS}} \approx 1$

the integrated W-term reproduces
the SIDIS collinear $d\sigma$ at LO,
which reasonably describes data

De Florian et al., P.R. D75 (07) 114010

$$\int dq_T \frac{d\sigma}{dx dz dq_T dQ} = \int dq_T W \Big|_{\text{NLL}} \propto f_1^q(x, Q) D_1^{q \rightarrow h}(z, Q)$$
$$= \frac{d\sigma}{dx dz dQ} \Big|_{\text{LO}}$$

Normalization problem in SIDIS

at NLL, $\mathcal{H}^{\text{SIDIS}} \approx 1$

the integrated W-term reproduces
the SIDIS collinear $d\sigma$ at LO,
which reasonably describes data

De Florian et al., P.R. D75 (07) 114010

at higher orders, $\mathcal{H}^{\text{SIDIS}} = 1 + c_1 \alpha_S + \dots$ $c_1 < 0$ spoils agreement

the integrated W-term contains
only some terms of the SIDIS
collinear $d\sigma$

$$\int dq_T \frac{d\sigma}{dx dz dq_T dQ} = \int dq_T W \Big|_{\text{NLL}} \propto f_1^q(x, Q) D_1^{q \rightarrow h}(z, Q)$$
$$= \frac{d\sigma}{dx dz dQ} \Big|_{\text{LO}}$$

$$\int dq_T W \Big|_{\text{NNLL}} \neq \frac{d\sigma}{dx dz dQ} \Big|_{\text{NLO}}$$

Y-term $\cancel{\rightarrow} 0$

Normalization problem in SIDIS

at NLL, $\mathcal{H}^{\text{SIDIS}} \approx 1$

the integrated W-term reproduces
the SIDIS collinear $d\sigma$ at LO,
which reasonably describes data

De Florian et al., P.R. D75 (07) 114010

at higher orders, $\mathcal{H}^{\text{SIDIS}} = 1 + c_1 \alpha_S + \dots$ $c_1 < 0$ spoils agreement

the integrated W-term contains
only some terms of the SIDIS
collinear $d\sigma$

$$\int dq_T W \Big|_{\text{NNLL}} \neq \frac{d\sigma}{dx dz dQ} \Big|_{\text{NLO}}$$

Y-term $\cancel{\rightarrow} 0$

We define the normalization factor

$$\omega(x, z, Q) = \frac{d\sigma_{\text{nomix}}}{dx dz dQ} \Big/ \int d\mathbf{q}_T W = 1 \quad \text{at NLL}$$

includes all NLO terms where
x- and z-dependence can be factorized
 \rightarrow includes W + part of the Y term...



Does not depend on fit parameters,
precomputed

Scale dependence of TMD

$$f_1^q(x, b_T^2; \mu_f, \zeta_f) =$$

$$\sum_i [C_{q \rightarrow i}(x, b_T^2; \mu_{b_*}) \otimes f_1^i(x, \mu_{b_*})] \quad \text{matching collinear PDF at small } b_T$$

$$\times \exp[S(\mu_f, \mu_{b_*})] \quad \text{Sudakov: evolution in } \mu \text{ scale; contains anomalous dimensions } \gamma_F, \gamma_K$$

$$\times \left[\frac{\zeta_f}{\mu_{b_*}^2} \right]^{K(b_*, \mu_{b_*})/2} \quad \text{evolution in } \zeta \text{ scale; contains Collins-Soper kernel K}$$

perturbative

perturbative α_S^n

accuracy	\mathcal{H} and C	K and γ_F	γ_K	PDF and a_S evol.	FF
LL	0	-	1	-	-
NLL	0	1	2	LO	LO
NLL'	1	1	2	NLO	NLO
NNLL	1	2	3	NLO	NLO
NNLL'	2	2	3	NNLO	NNLO
N^3LL	2	3	4	NNLO	NNLO NLO
N^3LL'	3	3	4	N^3LO	N^3LO

FF at NNLO
not yet
implemented

Borsa et al.,
P.R.L. 129 (22) 012002
arXiv:2202.05060

Abdul Khalek et al.,
P.L. B834 (22) 137456
arXiv:2204.10331

Scale dependence of TMD

$$f_1^q(x, b_T^2; \mu_f, \zeta_f) =$$

$$\mu_f \geq \mu_{b_*} = \frac{2e^{-\gamma_E}}{b_*(b_T)} \geq 1$$

prescription to smoothly connect to large b_T , avoiding Landau pole.
Introduces **nonperturbative** part

$$\begin{aligned}
 & \sum_i [C_{q \rightarrow i}(x, b_T^2; \mu_{b_*}) \otimes f_1^i(x, \mu_{b_*})] && \text{matching collinear PDF at small } b_T \\
 & \times \exp[S(\mu_f, \mu_{b_*})] && \text{Sudakov: evolution in } \mu \text{ scale; contains anomalous dimensions } \gamma_F, \gamma_K \\
 & \times \left[\frac{\zeta_f}{\mu_{b_*}^2} \right]^{K(b_*, \mu_{b_*})/2} && \text{evolution in } \zeta \text{ scale; contains Collins-Soper kernel } K \\
 & \times \left[\frac{\zeta_f}{Q_0^2} \right]^{g_K(b_T)/2} && \text{nonperturbative Collins-Soper kernel} \\
 & \times f_{\text{NP}}(x, b_T; Q_0) && \text{(arbitrary } Q_0=1 \text{ GeV)} \\
 & && \text{nonperturbative TMD at initial (arbitrary) scale } Q_0
 \end{aligned}$$

perturbative α_S^n

accuracy	\mathcal{H} and C	K and γ_F	γ_K	PDF and a_s evol.	FF
LL	0	-	1	-	-
NLL	0	1	2	LO	LO
NLL'	1	1	2	NLO	NLO
NNLL	1	2	3	NLO	NLO
NNLL'	2	2	3	NNLO	NNLO
N³LL	2	3	4	NNLO	NNLO NLO
N³LL'	3	3	4	N³LO	N³LO

FF at NNLO
not yet implemented

Borsa et al.,
P.R.L. 129 (22) 012002
arXiv:2202.05060

Abdul Khalek et al.,
P.L. B834 (22) 137456
arXiv:2204.10331

Most recent extractions of unpolarized TMD f_1

SIDIS

	Accuracy	HERMES	COMPASS	DY	Z production	N of points	χ^2/N_{points}
PV 2017 arXiv:1703.10157	NLL	✓	✓	✓	✓	8059	1.5
SV 2017 arXiv:1706.01473	NNLL'	✗	✗	✓	✓	309	1.23
BSV 2019 arXiv:1902.08474	NNLL'	✗	✗	✓	✓	457	1.17
SV 2019 arXiv:1912.06532	N^3LL	✓	✓	✓	✓	1039	1.06
PV 2019 arXiv:1912.07550	N^3LL	✗	✗	✓	✓	353	1.07
SV19 + flavor dep. arXiv:2201.07114	N^3LL	✗	✗	✓	✓	309	<1.08>
MAPTMD 2022 arXiv:2206.07598	N^3LL	✓	✓	✓	✓	2031	1.06
ART23 arXiv:2305.07473	N^4LL	✗	✗	✓	✓	627	0.96

increasing precision & accuracy

Most recent extractions of unpolarized TMD f_1

SIDIS

	Accuracy	HERMES	COMPASS	DY	Z production	N of points	χ^2/N_{points}
PV 2017 arXiv:1703.10157	NLL	✓	✓	✓	✓	8059	1.5
SV 2017 arXiv:1706.01473	NNLL'	✗	✗	✓	✓	309	1.23
BSV 2019 arXiv:1902.08474	NNLL'	✗	✗	✓	✓	457	1.17
SV 2019 arXiv:1912.06532	N^3LL	✓	✓	✓	✓	1039	1.06
PV 2019 arXiv:1912.07550	N^3LL	✗	✗	✓	✓	353	1.07
SV19 + flavor dep. arXiv:2201.07114	N^3LL	✗	✗	✓	✓	309	<1.08>
MAPTMD 2022 arXiv:2206.07598	N^3LL	✓	✓	✓	✓	2031	1.06
ART23 arXiv:2305.07473	N^4LL	✗	✗	✓	✓	627	0.96

increasing accuracy & precision

only three global fits

Main features of MAPTMD22 fit

- global fit of Drell-Yan and SIDIS data with
 - largest number of data points: **2031**
 - highest perturbative accuracy: **N³LL**
(with FF currently only at NLO)
- prescription to fix SIDIS normalization problem beyond NLL
(effectively introducing part of Y-term)
- number of fitted parameters: **21**
- extremely good description: **$\chi^2 / N_{\text{data}} = 1.06$**
- account of correlated (exp. and th.) errors with nuisance parameters, including PDF & FF uncertainties

MMHT2014

DSS14 (π), DSS17 (K)

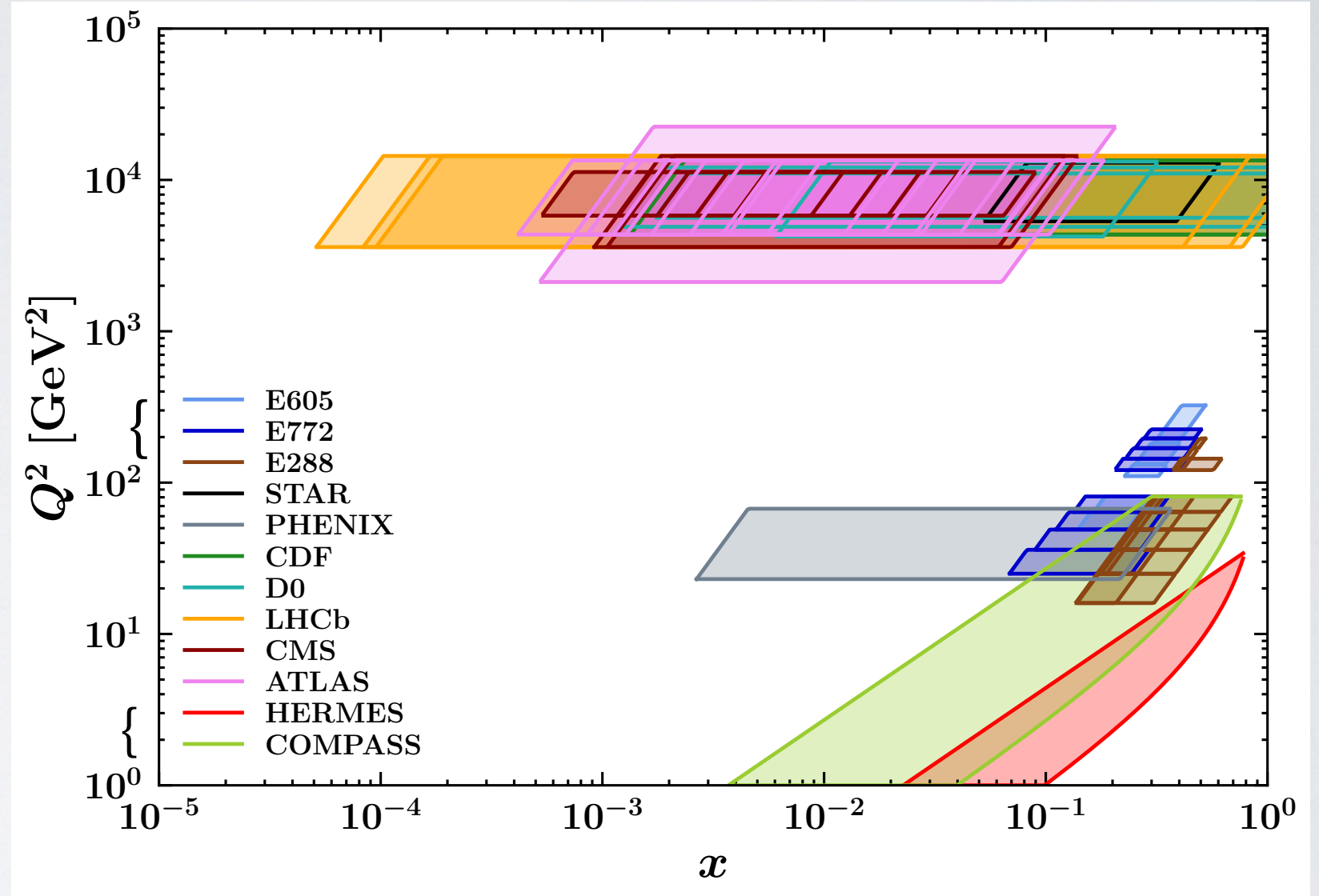
The MAPTMD22 data sets

N_{data} after cuts

Drell Yan { 233 fixed target
251 collider

1547 SIDIS

2031 data points



kinematic cuts

$$\langle Q \rangle > 1.4 \text{ GeV}$$

$$0.2 < z < 0.7$$

Drell-Yan

$$q_T < 0.2 Q$$

SIDIS

$$P_{hT} < \min \left[\min [0.2 Q, 0.5 Qz] + 0.3 \text{ GeV}, zQ \right]$$

Scale dependence of TMD

$$f_1^q(x, b_T^2; \mu_f, \zeta_f) =$$

$$\mu_f \geq \mu_{b_*} = \frac{2e^{-\gamma_E}}{b_*(b_T)} \geq 1$$

prescription to smoothly connect to large b_T , avoiding Landau pole.
Introduces **nonperturbative** part

$$\begin{aligned}
 & \sum_i [C_{q \rightarrow i}(x, b_T^2; \mu_{b_*}) \otimes f_1^i(x, \mu_{b_*})] && \text{matching collinear PDF at small } b_T \\
 & \times \exp[S(\mu_f, \mu_{b_*})] && \text{Sudakov: evolution in } \mu \text{ scale; contains anomalous dimensions } \gamma_F, \gamma_K \\
 & \times \left[\frac{\zeta_f}{\mu_{b_*}^2} \right]^{K(b_*, \mu_{b_*})/2} && \text{evolution in } \zeta \text{ scale; contains Collins-Soper kernel } K \\
 & \times \left[\frac{\zeta_f}{Q_0^2} \right]^{g_K(b_T)/2} && \text{nonperturbative Collins-Soper kernel} \\
 & \times f_{\text{NP}}(x, b_T; Q_0) && \text{(arbitrary } Q_0=1 \text{ GeV)} \\
 & && \text{nonperturbative TMD at initial (arbitrary) scale } Q_0
 \end{aligned}$$

perturbative

non perturbative

perturbative α_S^n

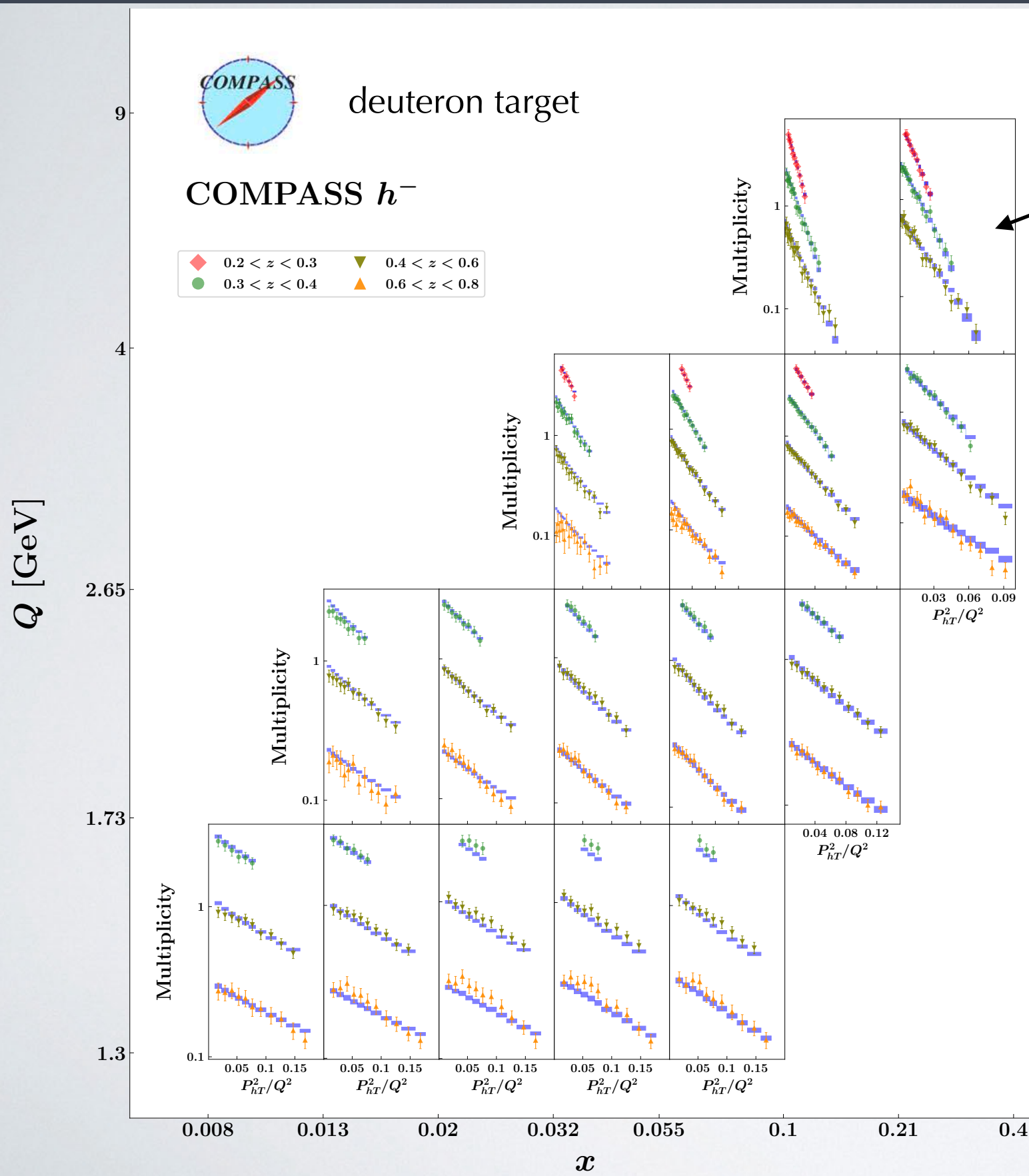
accuracy	\mathcal{H} and C	K and γ_F	γ_K	PDF and a_s evol.	FF
LL	0	-	1	-	-
NLL	0	1	2	LO	LO
NLL'	1	1	2	NLO	NLO
NNLL	1	2	3	NLO	NLO
NNLL'	2	2	3	NNLO	NNLO
N³LL	2	3	4	NNLO	NNLO NLO
N³LL'	3	3	4	N³LO	N³LO

FF at NNLO
not yet implemented

Borsa et al.,
P.R.L. 129 (22) 012002
arXiv:2202.05060

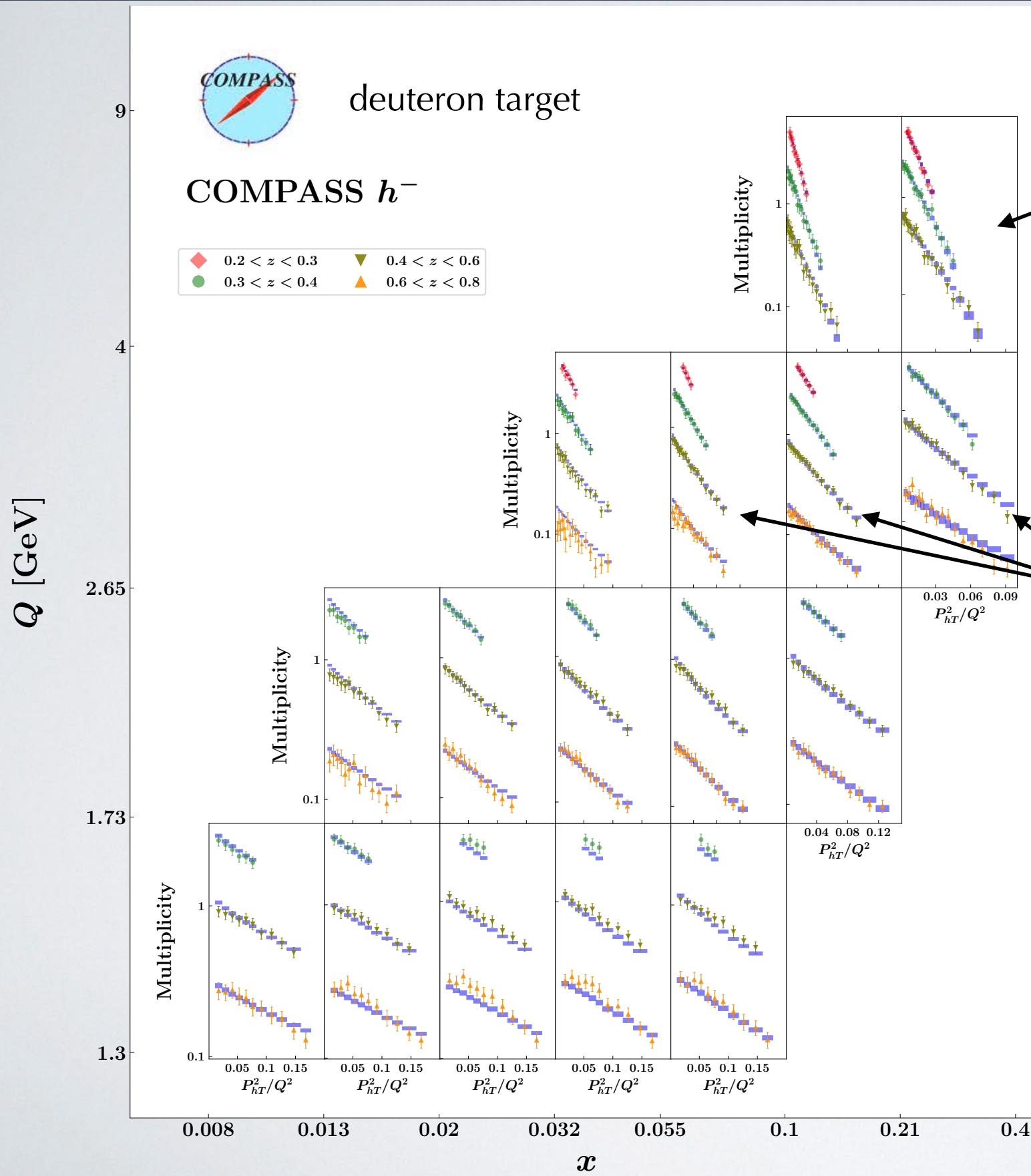
Abdul Khalek et al.,
P.L. B834 (22) 137456
arXiv:2204.10331

Data-driven nonperturbative TMD



at given (x, Q^2) ,
different slopes for different z

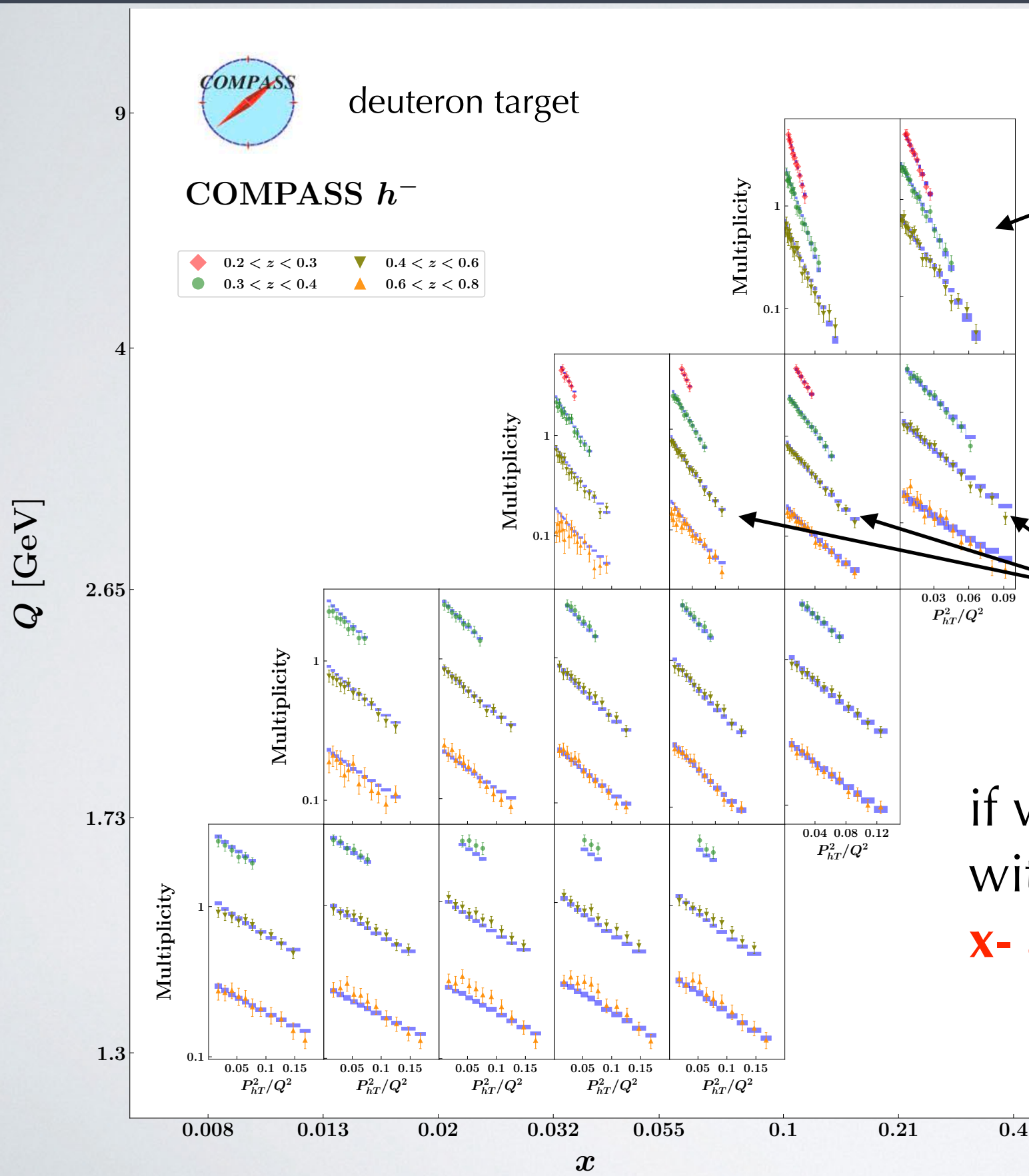
Data-driven nonperturbative TMD



at given (x, Q^2) ,
different slopes for different z

at given z ,
different slopes for different x

Data-driven nonperturbative TMD



at given (x, Q^2) ,
different slopes for different z

at given z ,
different slopes for different x

if we model nonperturbative TMDs
with Gaussians, we need
x- and z-dependent widths!

Parametrization of non-perturbative TMD

nonperturbative TMD PDF
Fourier Transform of sum
of 3 Gaussians with
x-dependent widths

$$f_{\text{NP}}(x, b_T; Q_0) = \text{F.T.} \left(e^{-k_\perp^2/g_{1A}(x)} + \lambda_B k_\perp^2 e^{-k_\perp^2/g_{1B}(x)} + \lambda_C e^{-k_\perp^2/g_{1C}(x)} \right)$$

with $g_{1X}(x) = N_{1X} \frac{(1-x)^{\alpha_X^2} x^{\sigma_X}}{(1-\hat{x})^{\alpha_X^2} \hat{x}^{\sigma_X}}$ $\hat{x} = 0.1$ **11 param.**

Parametrization of non-perturbative TMD

nonperturbative TMD PDF
 Fourier Transform of sum
 of 3 Gaussians with
 x-dependent widths

$$f_{\text{NP}}(x, b_T; Q_0) = \text{F.T.} \left(e^{-k_\perp^2/g_{1A}(x)} + \lambda_B k_\perp^2 e^{-k_\perp^2/g_{1B}(x)} + \lambda_C e^{-k_\perp^2/g_{1C}(x)} \right)$$

with $g_{1X}(x) = N_{1X} \frac{(1-x)^{\alpha_X^2} x^{\sigma_X}}{(1-\hat{x})^{\alpha_X^2} \hat{x}^{\sigma_X}}$ $\hat{x} = 0.1$ **11 param.**

nonperturbative TMD FF
 Fourier Transform of sum
 of 2 Gaussians with
 z-dependent widths

$$D_{\text{NP}}(z, b_T; Q_0) = \text{F.T.} \left(e^{-P_\perp^2/g_{3A}(z)} + \lambda_F P_\perp^2 e^{-P_\perp^2/g_{3B}(z)} \right)$$

with $g_{3X}(z) = N_{3X} \frac{(1-z)^{\gamma_X^2} (z^{\beta_X} + \delta_X^2)}{(1-\hat{z})^{\gamma_X^2} (\hat{z}^{\beta_X} + \delta_X^2)}$ $\hat{z} = 0.5$ **9 param.**

Parametrization of non-perturbative TMD

nonperturbative TMD PDF
 Fourier Transform of sum
 of 3 Gaussians with
 x-dependent widths

$$f_{\text{NP}}(x, b_T; Q_0) = \text{F.T.} \left(e^{-k_\perp^2/g_{1A}(x)} + \lambda_B k_\perp^2 e^{-k_\perp^2/g_{1B}(x)} + \lambda_C e^{-k_\perp^2/g_{1C}(x)} \right)$$

with $g_{1X}(x) = N_{1X} \frac{(1-x)^{\alpha_X^2} x^{\sigma_X}}{(1-\hat{x})^{\alpha_X^2} \hat{x}^{\sigma_X}}$ $\hat{x} = 0.1$ **11 param.**

nonperturbative TMD FF
 Fourier Transform of sum
 of 2 Gaussians with
 z-dependent widths

$$D_{\text{NP}}(z, b_T; Q_0) = \text{F.T.} \left(e^{-P_\perp^2/g_{3A}(z)} + \lambda_F P_\perp^2 e^{-P_\perp^2/g_{3B}(z)} \right)$$

with $g_{3X}(z) = N_{3X} \frac{(1-z)^{\gamma_X^2} (z^{\beta_X} + \delta_X^2)}{(1-\hat{z})^{\gamma_X^2} (\hat{z}^{\beta_X} + \delta_X^2)}$ $\hat{z} = 0.5$ **9 param.**

nonperturbative part of
 Collins-Soper kernel

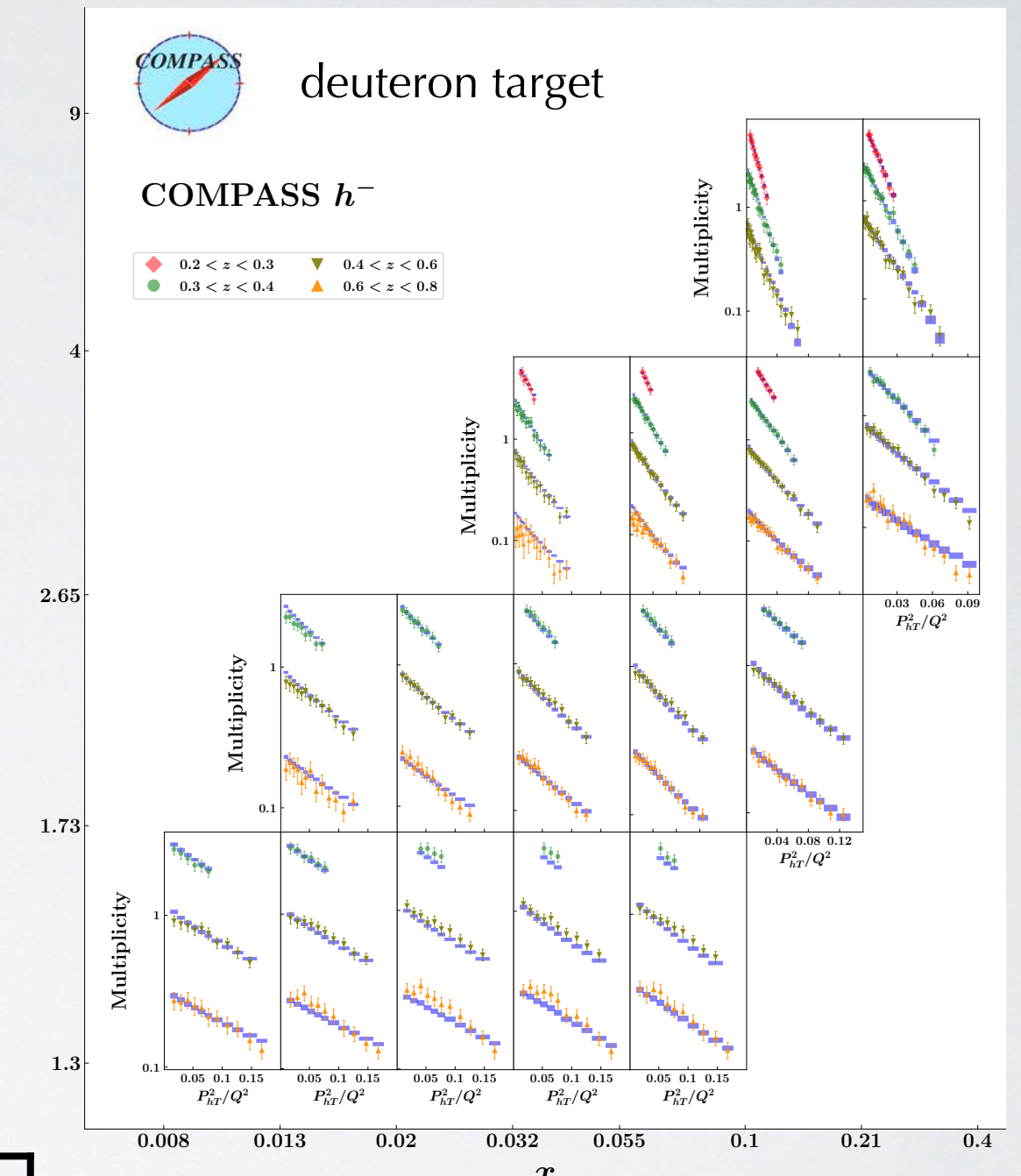
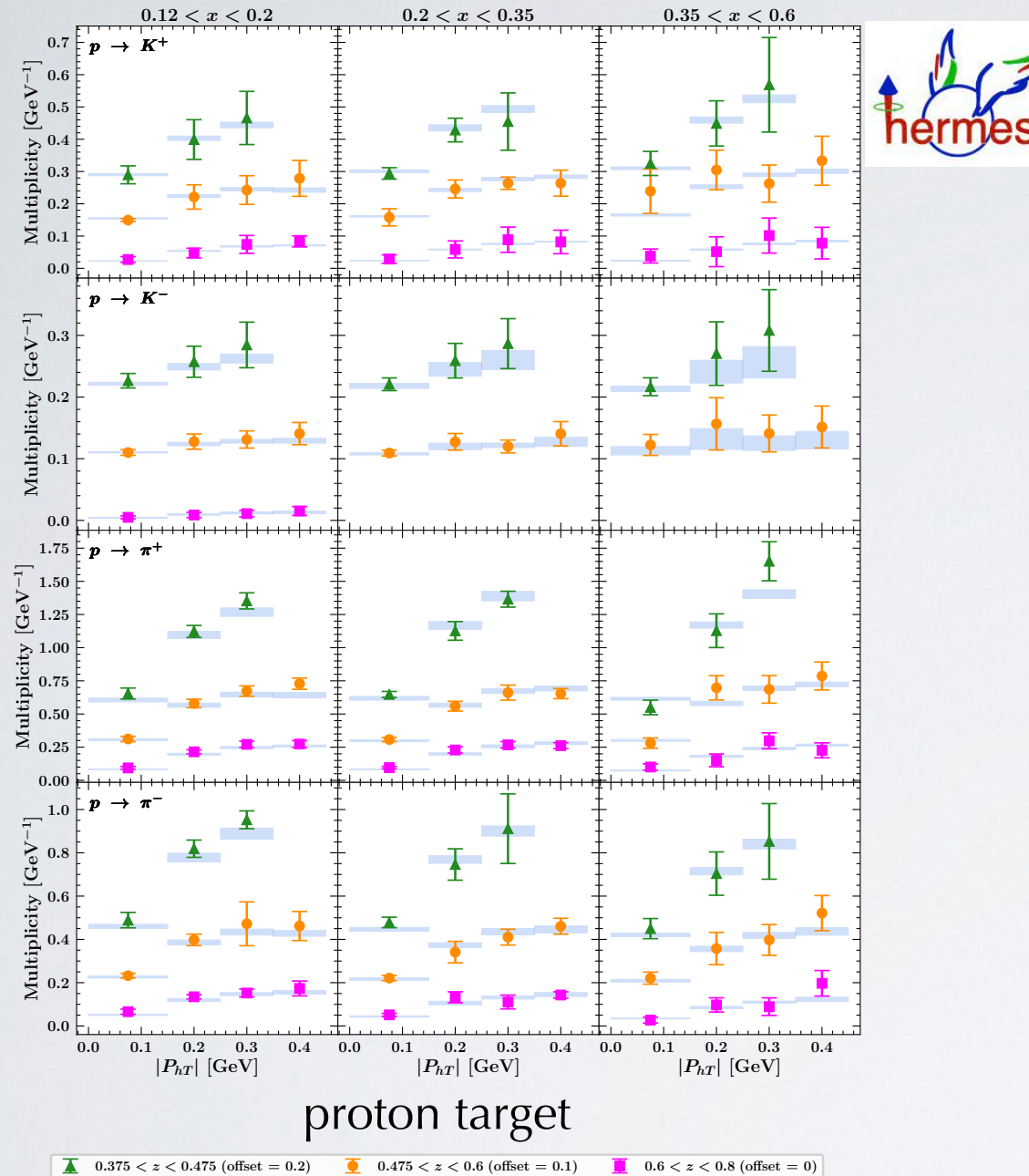
$$\left[\frac{\zeta_f}{Q_0^2} \right]^{g_K(b_T)/2}$$

$$g_K(b_T) = -g_2^2 \frac{b_T^2}{4}$$

1 param.

Total 21 param.

Fit results for SIDIS



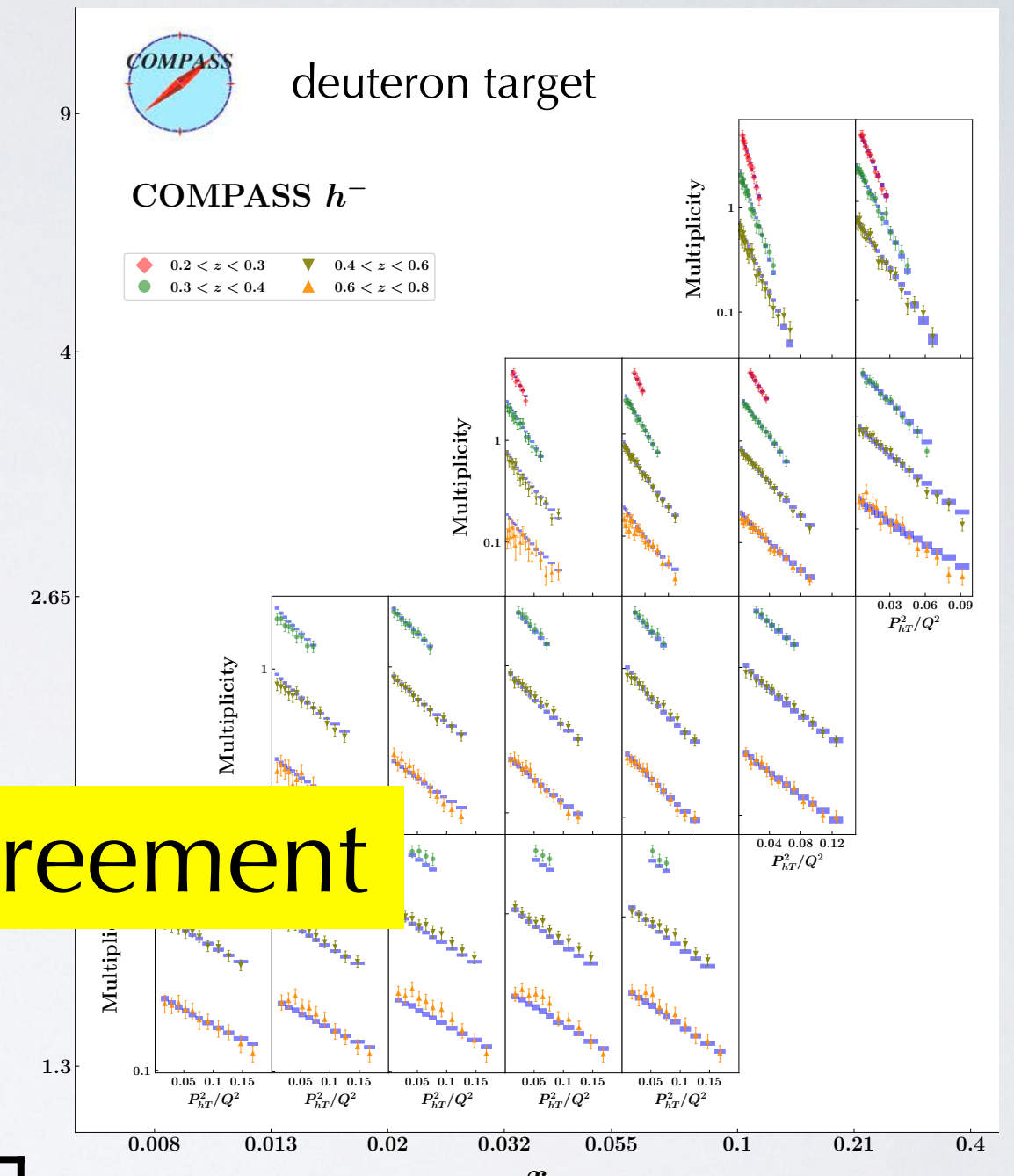
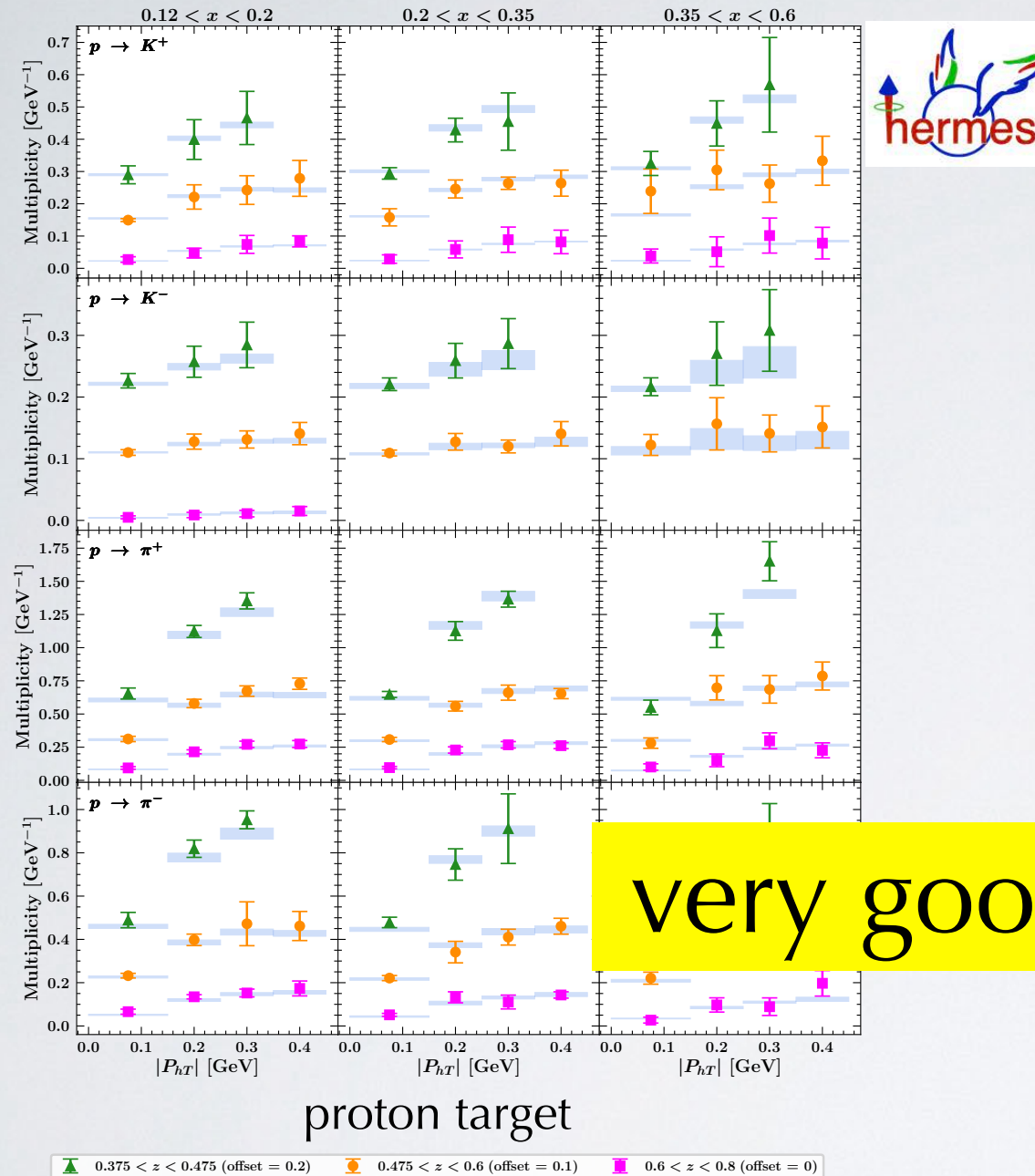
data set	N_{data}	χ_D^2	χ_λ^2	χ^2
HERMES	344	0.48	0.23	0.71
COMPASS	1203	0.62	0.3	0.92
SIDIS total	1547	0.59	0.28	0.87

χ_D^2 = uncorrelated error

χ_λ^2 = correlated error

$\chi^2 = \chi_D^2 + \chi_\lambda^2$

Fit results for SIDIS



data set	N_{data}	χ_D^2	χ_λ^2	χ^2
HERMES	344	0.48	0.23	0.71
COMPASS	1203	0.62	0.3	0.92
SIDIS total	1547	0.59	0.28	0.87

χ_D^2 = uncorrelated error

χ_λ^2 = correlated error

$$\chi^2 = \chi_D^2 + \chi_\lambda^2$$

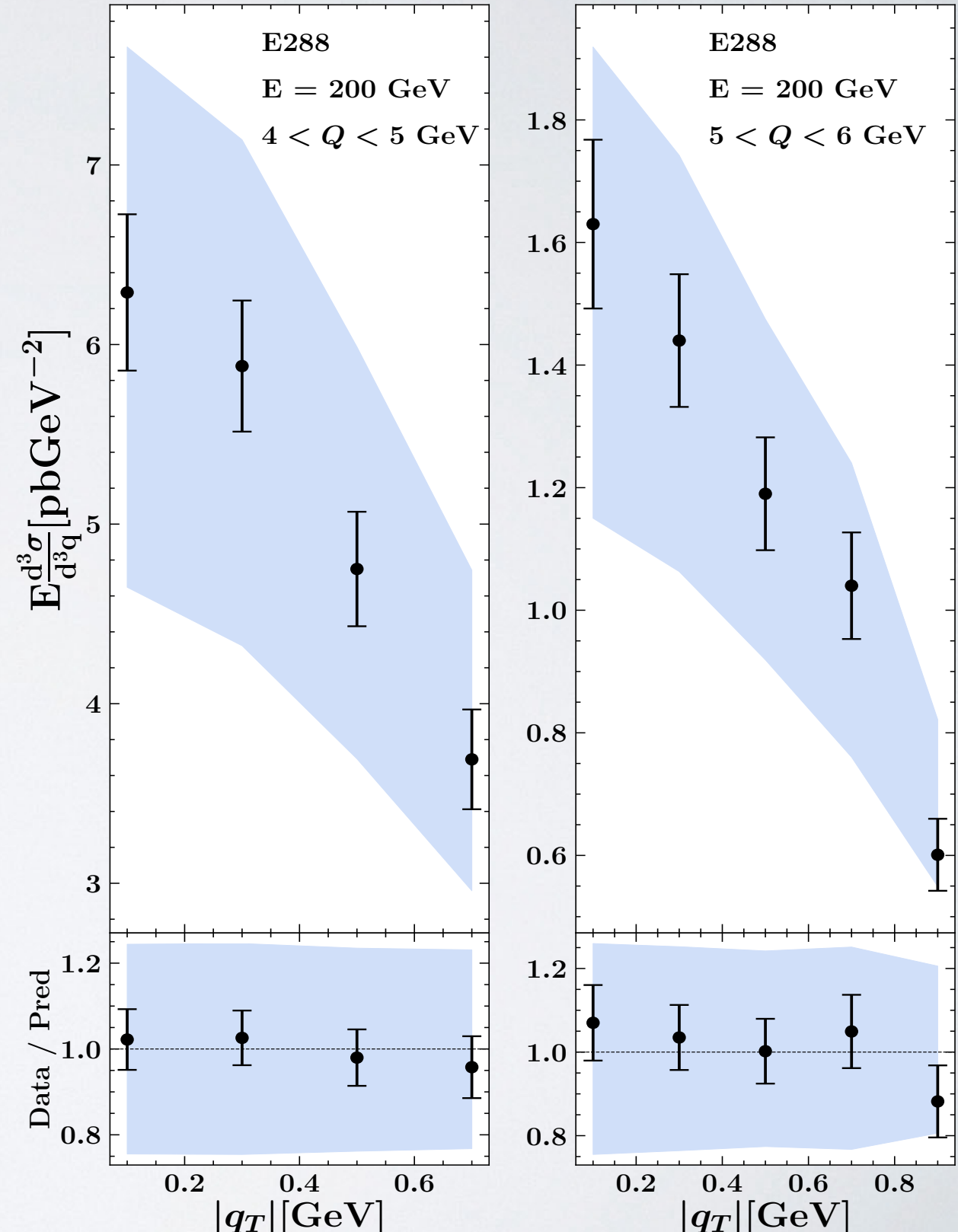
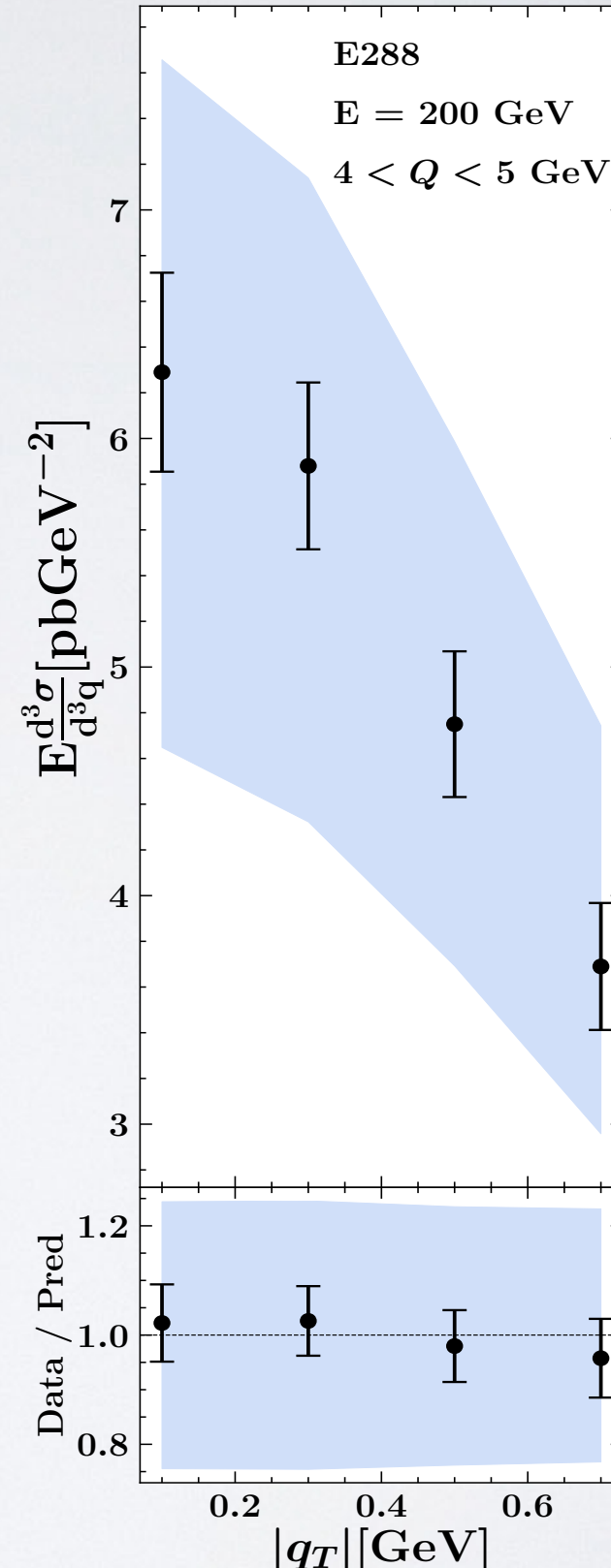
Fit results for fixed-target Drell-Yan

data set	N_{data}	χ_D^2	χ_λ^2	χ^2
SIDIS total	1547	0.59	0.28	0.87
Drell-Yan fixed target tot	233	0.84	0.4	1.24
Drell-Yan collider total	251	1.86	0.2	2.06

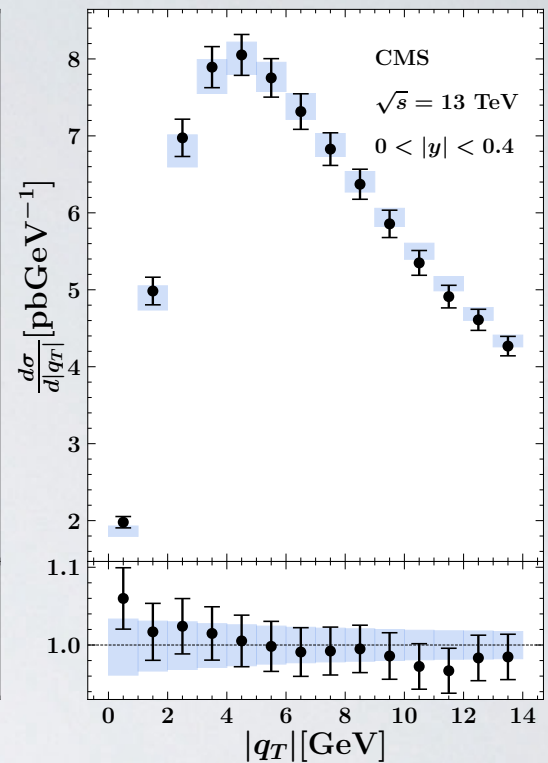
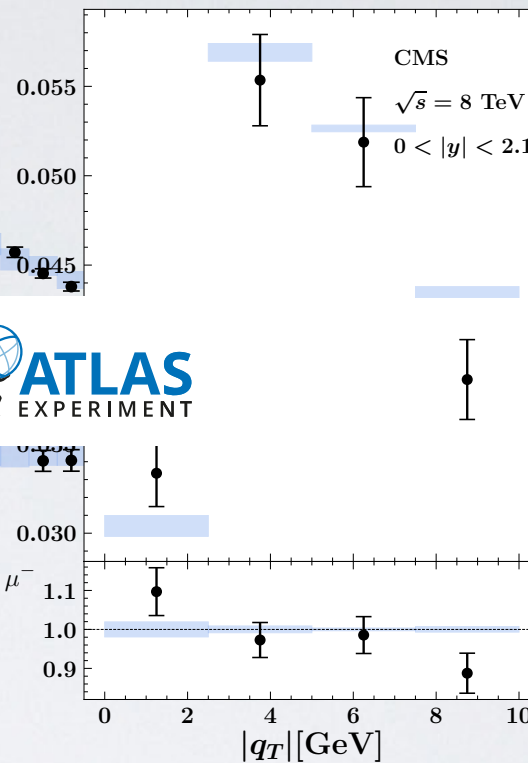
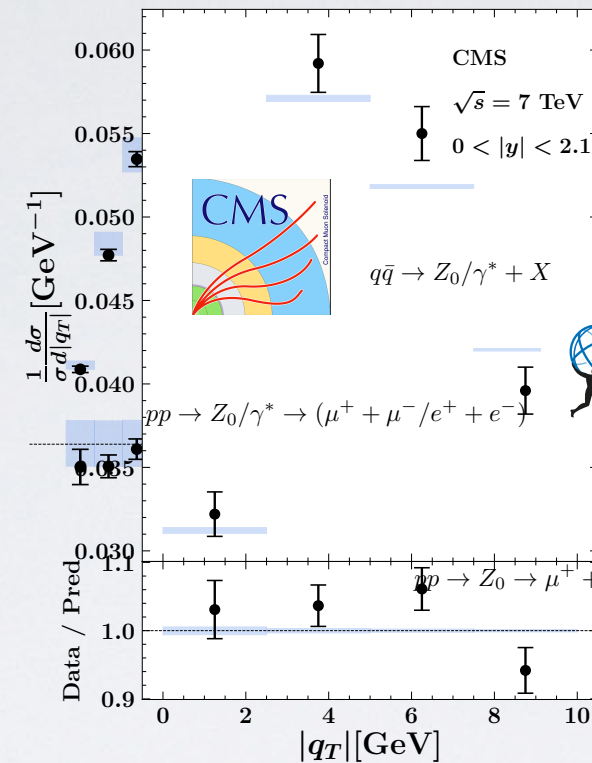
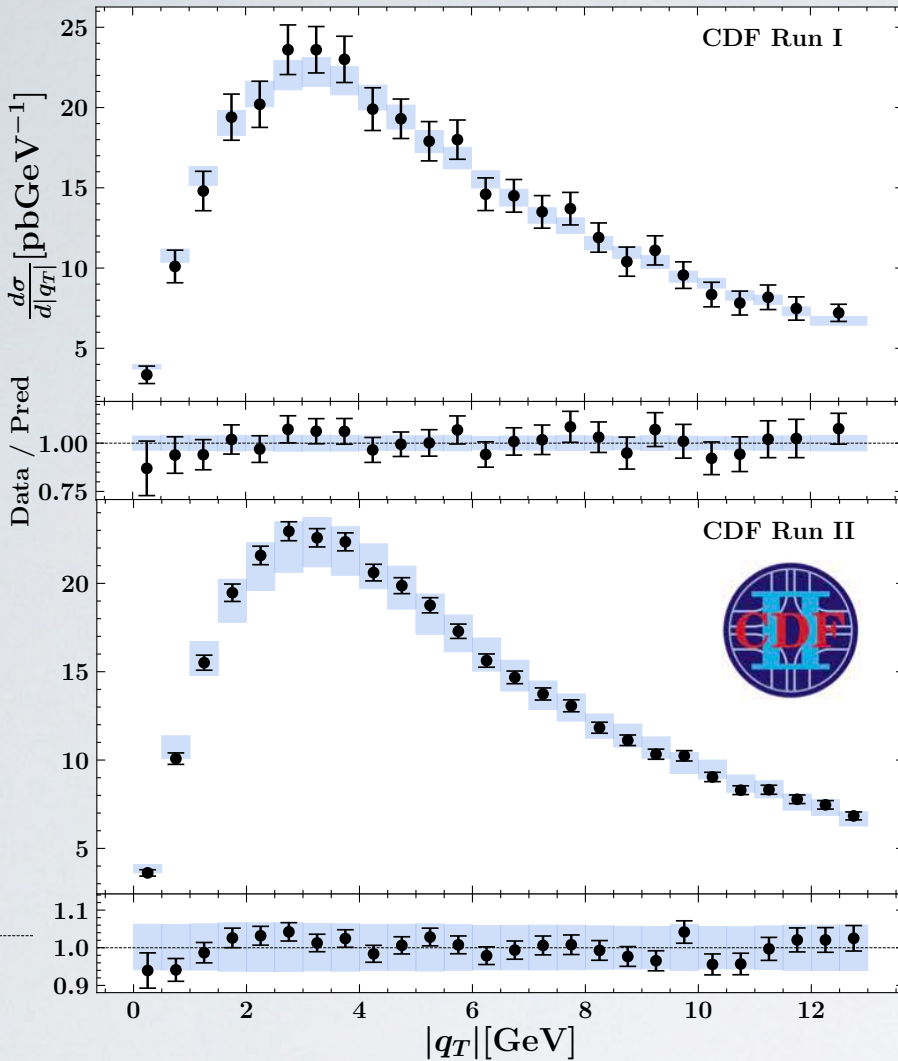
χ_D^2 = uncorrelated error
 χ_λ^2 = correlated error
 $\chi^2 = \chi_D^2 + \chi_\lambda^2$

good agreement

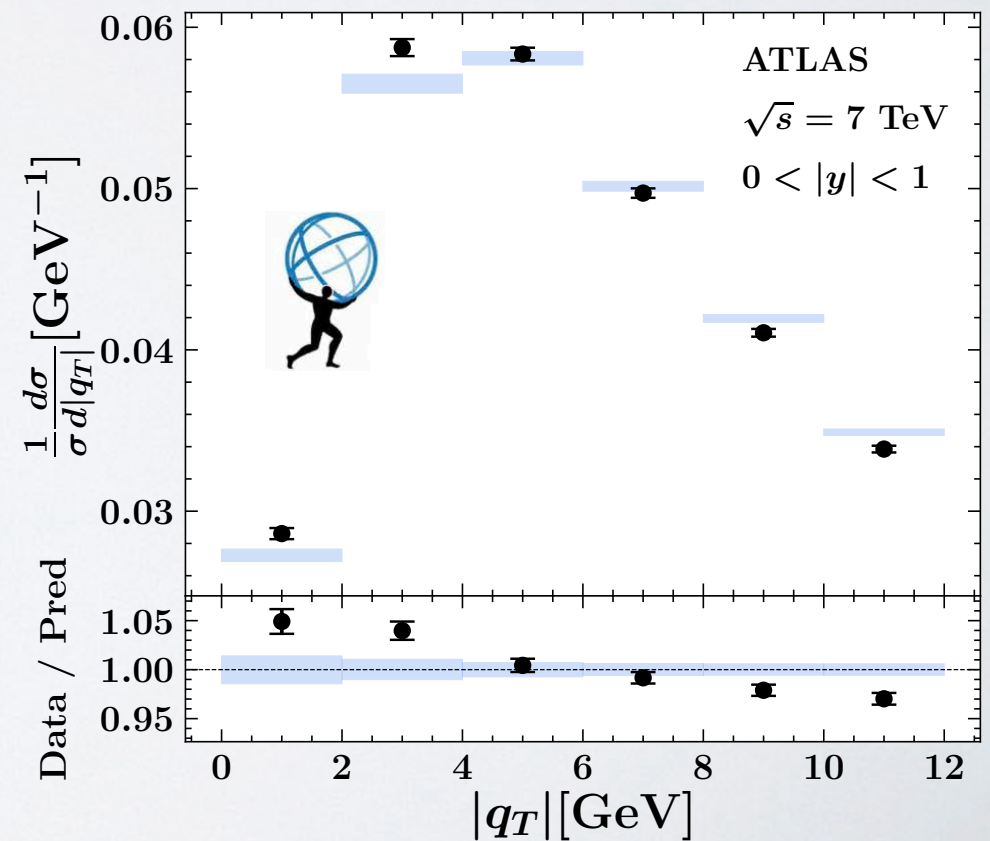
th. error band =
68% of all replicas



Fit results for collider Drell-Yan



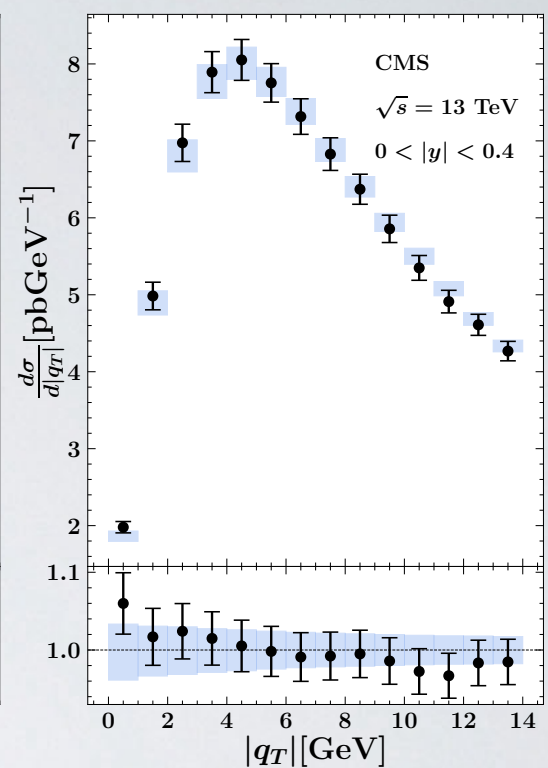
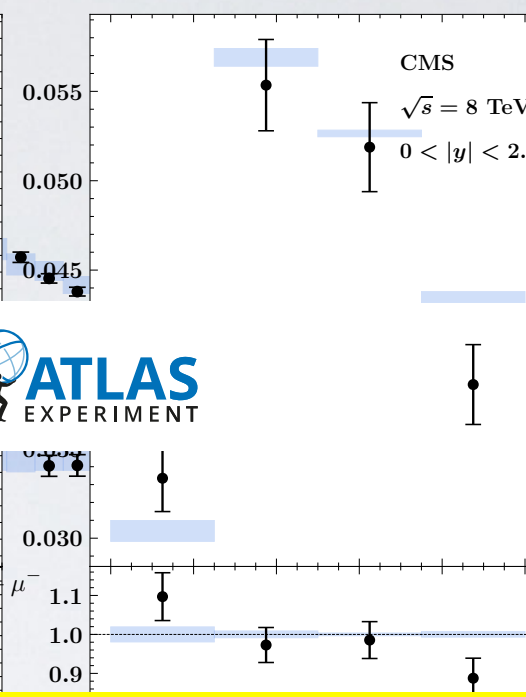
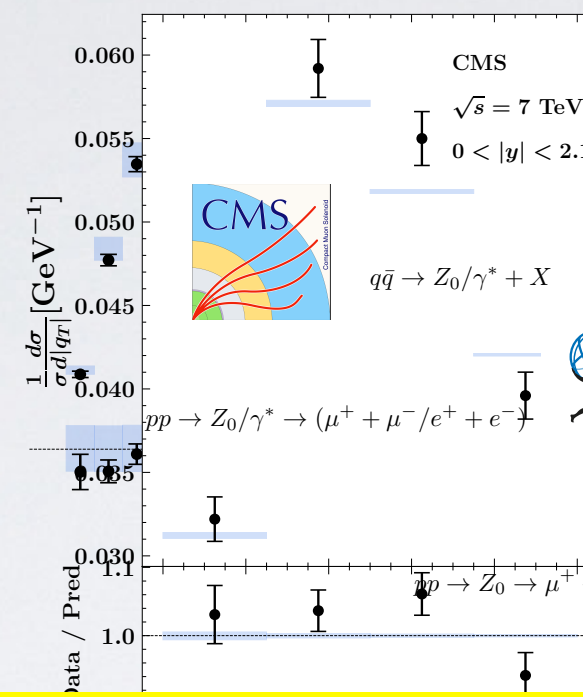
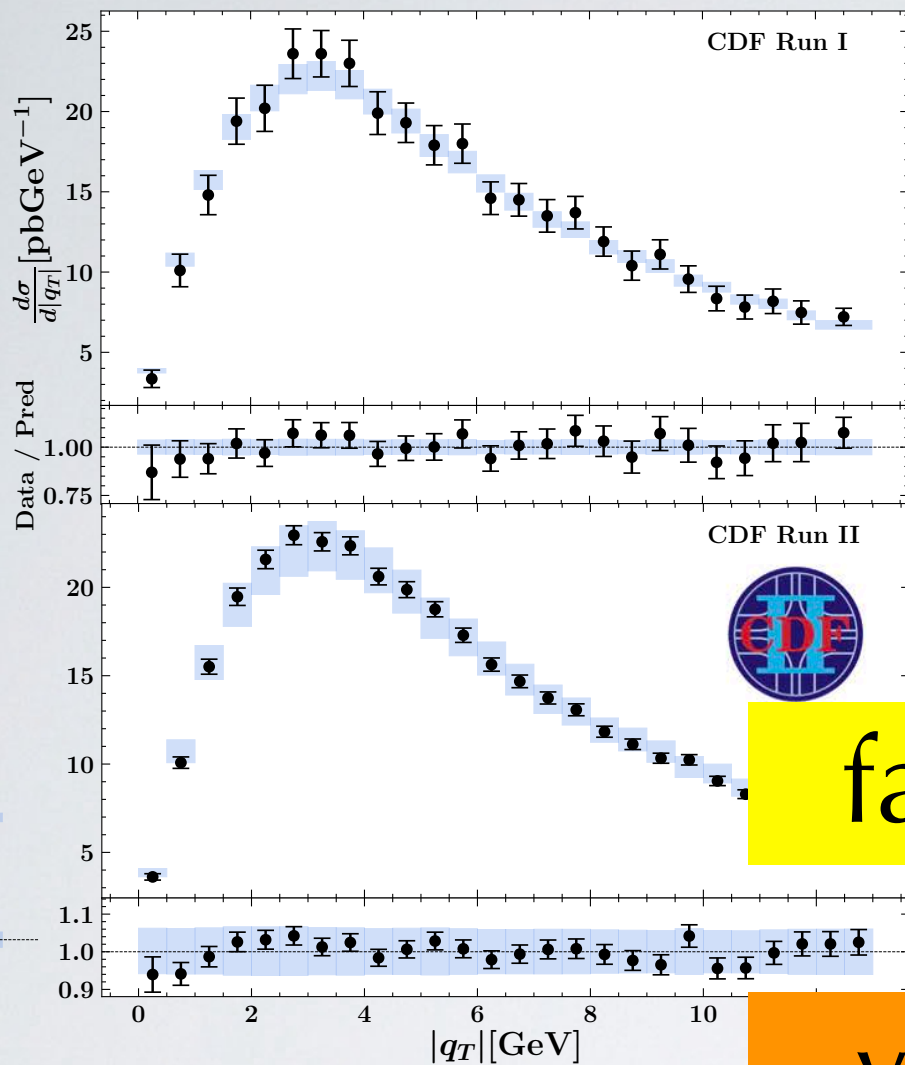
data set	N_{data}	χ_D^2	χ_λ^2	χ^2
SIDIS total	1547	0.59	0.28	0.87
Drell-Yan fixed target tot	233	0.85	0.4	1.24
Drell-Yan collider total	251	1.86	0.2	2.06
ATLAS total	72	4.56	0.48	5.05



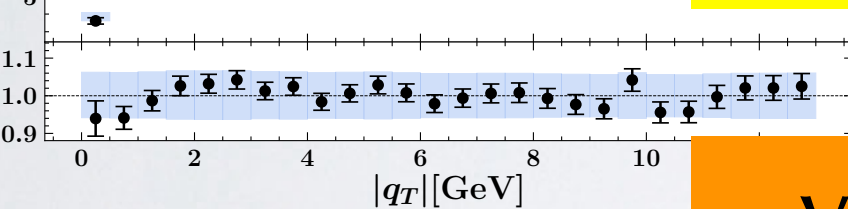
Fit results for collider Drell-Yan



Fit results for collider Drell-Yan

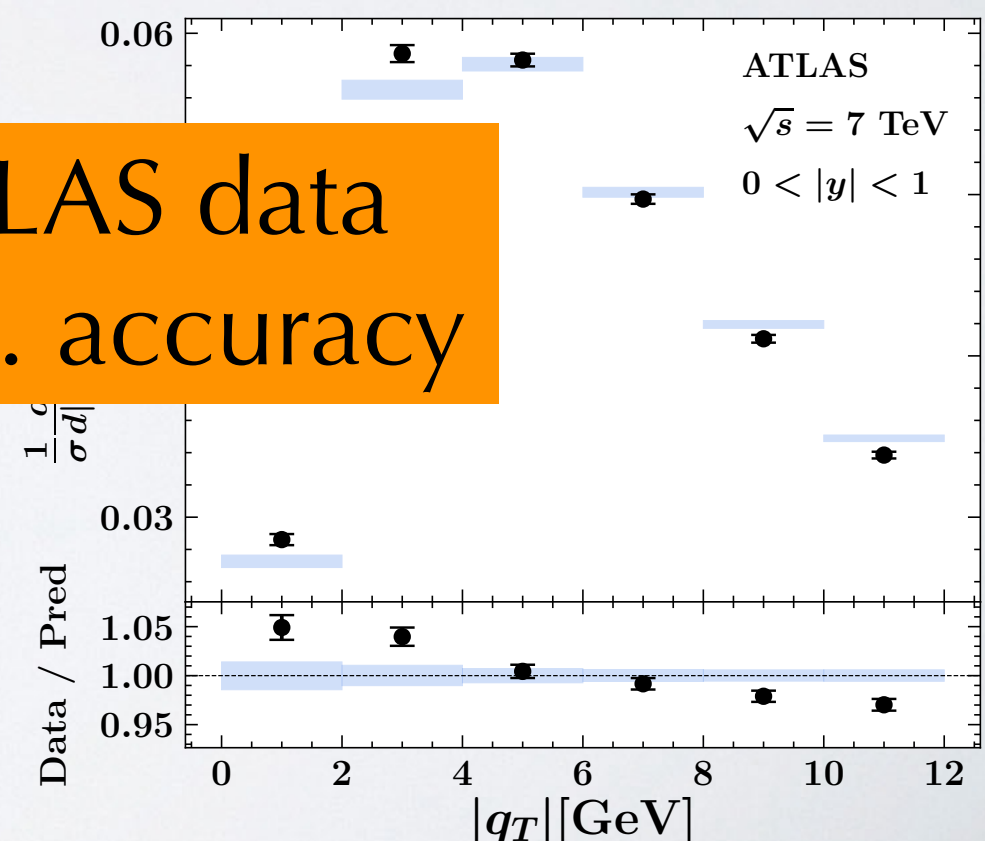


fairly good agreement

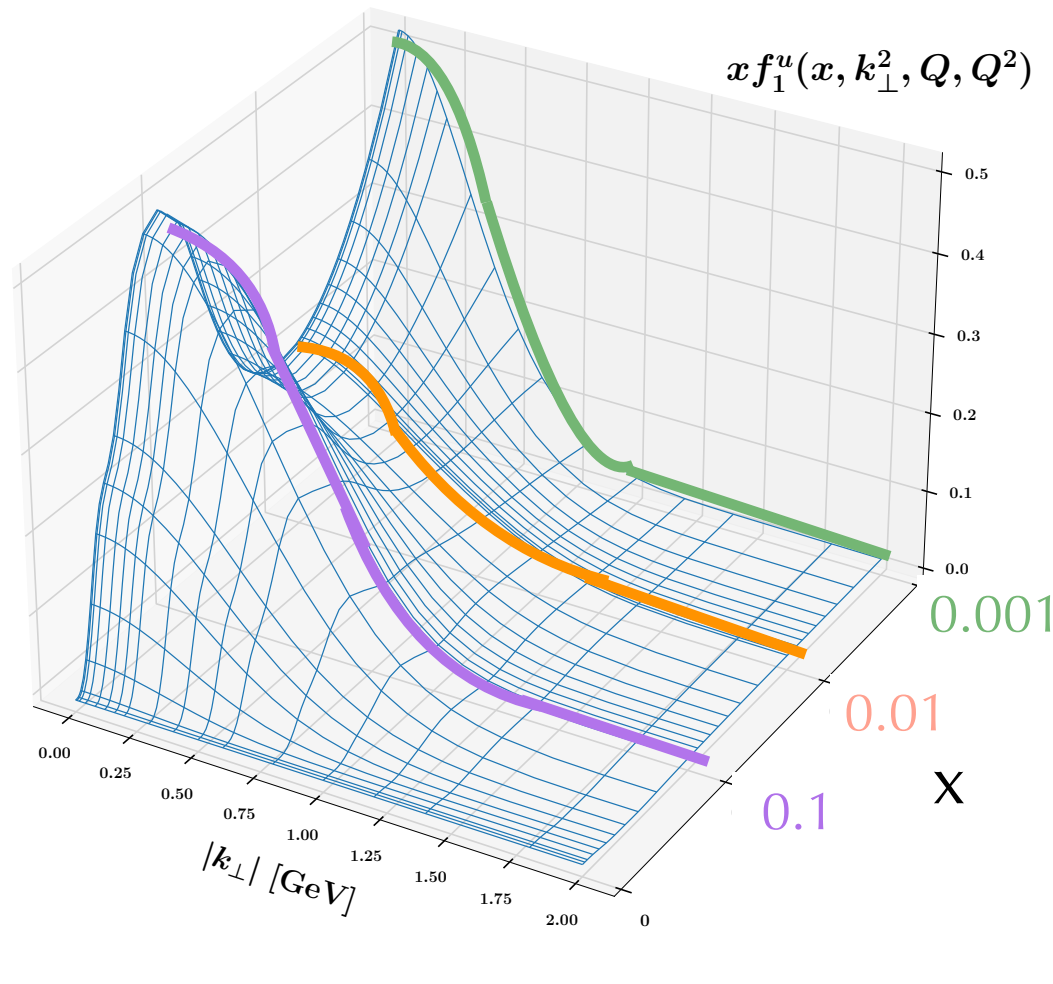


data set	N_{events}	χ^2/ν	$\Delta\sigma/\sigma$	$\Delta\sigma/\sigma$
SIDIS total	1547	0.59	0.28	0.87
Drell-Yan fixed target tot	233	0.85	0.4	1.24
Drell-Yan collider total	251	1.86	0.2	2.06
ATLAS total	72	4.56	0.48	5.05

very precise ATLAS data
require higher Th. accuracy

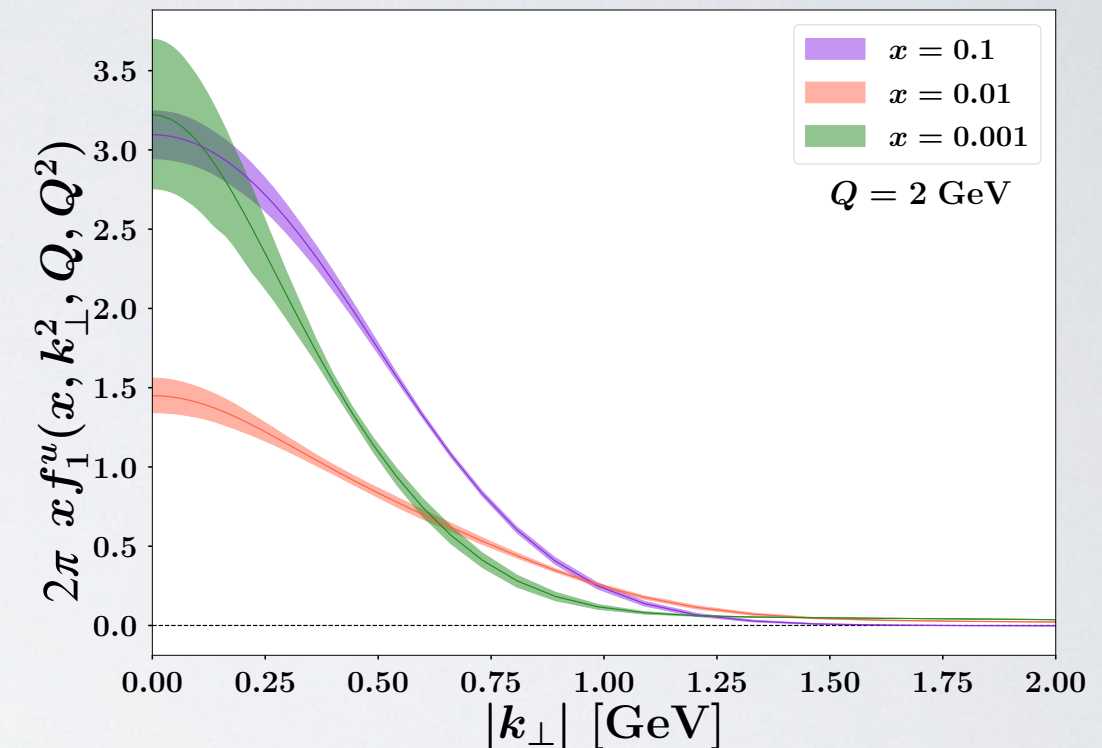


Visualizing MAPTMD22 TMD PDF



unpolarized up quark in the proton

$Q=2 \text{ GeV}$

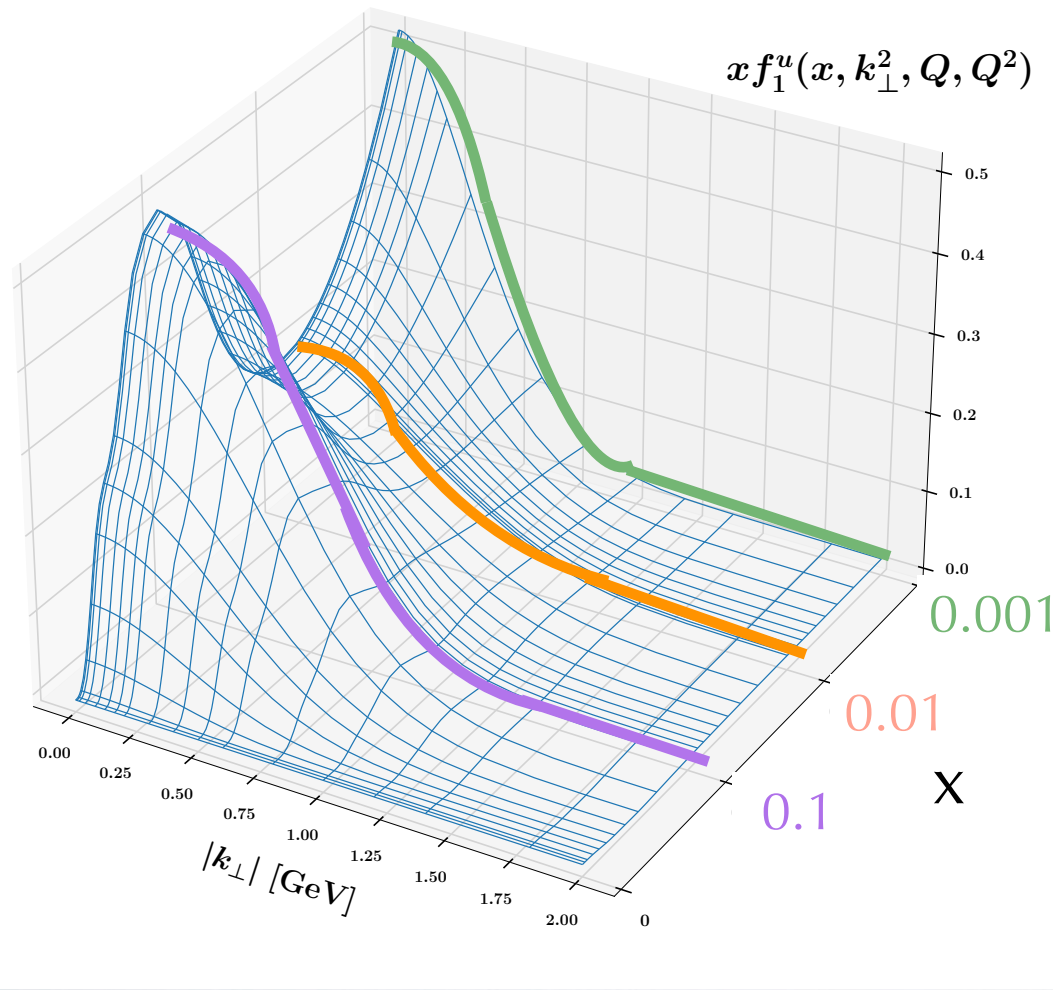


$$f_{\text{NP}}(x, k_\perp; Q_0) \sim \text{Gauss} + \lambda_B k_\perp^2 \text{Gauss} + \lambda_C \text{Gauss}$$

effect of x -dependent widths

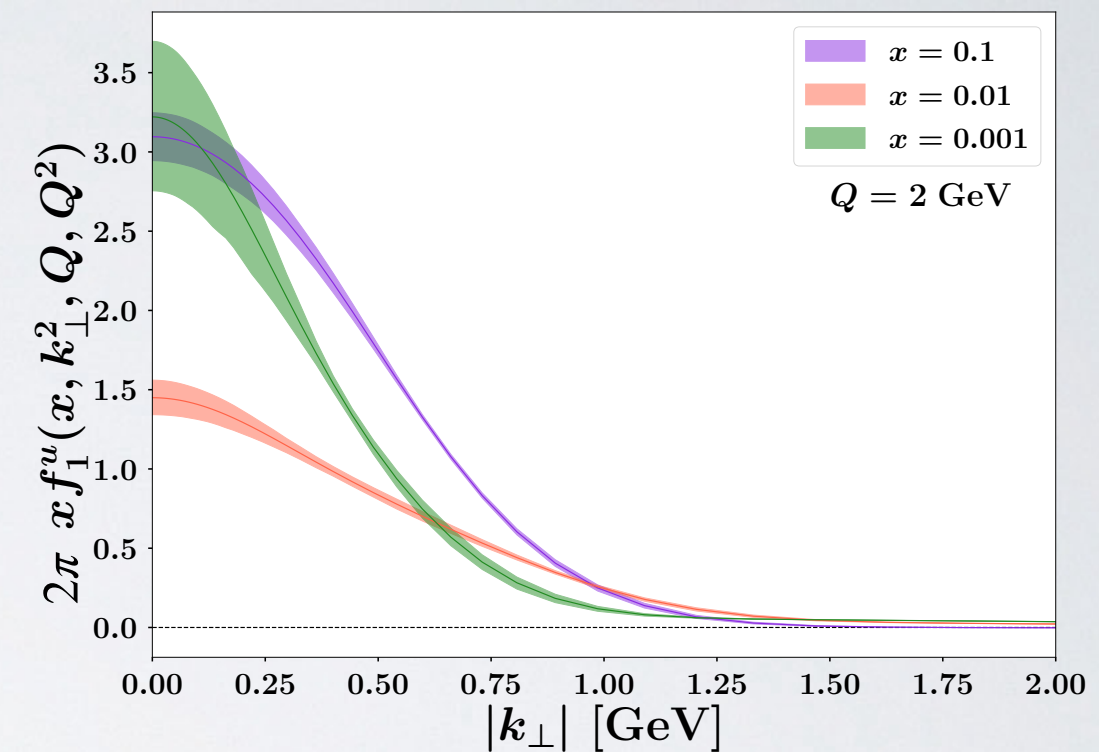
$$\langle k_\perp^2 \rangle(x = 0.1, Q = 1) = 0.3 \pm 0.05 \text{ GeV}^2$$

Visualizing MAPTMD22 TMD PDF



unpolarized up quark in the proton

$Q = 2 \text{ GeV}$



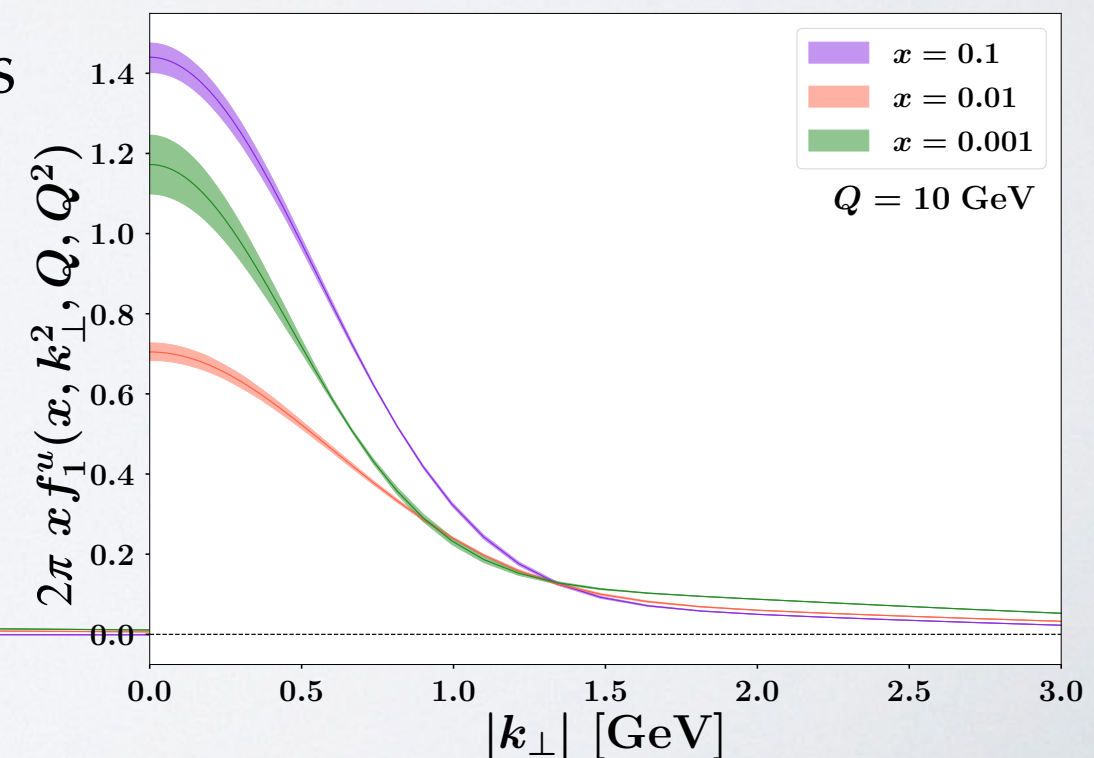
$$f_{\text{NP}}(x, k_{\perp}; Q_0) \sim \text{Gauss} + \lambda_B k_{\perp}^2 \text{Gauss} + \lambda_C \text{Gauss}$$

effect of x -dependent widths

$$\langle k_{\perp}^2 \rangle(x = 0.1, Q = 1) = 0.3 \pm 0.05 \text{ GeV}^2$$

$$e^{-g_2^2 b_T^2/4} \quad g_2 = 0.248 \pm 0.008 \text{ GeV}$$

effect of nonperturbative evolution



Visualizing the Collins-Soper evolution kernel

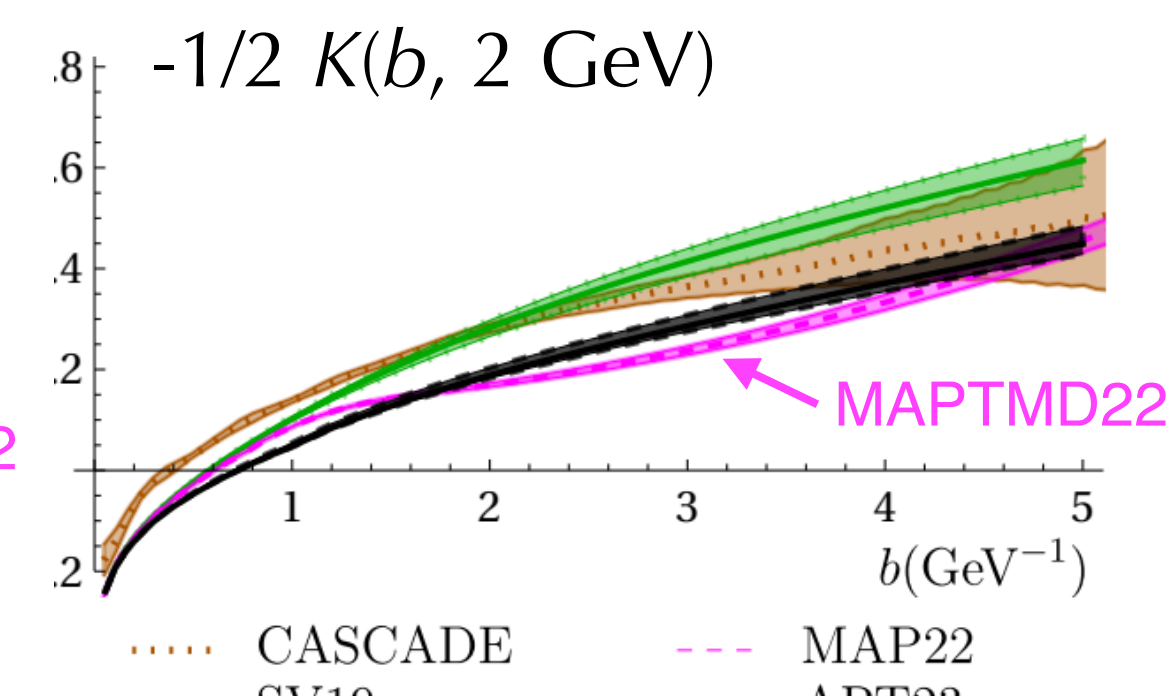
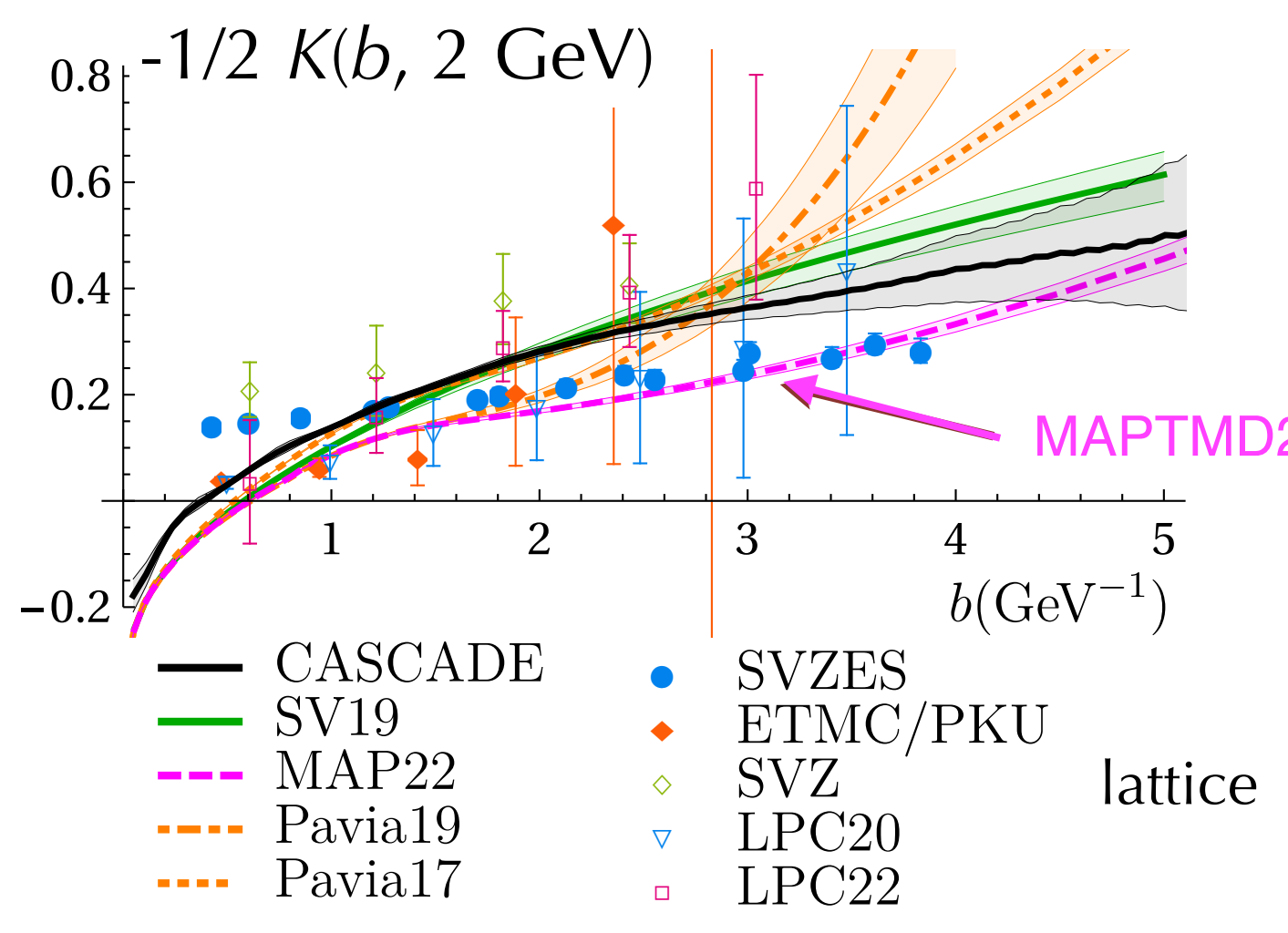
Collins-Soper kernel

drives evolution in rapidity ζ

$$K(b_T, \mu_{b_*}) = K(b_*, \mu_{b_*}) + g_K(b_T)$$

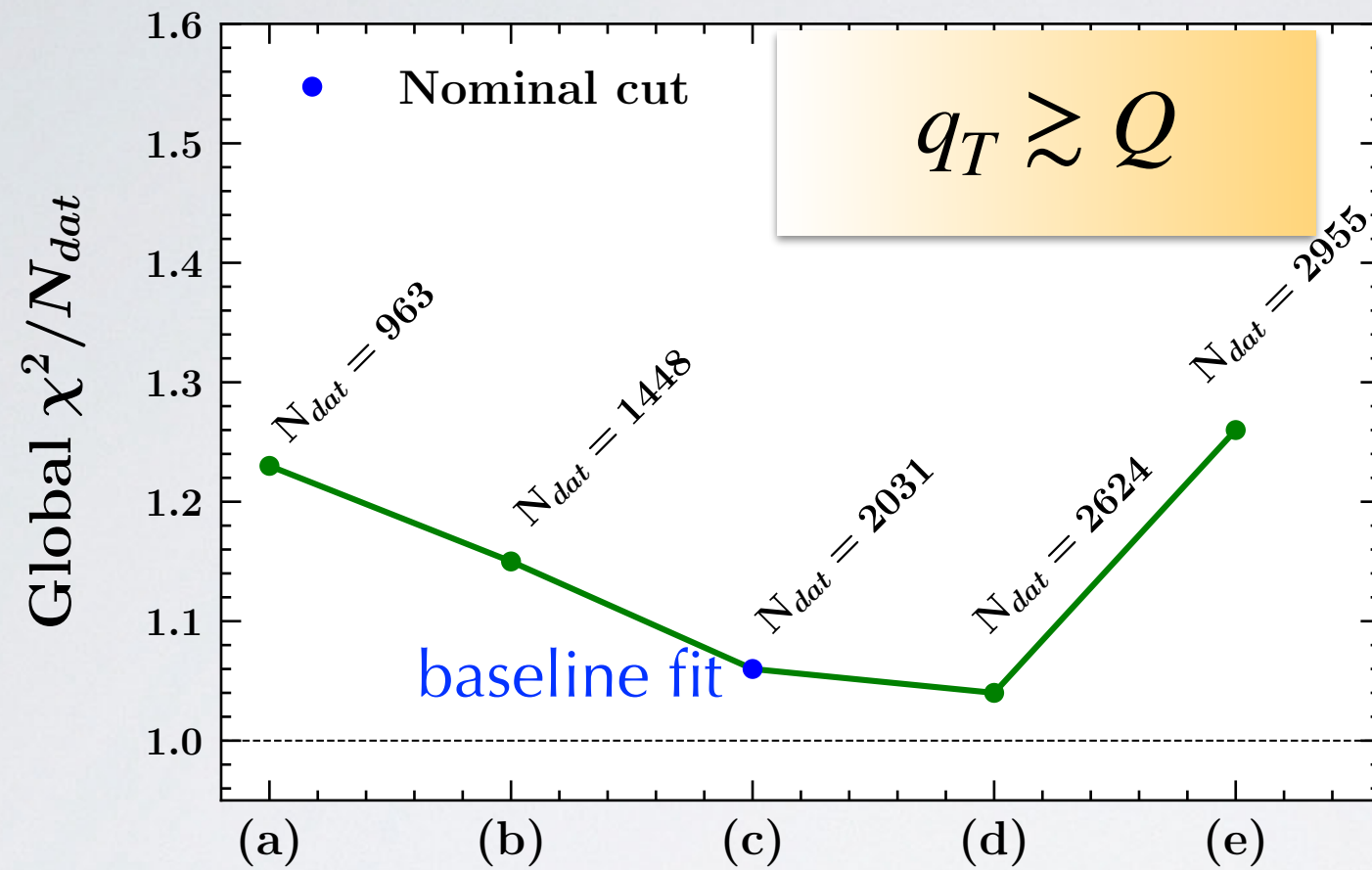
perturbative

non-perturbative
(fitted)



Moss et al., arXiv:2305.07473

Kinematic cuts and validity of TMD region



$$P_{hT} < \min \left[\min \left[c_1 Q, c_2 Qz \right] + c_3 \text{GeV}, zQ \right]$$

configurations

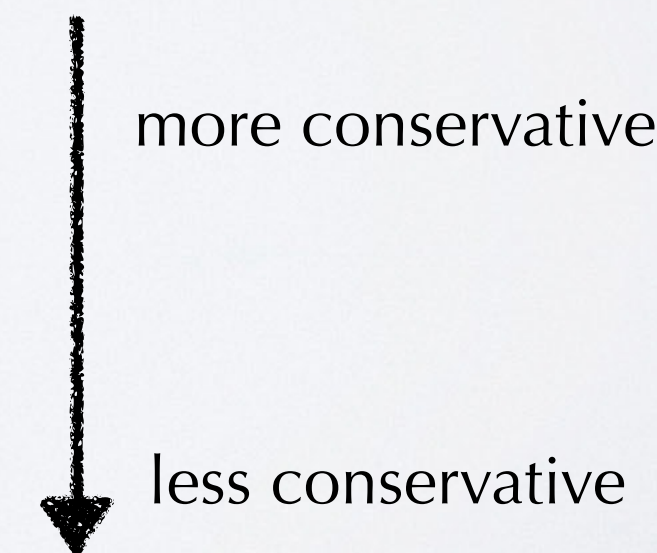
a) $c_1=c_2=0.4$, $c_3=0$ $q_T < 0.4 Q$

b) $c_1=0.15$, $c_2=0.4$, $c_3=0.2$

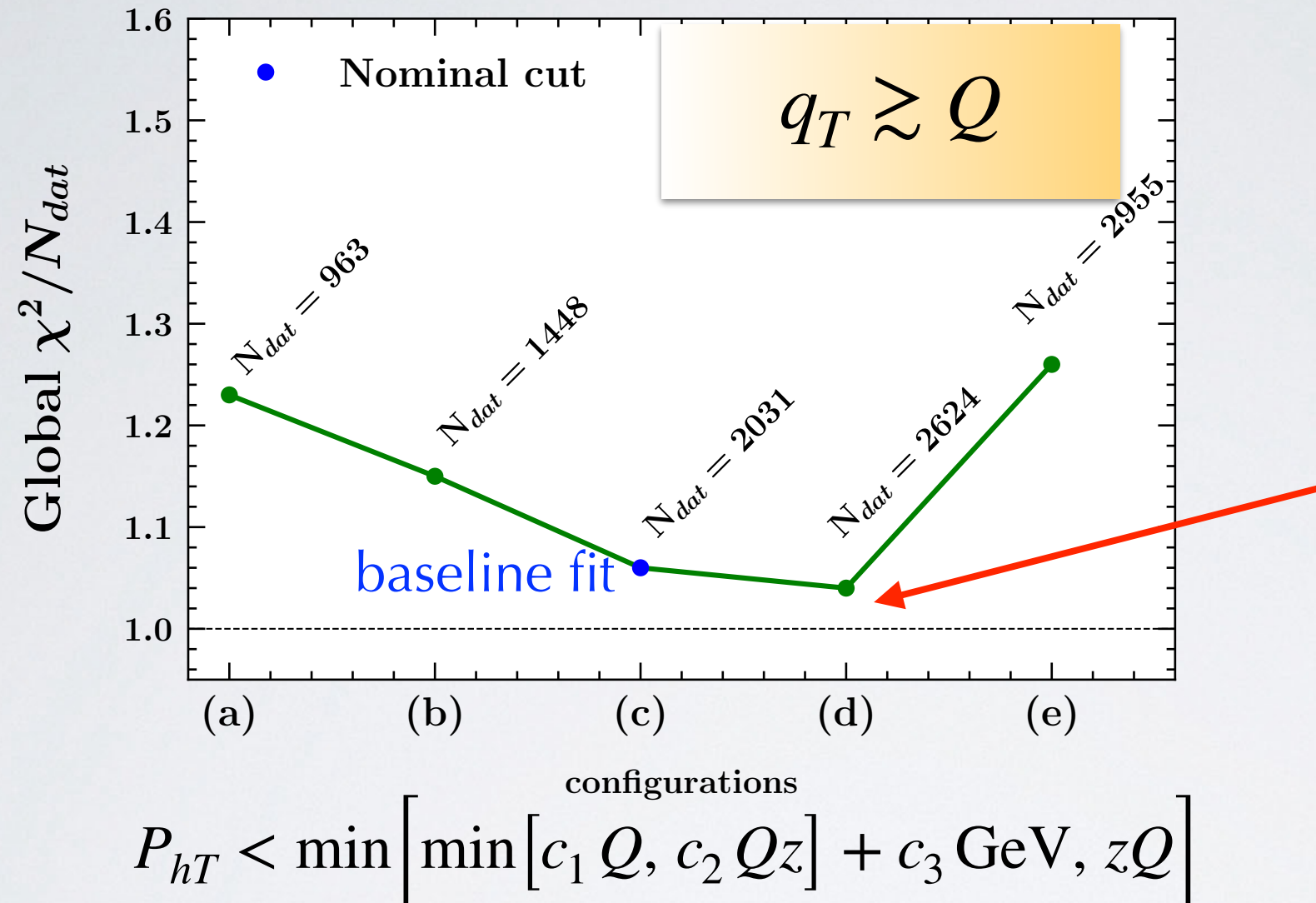
c) $c_1=0.2$, $c_2=0.5$, $c_3=0.3$ **baseline fit**

d) $c_1=0.2$, $c_2=0.6$, $c_3=0.4$ can be $q_T > Q$

e) $c_1=0.2$, $c_2=0.7$, $c_3=0.5$ can be $q_T > Q$



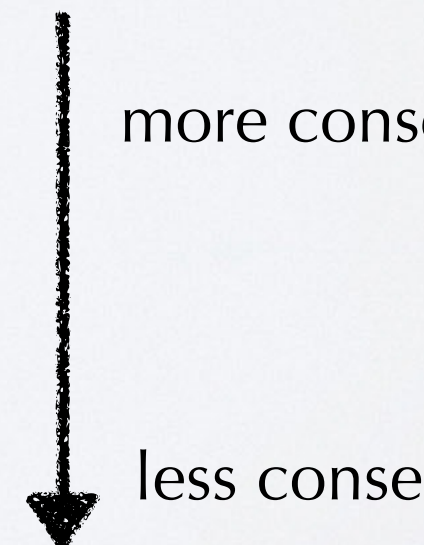
Kinematic cuts and validity of TMD region



- a) $c_1=c_2=0.4, c_3=0$ $q_T < 0.4 Q$
- b) $c_1=0.15, c_2=0.4, c_3=0.2$
- c) $c_1=0.2, c_2=0.5, c_3=0.3$ **baseline fit**
- d) $c_1=0.2, c_2=0.6, c_3=0.4$ can be $q_T > Q$
- e) $c_1=0.2, c_2=0.7, c_3=0.5$ can be $q_T > Q$

better χ^2 with less conservative cuts allowing for $q_T > Q$

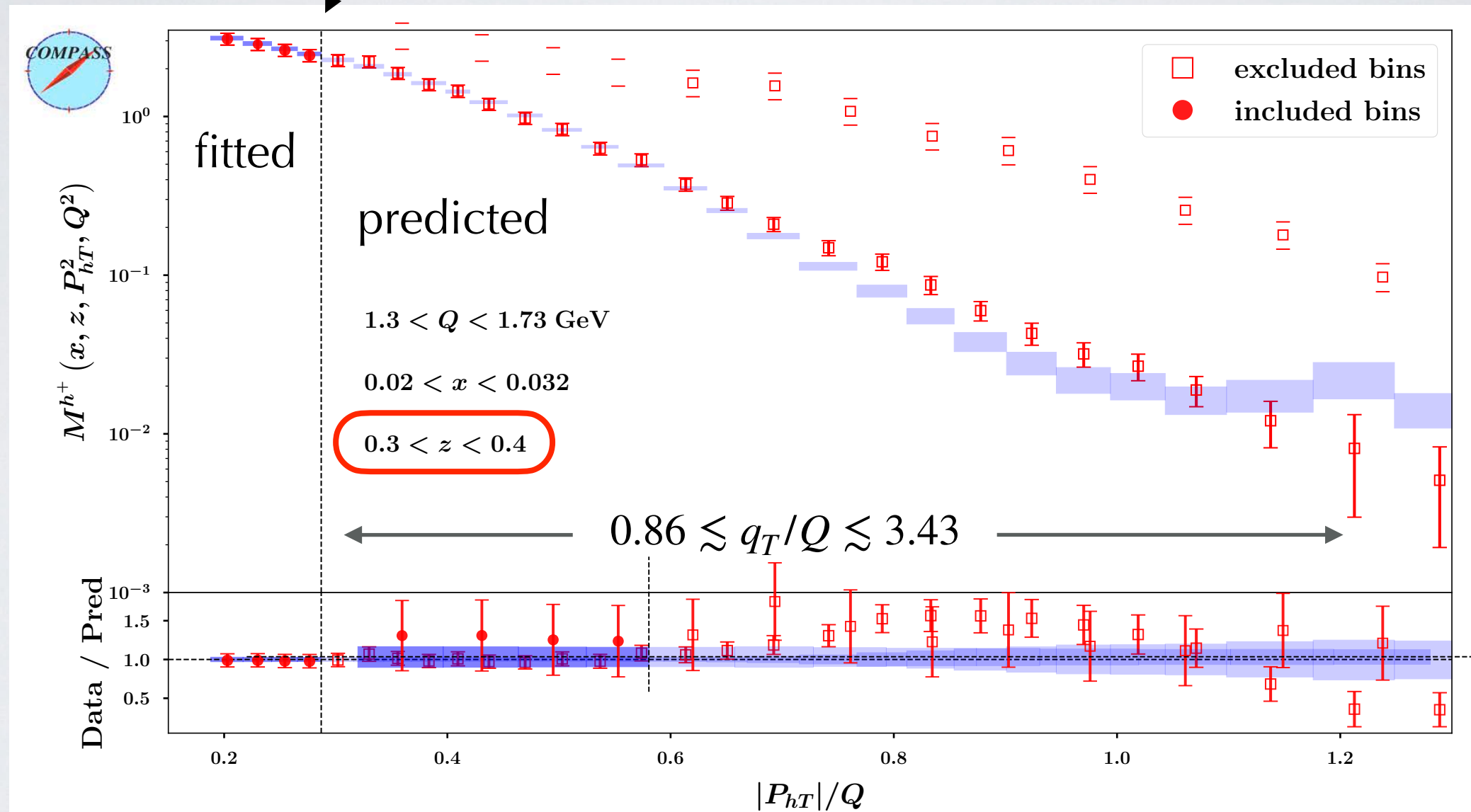
Where is the limit for TMD factorization??



Kinematic cuts and validity of TMD region

cut of
baseline fit

$$P_{hT} < \min \left[\min [0.2 Q, 0.5 Qz] + 0.3 \text{ GeV}, zQ \right]$$



validity of TMD factorization seems to extend well beyond $P_{hT}/z \ll Q$!

The MAPTMDPion22 fit

Extracting TMDs for the pion

	Framework	DY	N of points	χ^2/N_{points}
Wang et al., 2017 arXiv:1707.05207	NLL	✓	96	1.61
Vladimirov, 2019 arXiv:1907.10356	NNLL'	✓	80	1.44
MAPTMDPion22, 2022 arXiv:2210.01733	N ³ LL	✓	138	1.54
JAM 2023 arXiv:2302.01192	NNLL	✓	93	1.37

MAPTMDPion22: - best theoretical accuracy: **N³LL**
[arXiv:2210.01733](#)
 - largest number of included data: **138**
 - same consistent framework of MAPTMD22

$$f_{\text{NP}}^\pi(x, b_T; Q_0) = e^{-g_{1\pi}(x) b_T^2 / 4} \quad g_{1\pi}(x) = N_{1\pi} \frac{(1-x)^{\alpha_\pi^2} x^{\sigma_\pi}}{(1-\hat{x})^{\alpha_\pi^2} \hat{x}^{\sigma_\pi}} \quad 3 \text{ param.}$$

$$\hat{x} = 0.1$$

The MAPTMDPion22 data sets

$\pi^- W \rightarrow \mu^+ \mu^- X$

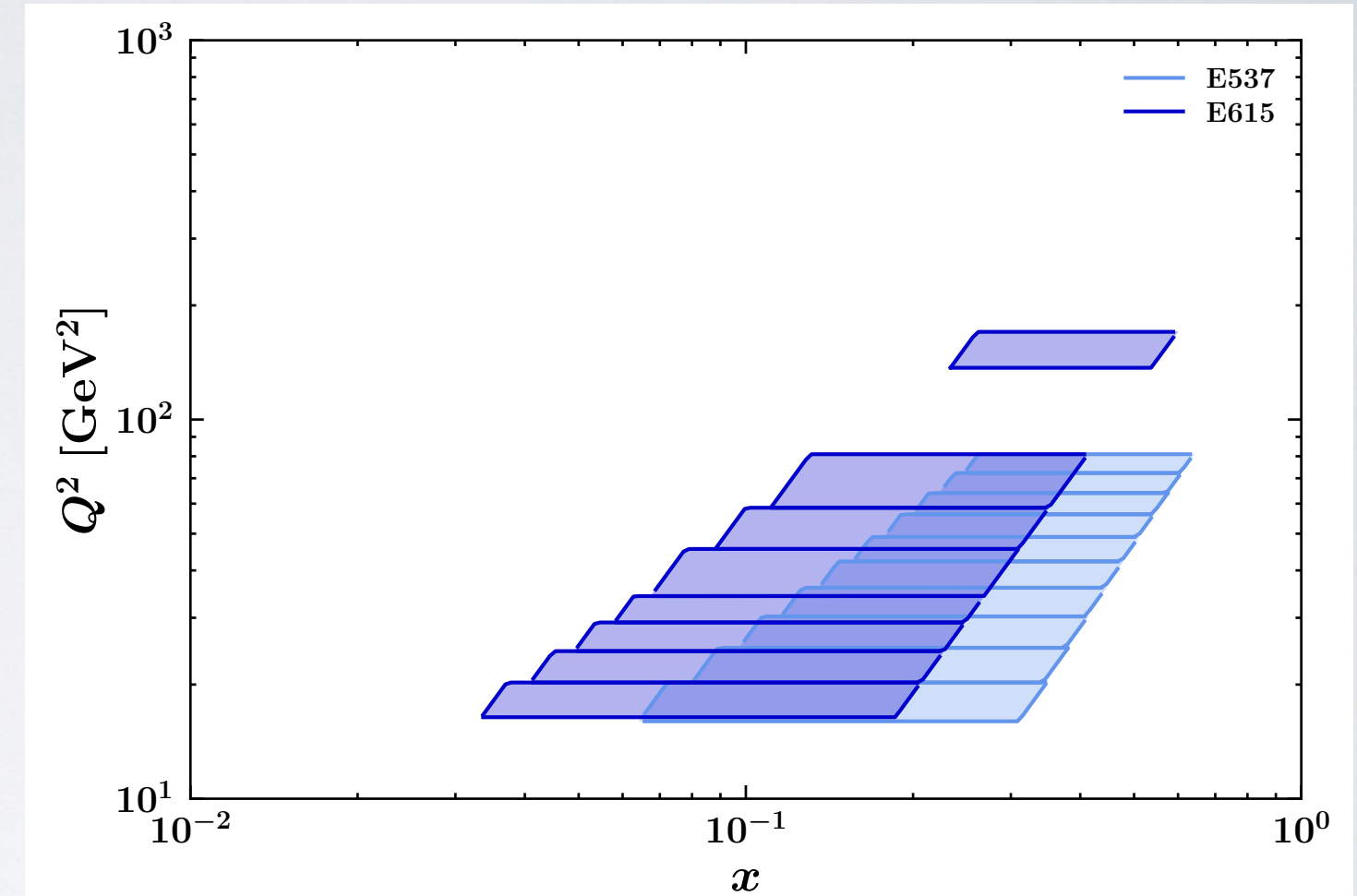
E615: $\sqrt{s} = 21.8$ GeV $0 < x_F < 1$
 $4.05 < Q < 13.05$ GeV
Stirling et al., 1993

E537: $\sqrt{s} = 15.3$ GeV $-0.1 < x_F < 1$
 $4 < Q < 9$ GeV
Anassontzis et al., 1988

Kinematical cut $q_T < 0.3 Q + 0.6$

N_{data} after cut: **74** + **64**

Many sources of (large) errors:



E615: stat. 5% syst. 16% (normalization)

E537: stat. 15-20% syst. 8%

Th.: 5-8% on PDF from xFitter20

The MAPTMDPion22 data sets

$\pi^- W \rightarrow \mu^+ \mu^- X$

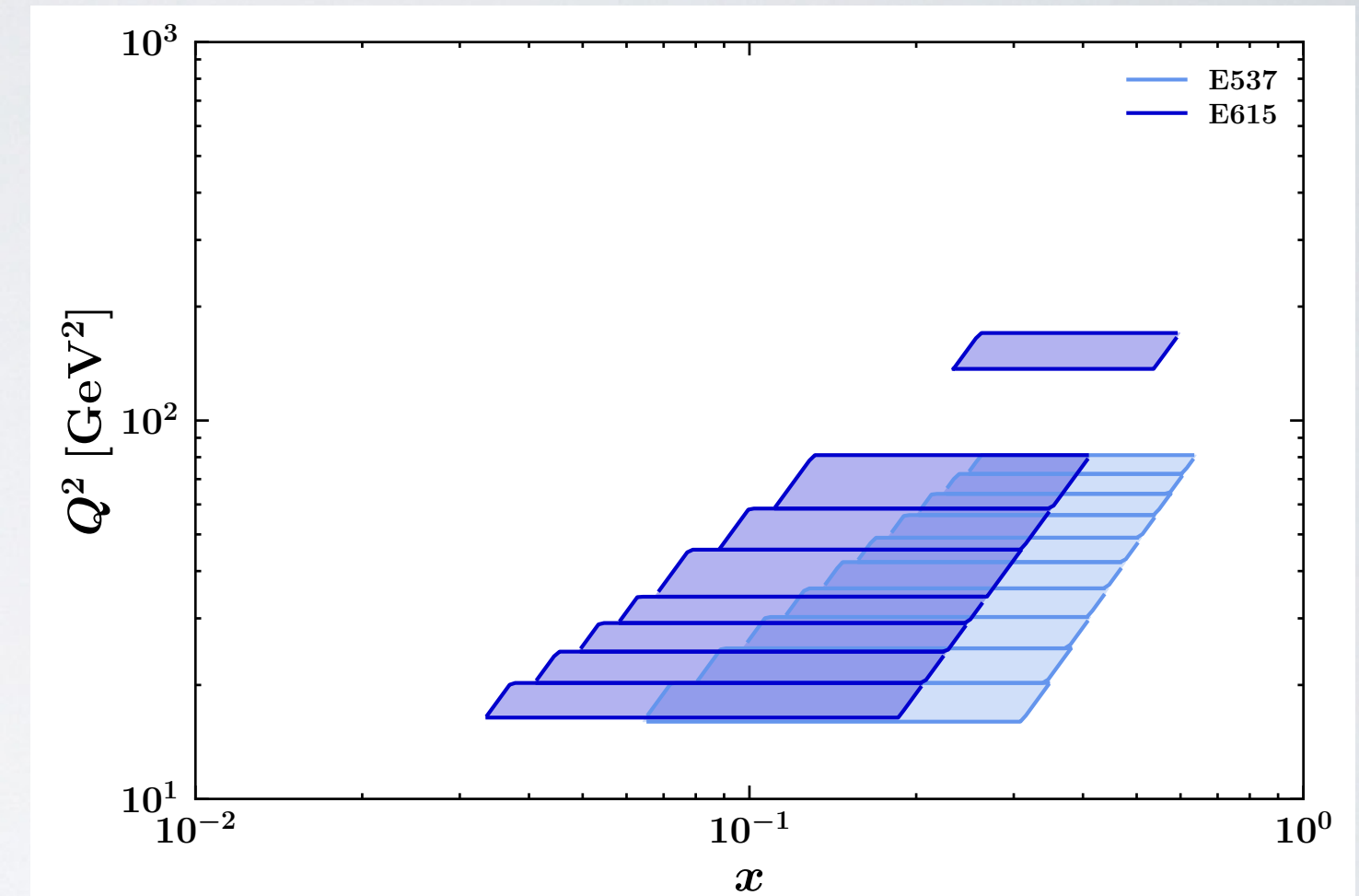
E615: $\sqrt{s} = 21.8$ GeV $0 < x_F < 1$
 $4.05 < Q < 13.05$ GeV
Stirling et al., 1993

E537: $\sqrt{s} = 15.3$ GeV $-0.1 < x_F < 1$
 $4 < Q < 9$ GeV
Anassontzis et al., 1988

Kinematical cut $q_T < 0.2 Q$

N_{data} after cut: **74** + **64**

Many sources of (large) errors:

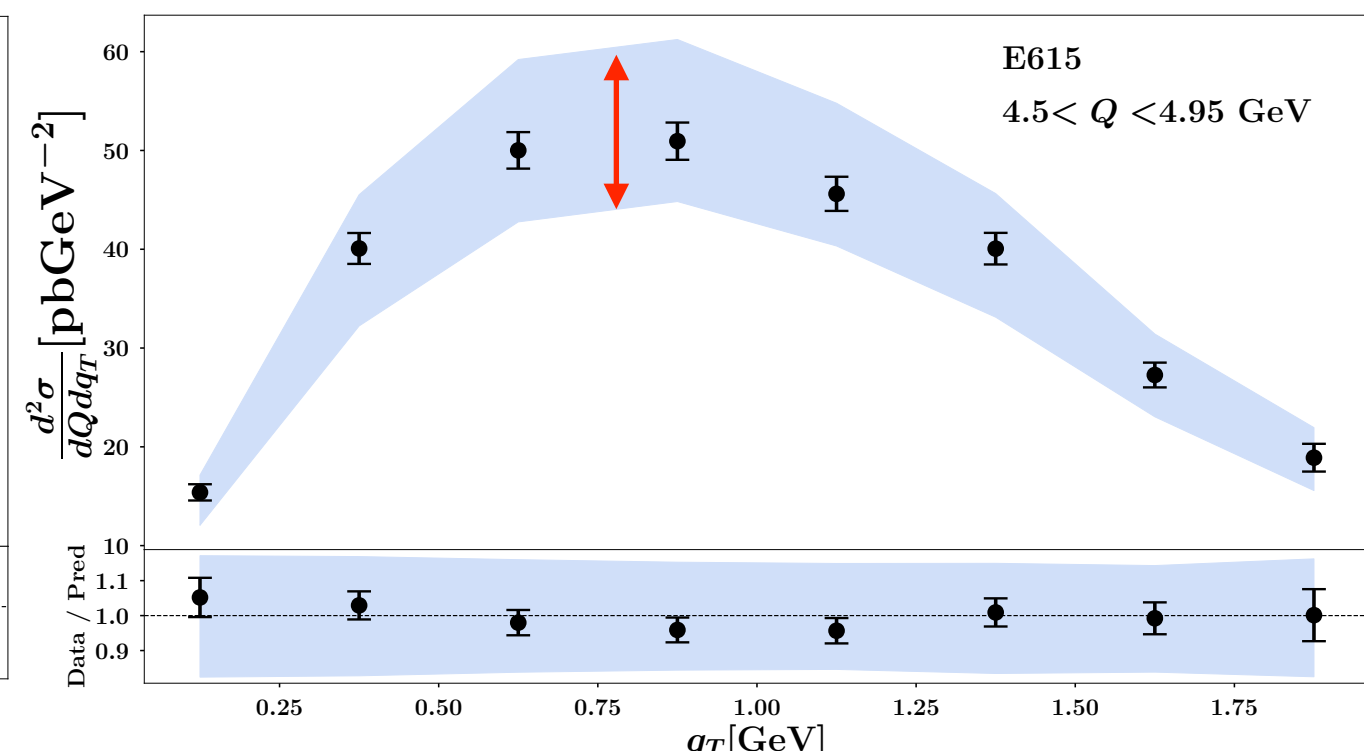
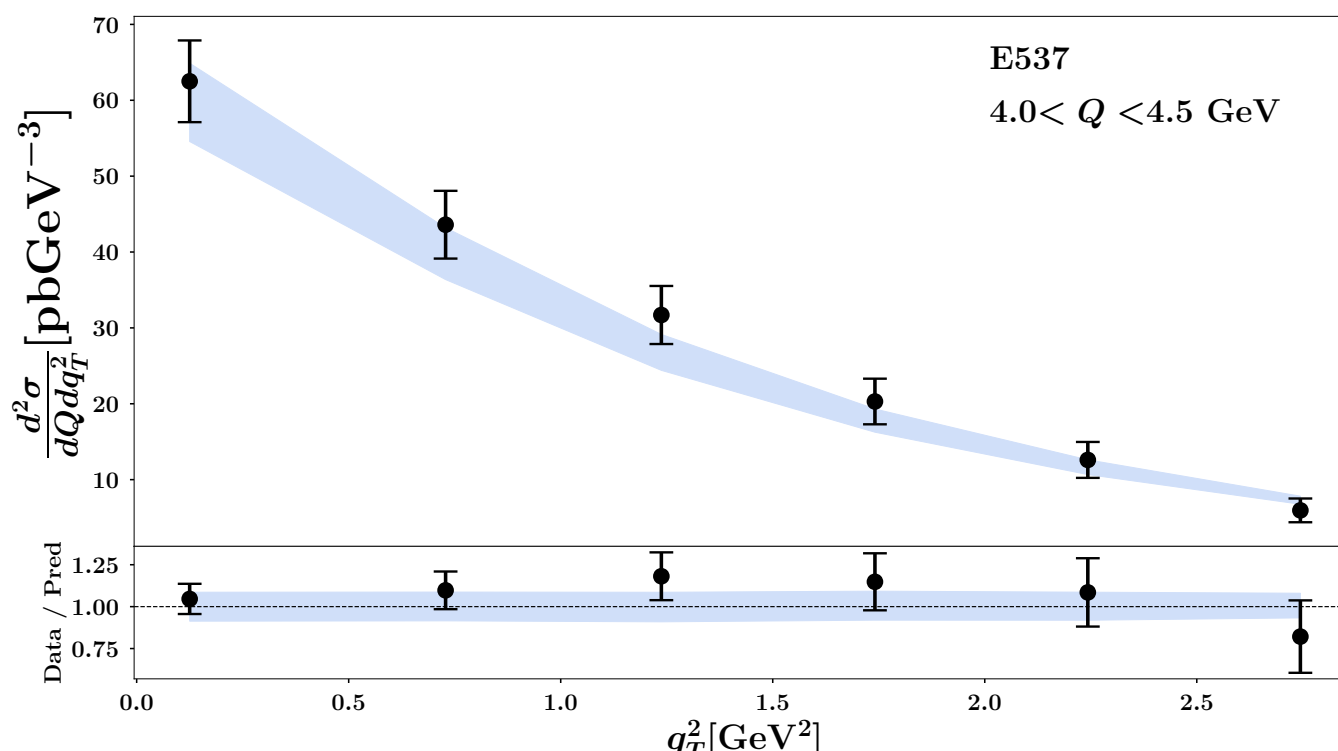


E615: stat. 5% syst. 16% (normalization)
E537: stat. 15-20% syst. 8%

Th.: 5-8% on PDF from xFitter20

Fit results

arXiv:2210.01733



MAPTMDPion22:

- good agreement in shape
- large normalization errors (for E615)

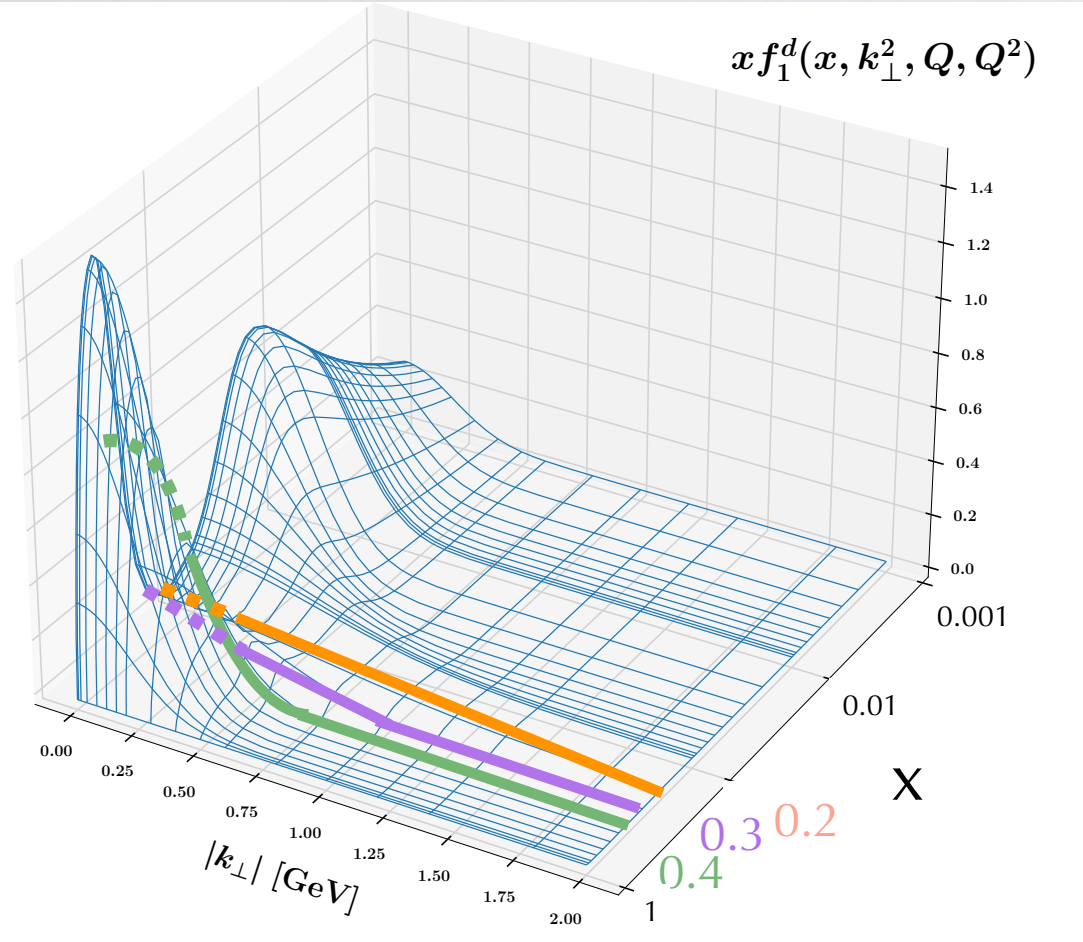
data set	N_{data}	χ_D^2	χ_λ^2	χ^2
E537	64	1.0	0.57	1.57
E615	74	0.31	1.22	1.53
total	138	0.63	0.92	1.55

χ_D^2 = uncorrelated error

χ_λ^2 = correlated error

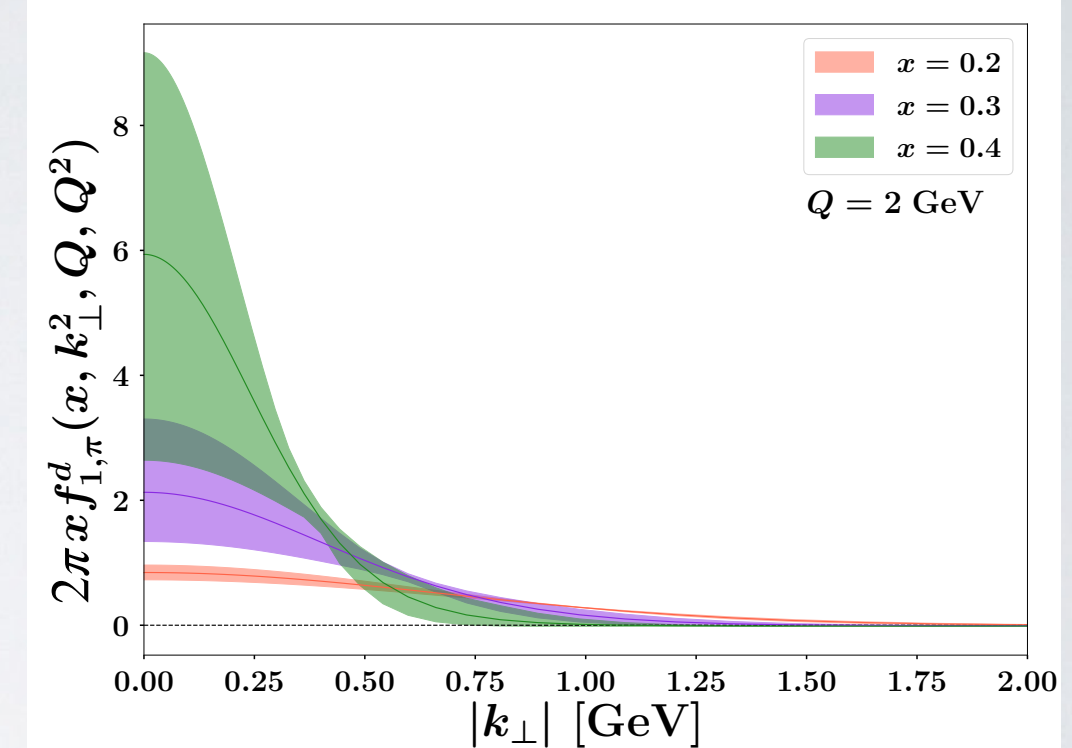
$\chi^2 = \chi_D^2 + \chi_\lambda^2$

Visualizing MAPTMDPion22 TMD PDF

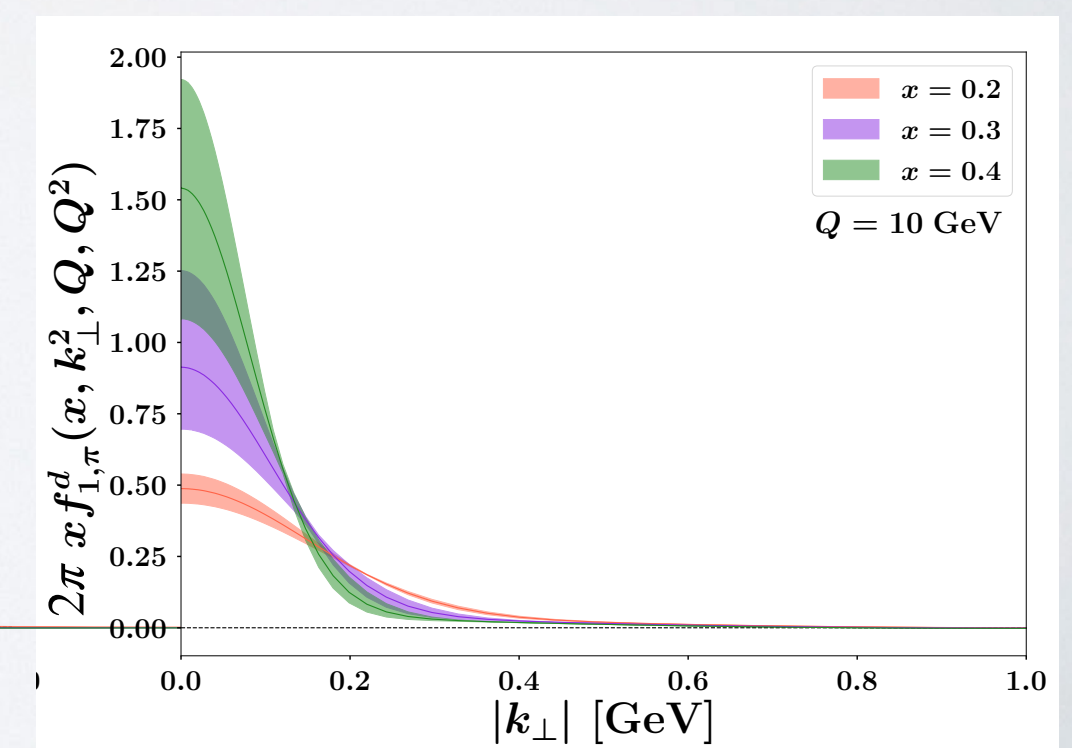


unpolarized down quark in π^-

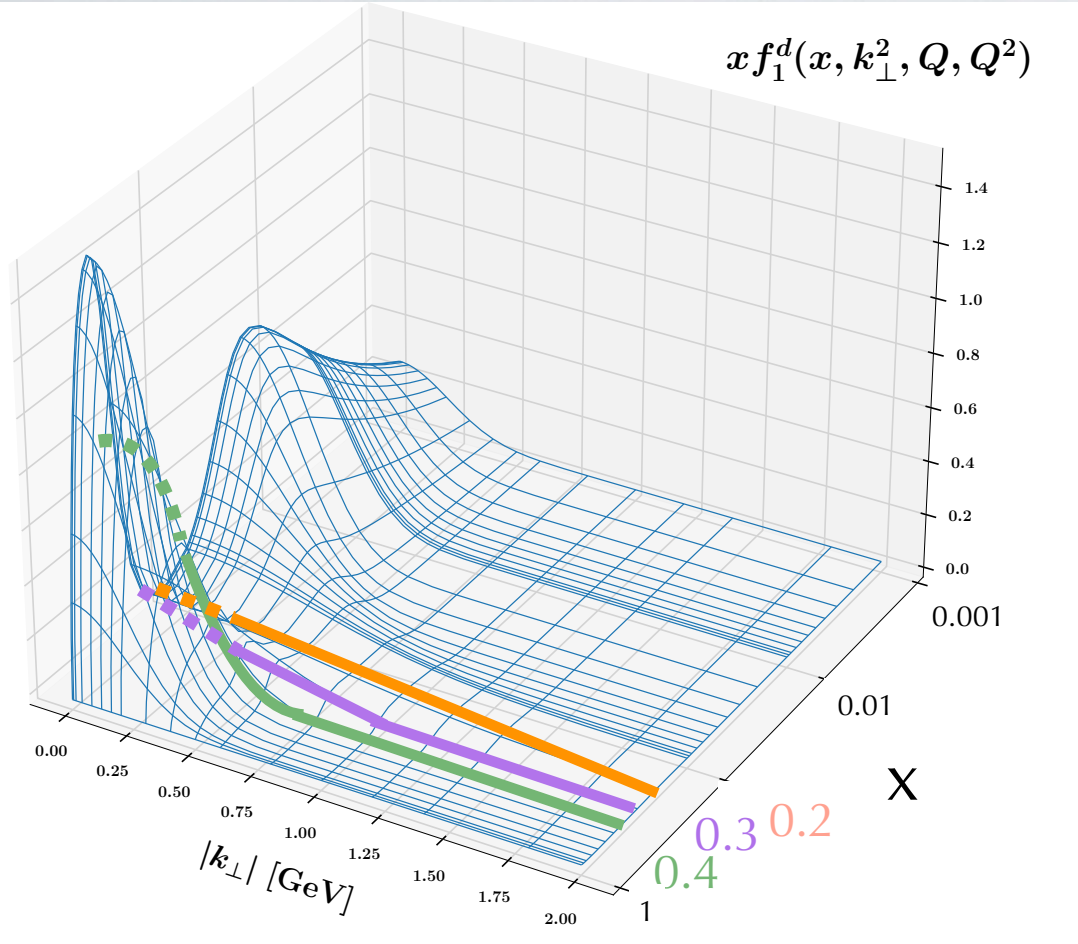
$Q = 2 \text{ GeV}$



$e^{-g_2^2 b_T^2/4}$ same nonperturbative evolution as for proton

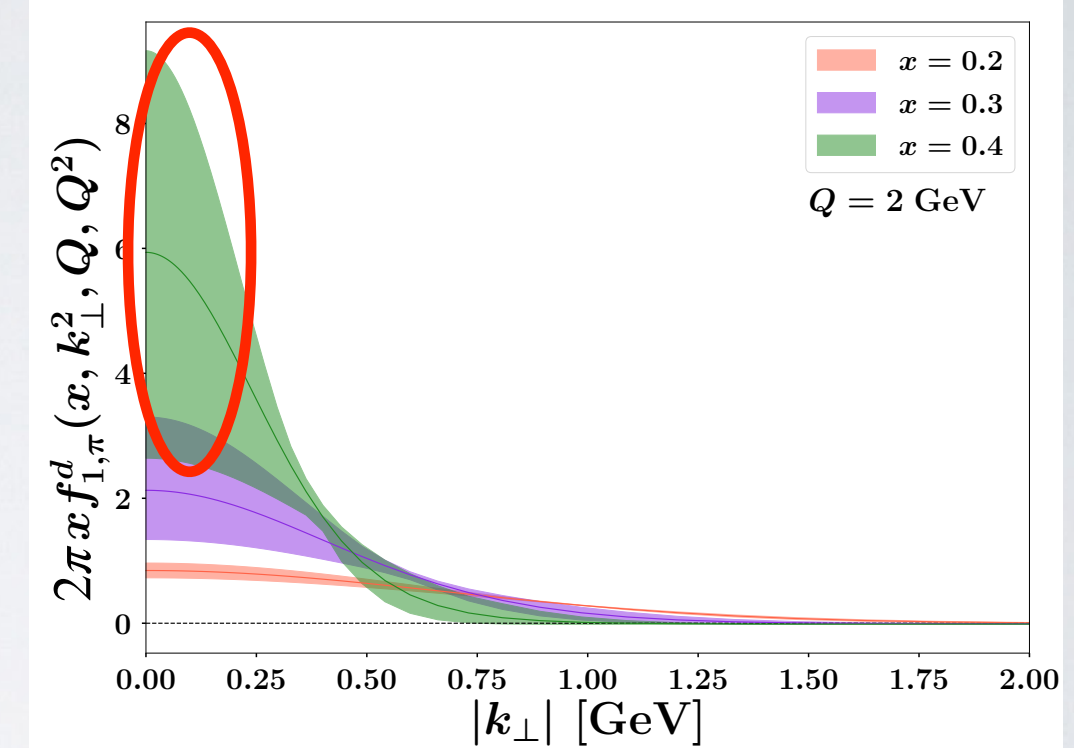


Visualizing MAPTMDPion22 TMD PDF



unpolarized down quark in π^-

$Q = 2 \text{ GeV}$



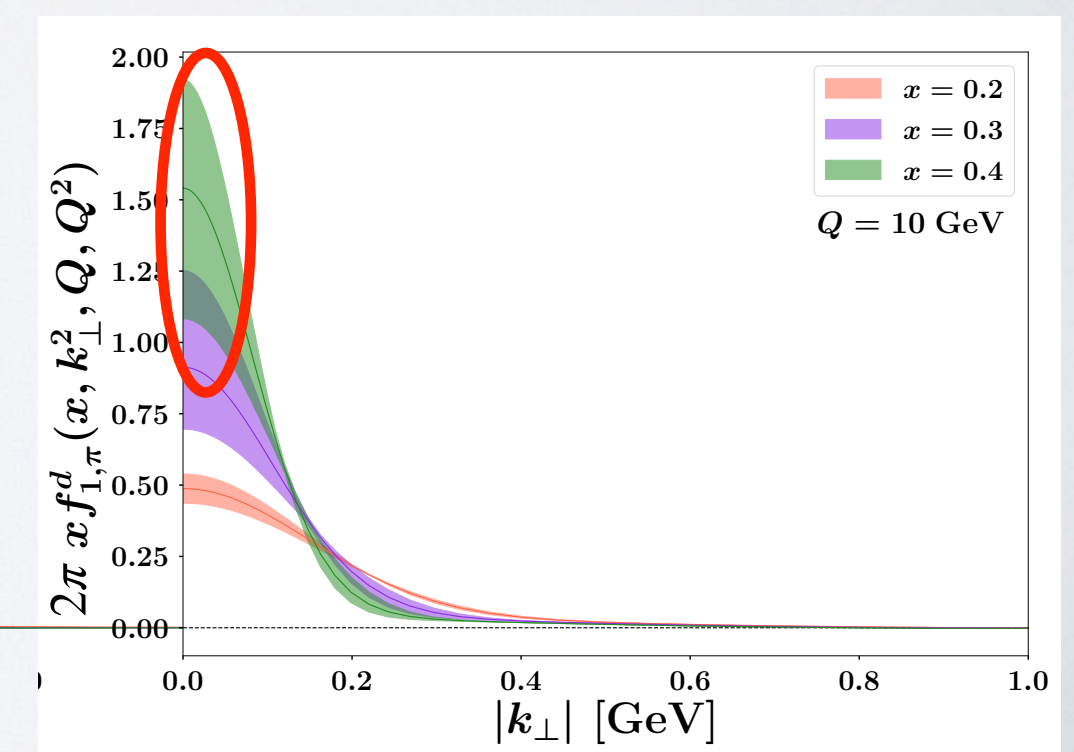
$e^{-g_2^2 b_T^2/4}$ same nonperturbative evolution as for proton

$$N_{1\pi} = 0.47 \pm 0.12 \quad \sigma_{1\pi} = 4.50 \pm 2.25 \quad \alpha_{1\pi} = 4.40 \pm 1.34$$



$\langle k_\perp^2 \rangle (x = 0.1, Q = 1)$ larger than in the proton

data not very sensitive to nonperturbative parameters => **need new data!**



Summary and Outlook

- **MAPTMD22**: a **global fit at N^3LL** of SIDIS and Drell-Yan data from LHC, Tevatron, RHIC; **2031 data pts.**, **21 parameters**, $\chi^2/N_{\text{data}} = 1.06$: the current most robust and precise extraction of unpolarized quark TMDs in the proton, accuracy comparable to modern PDF fits
- surprisingly, MAPTMD22 performs **well** in SIDIS well **outside TMD factorization limit** $q_T \ll Q$

Summary and Outlook

- **MAPTMD22**: a **global fit** at **N^3LL** of SIDIS and Drell-Yan data from LHC, Tevatron, RHIC; **2031 data pts.**, **21 parameters**, $\chi^2/N_{\text{data}} = 1.06$: the current most robust and precise extraction of unpolarized quark TMDs in the proton, accuracy comparable to modern PDF fits
 - surprisingly, MAPTMD22 performs **well** in SIDIS well **outside** TMD factorization limit $q_T \ll Q$
 - **MAPTMDPion22**: extraction of unpolarized quark TMDs in the pion from Drell-Yan data, consistent with MAPTMD22, at **highest accuracy** (**N^3LL**), including **largest set** of data (**138**)
-

Summary and Outlook

- **MAPTMD22:** a **global fit** at **N^3LL** of SIDIS and Drell-Yan data from LHC, Tevatron, RHIC; **2031 data pts.**, **21 parameters**, $\chi^2/N_{\text{data}} = 1.06$: the current most robust and precise extraction of unpolarized quark TMDs in the proton, accuracy comparable to modern PDF fits
- surprisingly, MAPTMD22 performs **well** in SIDIS well **outside** TMD factorization limit $q_T \ll Q$
- **MAPTMDPion22:** extraction of unpolarized quark TMDs in the pion from Drell-Yan data, consistent with MAPTMD22, at **highest accuracy** (**N^3LL**), including **largest set** of data (**138**)

-
- introduce flavor-dependent k_\perp distributions (ongoing...)
 - include upcoming Compass data for pion-induced Drell-Yan
 - improve perturbative accuracy (very precise ATLAS data...)



THANK YOU
for your
ATTENTION!

Backup

Drell-Yan observables

collider

Exp: normalized cross section differential in q_T in each bin

Th: for each bin $[i,f]$

DYNNLO
with MMHT14 PDFs

$$\frac{1}{\sigma_{\text{fiducial}}} \frac{1}{(\Delta q_T)_{if}} \int_{q_{Ti}}^{q_{Tf}} dq_T \int_{y_i}^{y_f} dy \int_{Q_i}^{Q_f} dQ \frac{d\sigma}{dq_T dy dQ}$$

fixed target

E288: cross section differential in average \bar{q}_T and \bar{y}

Th: for each bin $[i,f]$

$$\frac{1}{2\pi\bar{q}_T} \int_{Q_i}^{Q_f} dQ \frac{d\sigma}{dq_T dy dQ} \Big|_{y=\bar{y}, q_T=\bar{q}_T}$$

E772: cross section differential in average \bar{q}_T and $x_F = x_A - x_B$ bins

Th: for each bin $[i,f]$

$$\frac{1}{(\Delta x_F)_{if}} \int_{x_{Fi}}^{x_{Ff}} dx_F \int_{Q_i}^{Q_f} dQ \frac{2E}{\pi\sqrt{s}} \frac{d\sigma}{dq_T^2 dx_F dQ} \Big|_{q_T=\bar{q}_T}$$

E605: cross section differential in average \bar{q}_T and \bar{x}_F

Th: for each bin $[i,f]$

$$\int_{Q_i}^{Q_f} dQ \frac{2E}{\pi\sqrt{s}} \frac{d\sigma}{dq_T^2 dx_F dQ} \Big|_{x_F=\bar{x}_F, q_T=\bar{q}_T}$$

SIDIS observable

Exp: differential SIDIS cross section divided by DIS one

$$M(x, z, P_{hT}, Q) = \frac{d\sigma^{\text{SIDIS}}}{dx dz dP_{hT} dQ} \Bigg/ \frac{d\sigma^{\text{DIS}}}{dx dQ}$$

Multiplicity

Th: for each bin [i,f]

$$\mathcal{O}^{\text{SIDIS}} = \frac{1}{(\Delta Q)_{if}} \int_{Q_i}^{Q_f} dQ \frac{1}{(\Delta x)_{if}} \int_{x_i}^{x_f} dx \frac{1}{(\Delta z)_{if}} \int_{z_i}^{z_f} dz \frac{1}{(\Delta P_{hT})_{if}} \int_{P_{hTi}}^{P_{hTf}} dP_{hT} \frac{d\sigma^{\text{SIDIS}}}{dx dz dP_{hT} dQ}$$

$$\mathcal{O}^{\text{DIS}} = \frac{1}{(\Delta Q)_{if}} \int_{Q_i}^{Q_f} dQ \frac{1}{(\Delta x)_{if}} \int_{x_i}^{x_f} dx \frac{d\sigma^{\text{DIS}}}{dx dQ}$$

$$M^{\text{th}}(x_{if}, z_{if}, P_{hTif}, Q_{if}) = \frac{\mathcal{O}^{\text{SIDIS}}}{\mathcal{O}^{\text{DIS}}}$$

Error treatment

bootstrap method: fitting 250 replicas of fluctuated exp. data

quality indicator: χ_0^2 of central replica (fitting not “ ” “ ”)

MAPTMD22 at $N^3LL^{(-)}$: $N_{\text{data}} = 2031$, 21 parameters, $\chi_0^2/N_{\text{data}} = 1.06$

$$\chi_0^2 \sim \langle \chi^2 \rangle_{\text{replicas}}$$

(exp. / th.) errors can be uncorrelated or correlated

$$\chi^2 = \chi_D^2 + \chi_\lambda^2$$

penalty for correlated errors

$$\sum_{\text{bins}} \left(\frac{\text{exp} - \bar{\text{th}}}{\sigma} \right)^2$$
$$\bar{\text{th}} = \text{th} + \sum_{\alpha} \lambda_{\alpha} \sigma_{\text{corr}}^{(\alpha)}$$
$$\chi_\lambda^2 = \sum_{\alpha} \lambda_{\alpha}^2$$

nuisance params.

$$\sigma^2 = \sigma_{\text{stat}}^2 + \sigma_{\text{uncorr}}^2$$

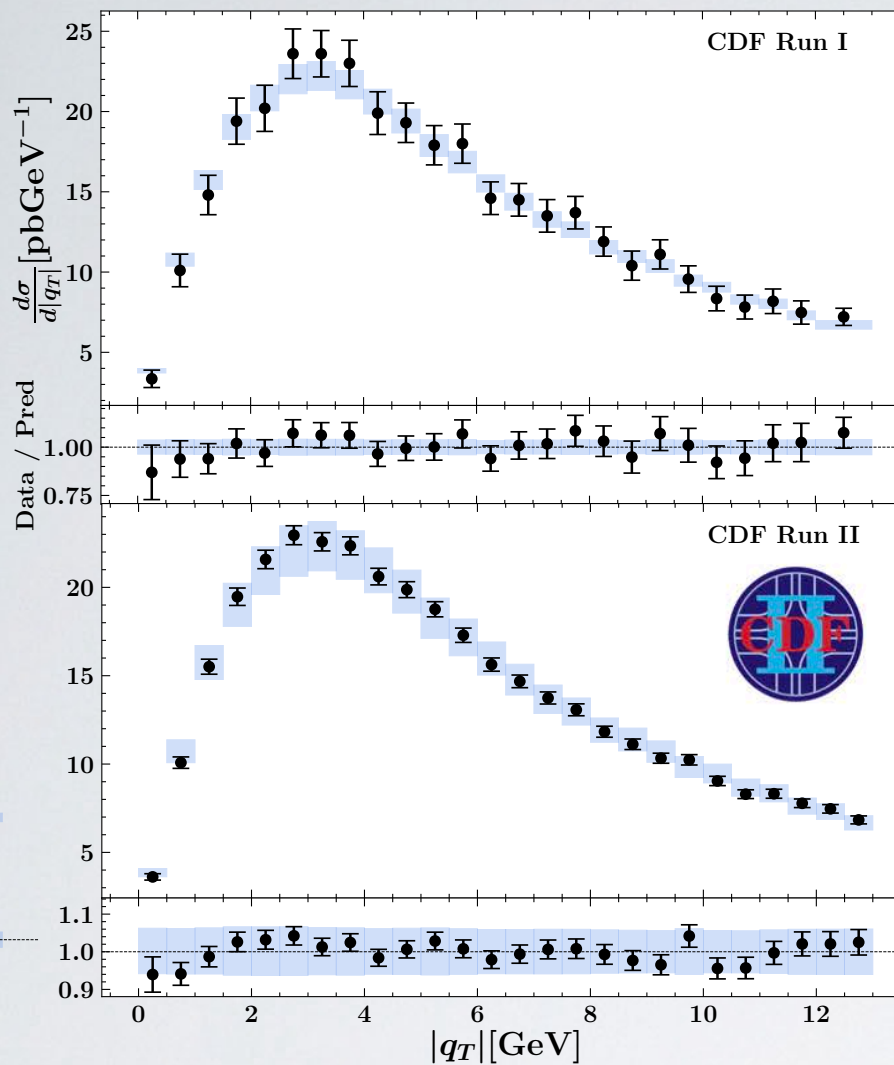
Examples of (partly) correlated errors :

- exp.: some normalization systematic errors

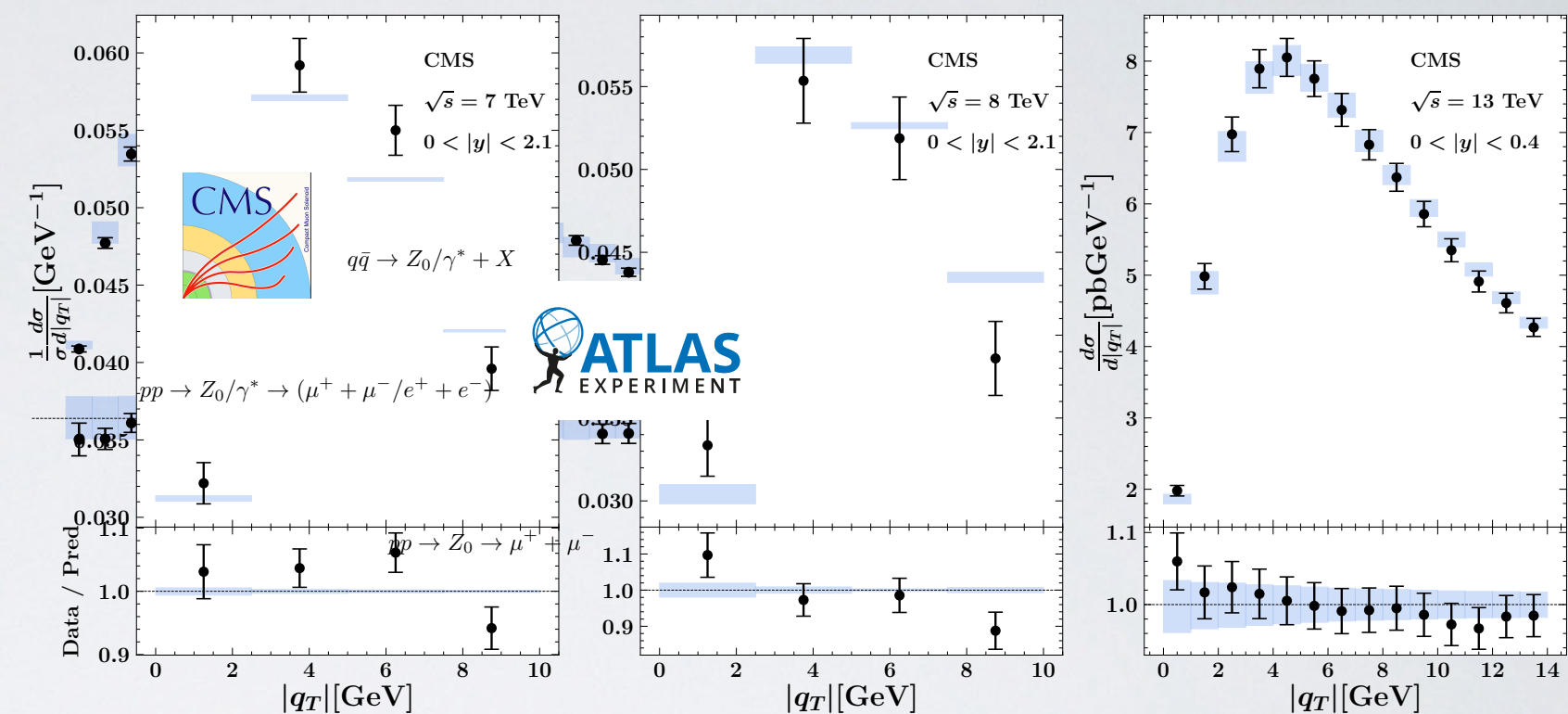
- th. : uncertainties of PDFs MMHT2014

FFs DSS14 for π^\pm
DSS17 for K^\pm

MAPTMD22 N³LL⁽⁻⁾ global fit $\chi^2_0/N_{\text{data}} = 1.06$

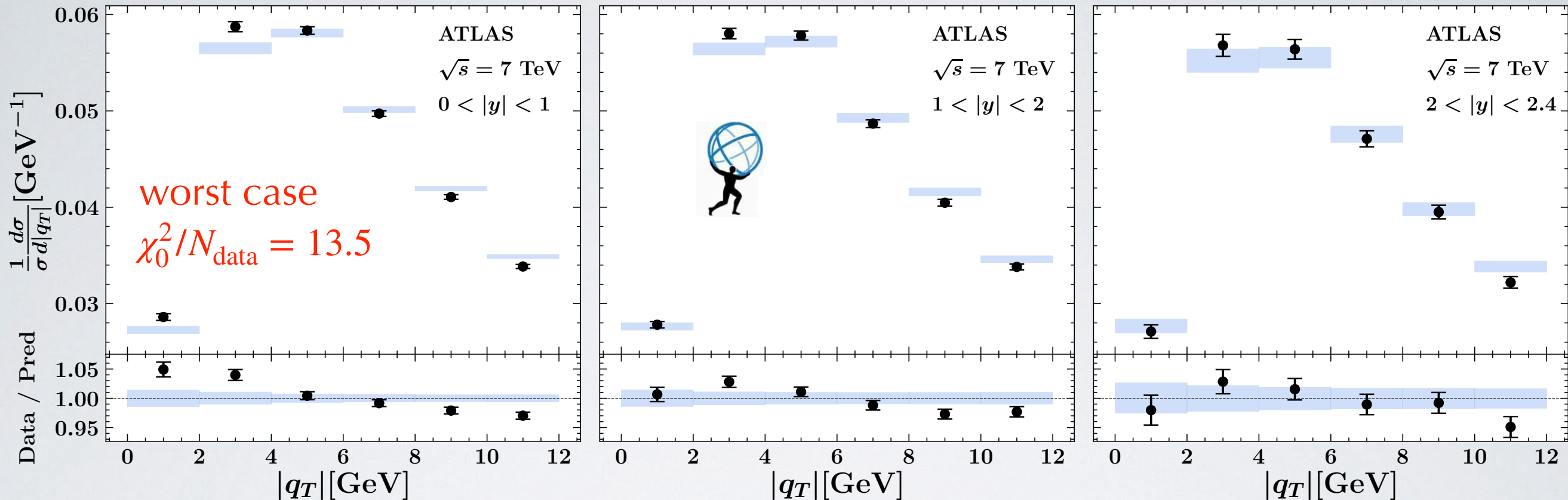


th. error band =
68% of all replicas



data set	N_{data}	χ^2_D	χ^2_λ	χ^2_0
Tevatron total	71	0.87	0.06	0.93
PHENIX 200	2	2.21	0.88	3.08
STAR 510	7	1.05	0.10	1.15
LHCb total	21	1.15	0.3	1.45
ATLAS total	72	4.56	0.48	5.05
CMS total	78	0.53	0.02	0.55
collider total	251	1.86	0.2	2.06
fixed target tot	233	0.85	0.4	1.24

MAPTMD22 N³LL⁽⁻⁾ global fit $\chi^2_0/N_{\text{data}} = 1.06$



extremely small exp. errors
→ very sensitive to small th. corrections

Examples:

- numerical implementation of lepton cuts
- power corrections
- effects of matching Y term

Chen et al.,
arXiv:2203.01565
Camarda et al.,
arXiv:2111.14509
Buonocore et al.,
arXiv:2111.13661

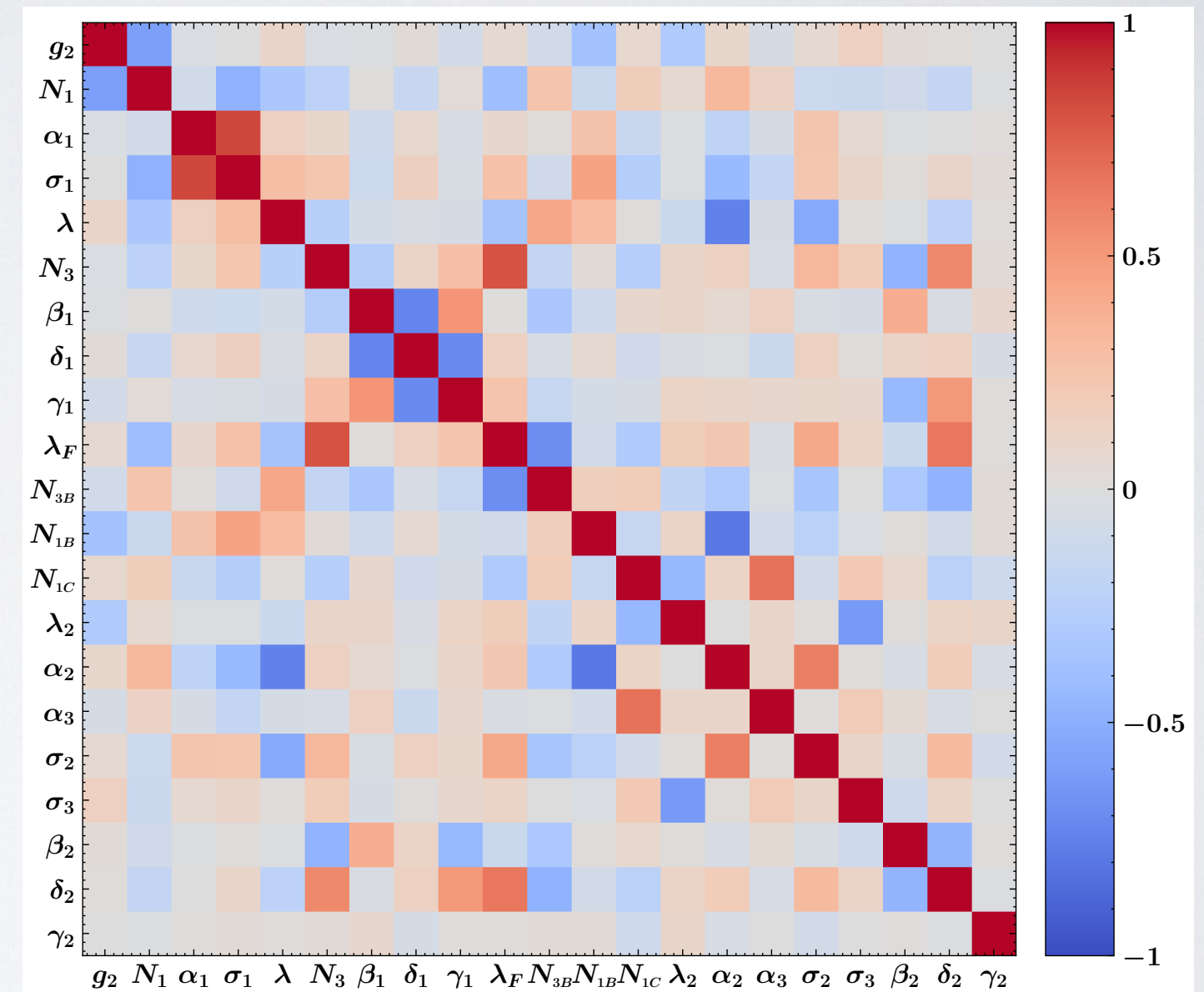
data set	N_{data}	χ^2_D	χ^2_λ	χ^2_0
ATLAS 7 TeV	18	6.43	0.92	7.35
ATLAS 8 TeV	48	3.7	0.32	4.02
ATLAS 13 TeV	6	5.09	0.5	6.4
ATLAS total	72	4.56	0.48	5.05
collider total	251	1.86	0.2	2.06

Backup: chi2 breakout

Data set	N ³ LL ⁻			
	N_{dat}	χ^2_D	χ^2_λ	χ^2_0
CDF Run I	25	0.45	0.09	0.54
CDF Run II	26	0.995	0.004	1.0
D0 Run I	12	0.67	0.01	0.68
D0 Run II	5	0.89	0.21	1.10
D0 Run II (μ)	3	3.96	0.28	4.2
<i>Tevatron total</i>	71	0.87	0.06	0.93
LHCb 7 TeV	7	1.24	0.49	1.73
LHCb 8 TeV	7	0.78	0.36	1.14
LHCb 13 TeV	7	1.42	0.06	1.48
<i>LHCb total</i>	21	1.15	0.3	1.45
ATLAS 7 TeV	18	6.43	0.92	7.35
ATLAS 8 TeV	48	3.7	0.32	4.02
ATLAS 13 TeV	6	5.9	0.5	6.4
<i>ATLAS total</i>	72	4.56	0.48	5.05
CMS 7 TeV	4	2.21	0.10	2.31
CMS 8 TeV	4	1.938	0.001	1.94
CMS 13 TeV	70	0.36	0.02	0.37
<i>CMS total</i>	78	0.53	0.02	0.55
PHENIX 200	2	2.21	0.88	3.08
STAR 510	7	1.05	0.10	1.15
DY collider total	251	1.86	0.2	2.06
E288 200 GeV	30	0.35	0.19	0.54
E288 300 GeV	39	0.33	0.09	0.42
E288 400 GeV	61	0.5	0.11	0.61
E772	53	1.52	1.03	2.56
E605	50	1.26	0.44	1.7
DY fixed-target total	233	0.85	0.4	1.24
HERMES ($p \rightarrow \pi^+$)	45	0.86	0.42	1.28
HERMES ($p \rightarrow \pi^-$)	45	0.61	0.31	0.92
HERMES ($p \rightarrow K^+$)	45	0.49	0.04	0.53
HERMES ($p \rightarrow K^-$)	37	0.18	0.13	0.31
HERMES ($d \rightarrow \pi^+$)	41	0.68	0.45	1.13
HERMES ($d \rightarrow \pi^-$)	45	0.63	0.35	0.97
HERMES ($d \rightarrow K^+$)	45	0.2	0.02	0.22
HERMES ($d \rightarrow K^-$)	41	0.14	0.08	0.22
<i>HERMES total</i>	344	0.48	0.23	0.71
COMPASS ($d \rightarrow h^+$)	602	0.55	0.31	0.86
COMPASS ($d \rightarrow h^-$)	601	0.68	0.3	0.98
<i>COMPASS total</i>	1203	0.62	0.3	0.92
SIDIS total	1547	0.59	0.28	0.87
Total	2031	0.77	0.29	1.06

Backup: N3LL(-) fit parameters

Parameter	Average over replicas
g_2 [GeV]	0.248 ± 0.008
N_1 [GeV 2]	0.316 ± 0.025
α_1	1.29 ± 0.19
σ_1	0.68 ± 0.13
λ [GeV $^{-1}$]	1.82 ± 0.29
N_3 [GeV 2]	0.0055 ± 0.0006
β_1	10.23 ± 0.29
δ_1	0.0094 ± 0.0012
γ_1	1.406 ± 0.084
λ_F [GeV $^{-2}$]	0.078 ± 0.011
N_{3B} [GeV 2]	0.2167 ± 0.0055
N_{1B} [GeV 2]	0.134 ± 0.017
N_{1C} [GeV 2]	0.0130 ± 0.0069
λ_2 [GeV $^{-1}$]	0.0215 ± 0.0058
α_2	4.27 ± 0.31
α_3	4.27 ± 0.13
σ_2	0.455 ± 0.050
σ_3	12.71 ± 0.21
β_2	4.17 ± 0.13
δ_2	0.167 ± 0.006
γ_2	0.0007 ± 0.0110



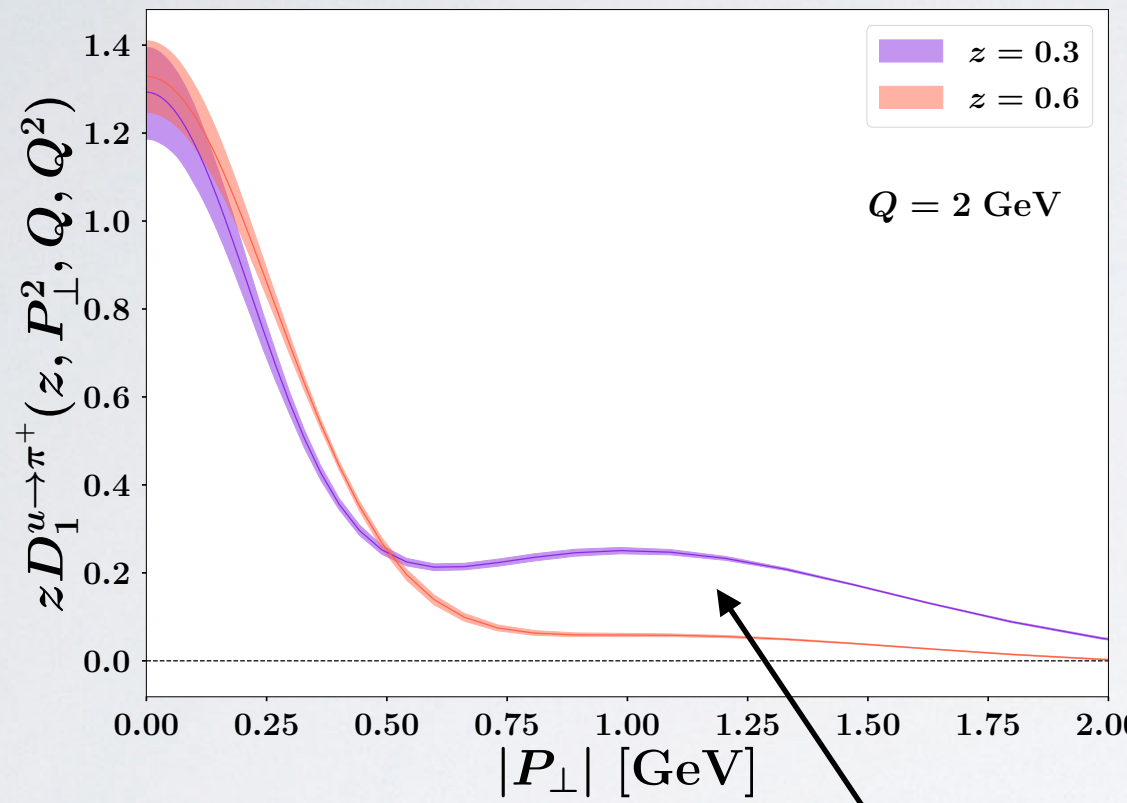
Backup: NNLL and NLL fits

	N ³ LL ⁻		NNLL		NLL	
Data set	N_{dat}	$\langle \chi^2 \rangle \pm \delta \langle \chi^2 \rangle$	N_{dat}	$\langle \chi^2 \rangle \pm \delta \langle \chi^2 \rangle$	N_{dat}	$\langle \chi^2 \rangle \pm \delta \langle \chi^2 \rangle$
ATLAS	72	5.01 ± 0.26	/	/	/	/
PHENIX 200	2	3.26 ± 0.31	2	0.81 ± 0.11	/	/
STAR 510	7	1.16 ± 0.04	7	0.99 ± 0.03	/	/
Other sets	170	0.83 ± 0.01	170	2.37 ± 0.11	/	/
DY collider	251	2.06 ± 0.07	179	2.3 ± 0.1	/	/
E772	53	2.48 ± 0.12	53	2.05 ± 0.22	/	/
Other sets	180	0.87 ± 0.04	180	0.71 ± 0.04	180	0.81 ± 0.04
DY fixed-target	233	1.24 ± 0.04	233	1.01 ± 0.05	180	0.81 ± 0.04
HERMES	344	0.71 ± 0.04	344	1.1 ± 0.06	344	0.51 ± 0.02
COMPASS	1203	0.95 ± 0.02	1203	0.6 ± 0.06	1203	0.41 ± 0.01
SIDIS	1547	0.89 ± 0.02	1547	0.71 ± 0.05	1547	0.43 ± 0.01
Total	2031	1.08 ± 0.01	1959	0.89 ± 0.01	1727	0.47 ± 0.01

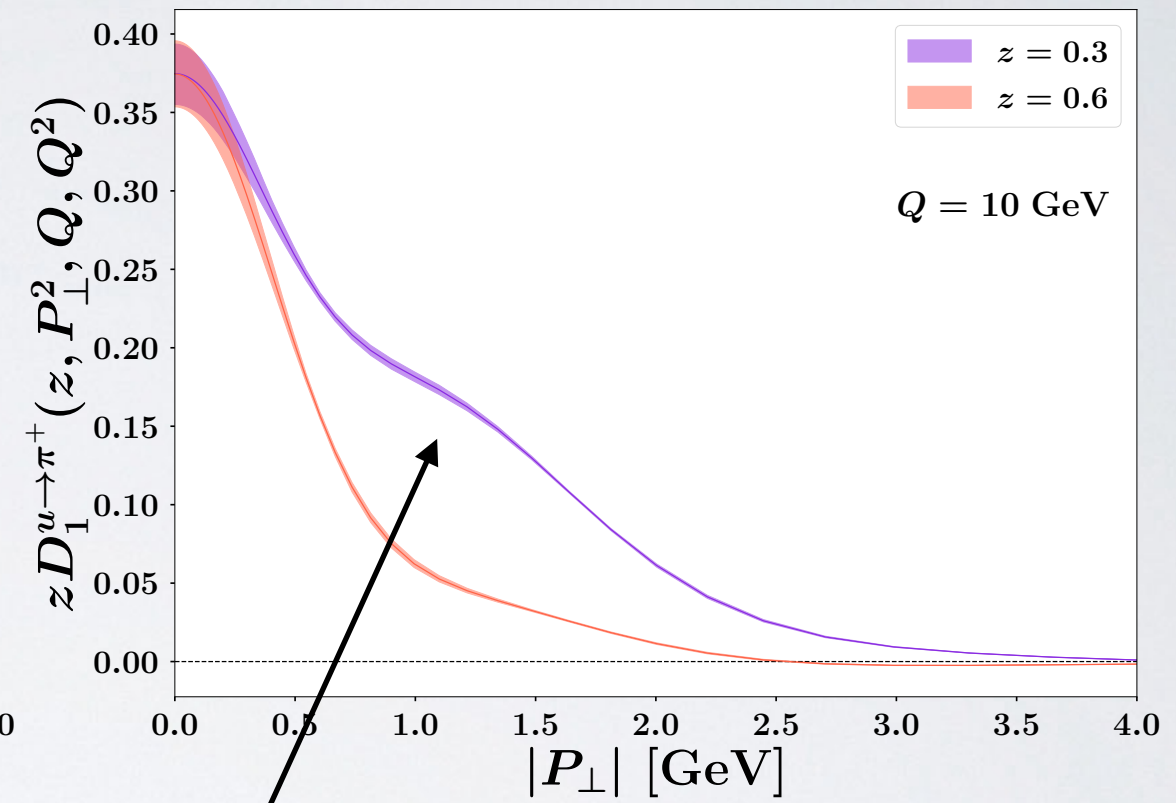
data sets requiring higher pert. accuracy need to be excluded.
 Still, these fits useful for polarized situations with less available accuracy

Visualizing MAPTMD22 TMD FF

up $\rightarrow \pi^+$



$Q = 2$ GeV

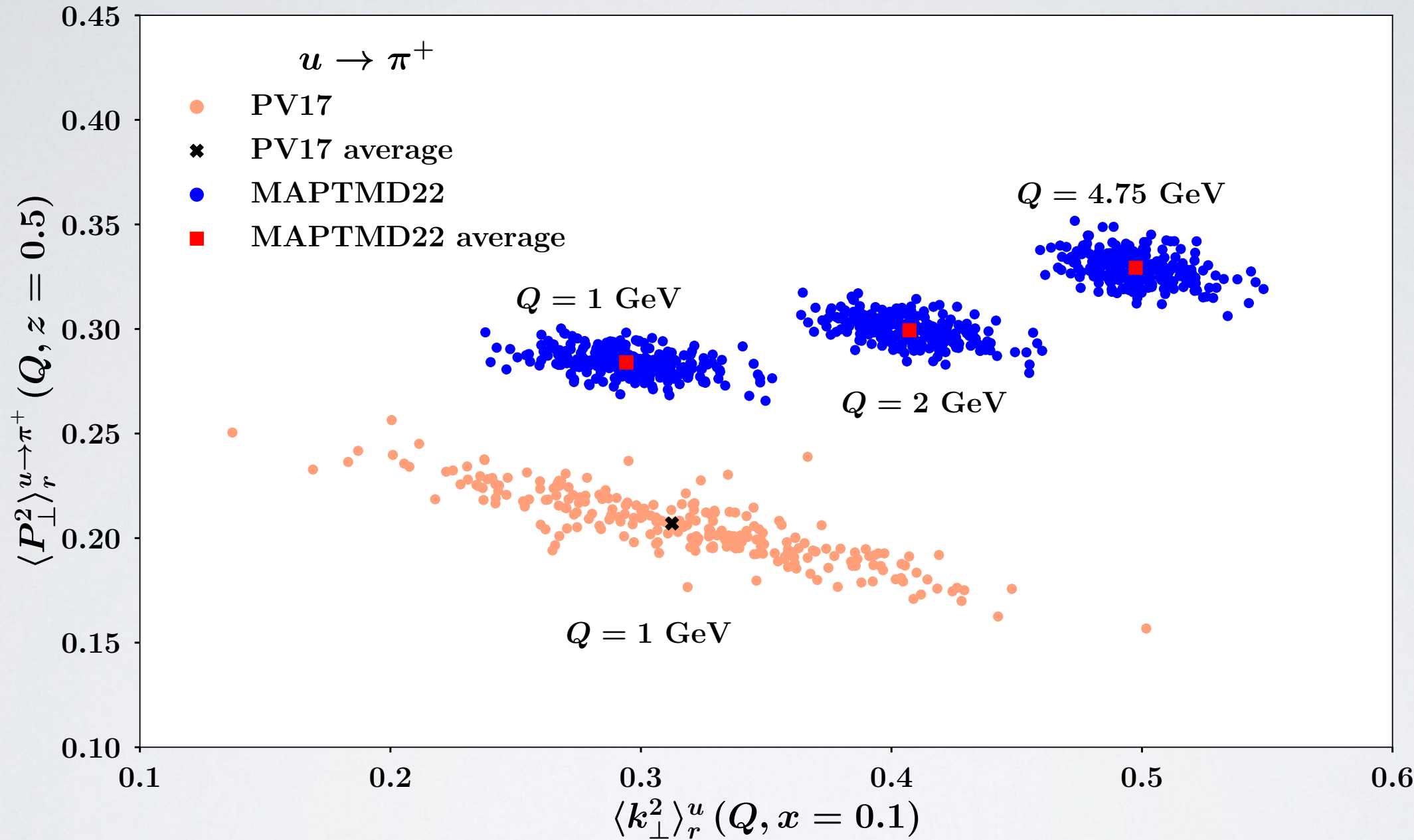


$Q = 10$ GeV

$$D_{\text{NP}}(z, P_\perp; Q_0) \sim \text{Gauss} + \lambda_F P_\perp^2 \text{Gauss}$$

$$\lambda_F = 0.078 \pm 0.011 \text{ GeV}^{-2}$$

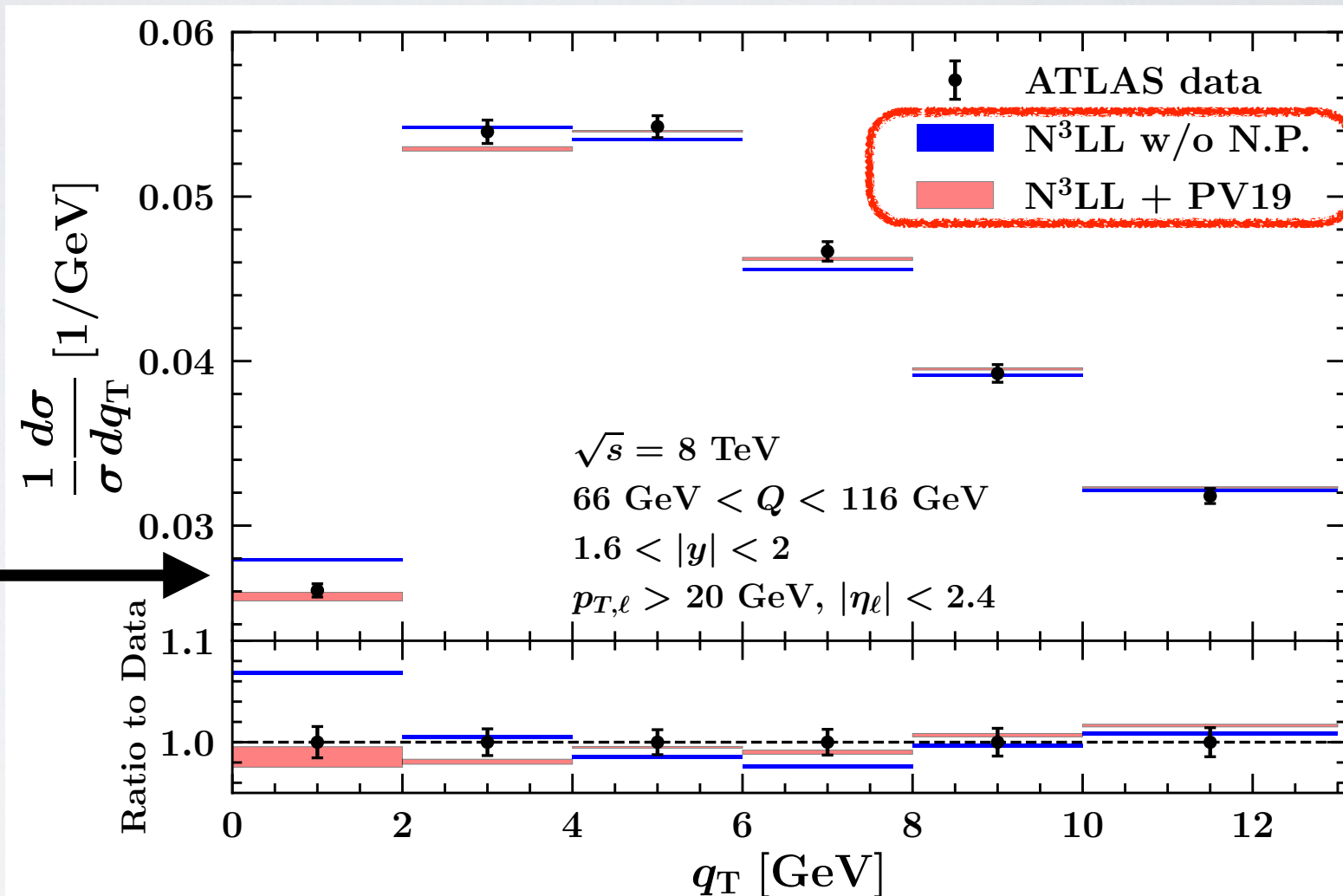
Backup: avg. transverse momenta



PV17 (NLL) \leftrightarrow MAPTMD22 (N3LL(-)) \rightarrow less anticorrelation

TMD impact at the LHC

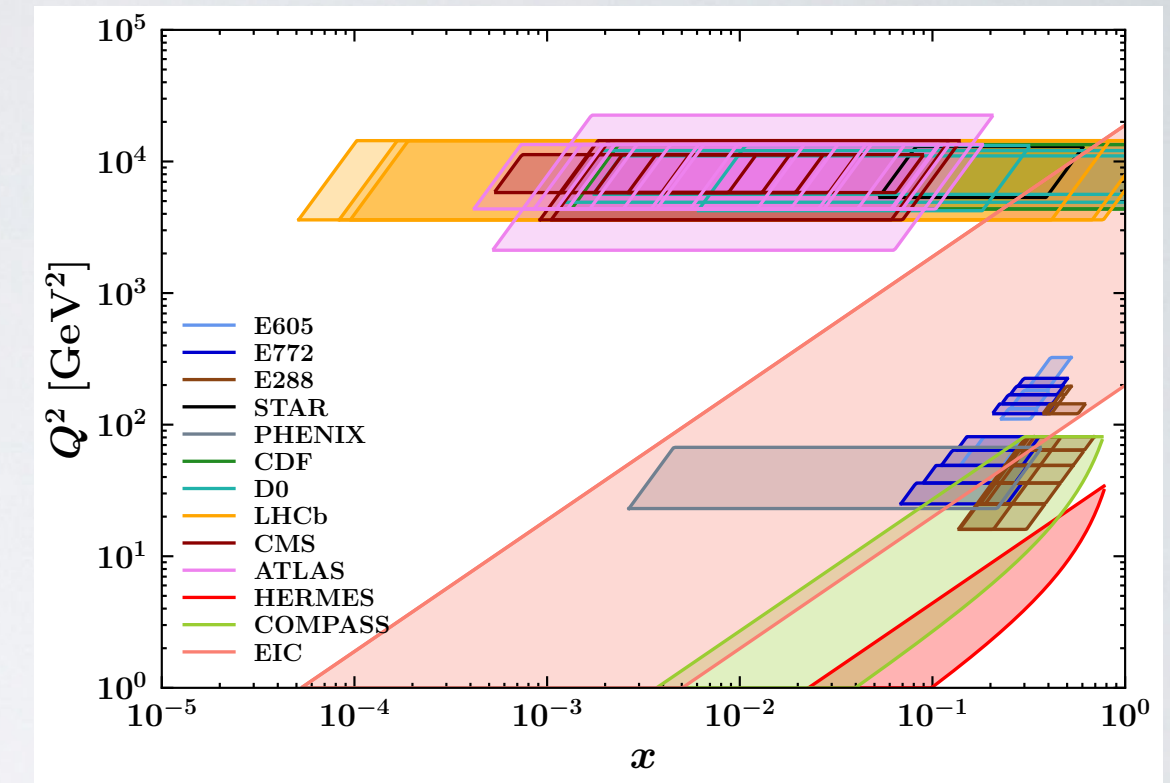
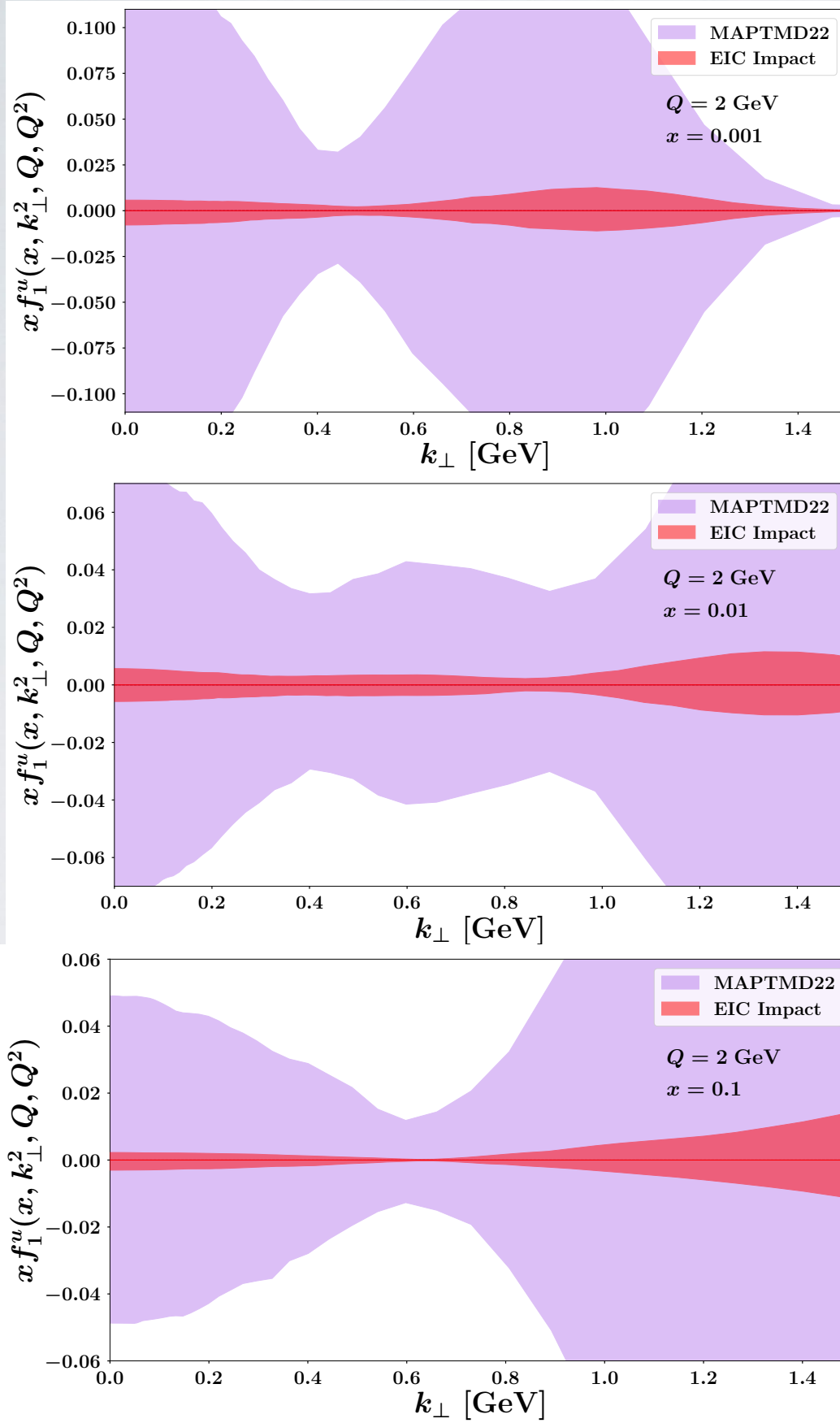
q_T distribution of Z in ATLAS kin.



effect of intrinsic
parton k_\perp
from PV 2019 fit

see also later for potential impact on W mass extraction

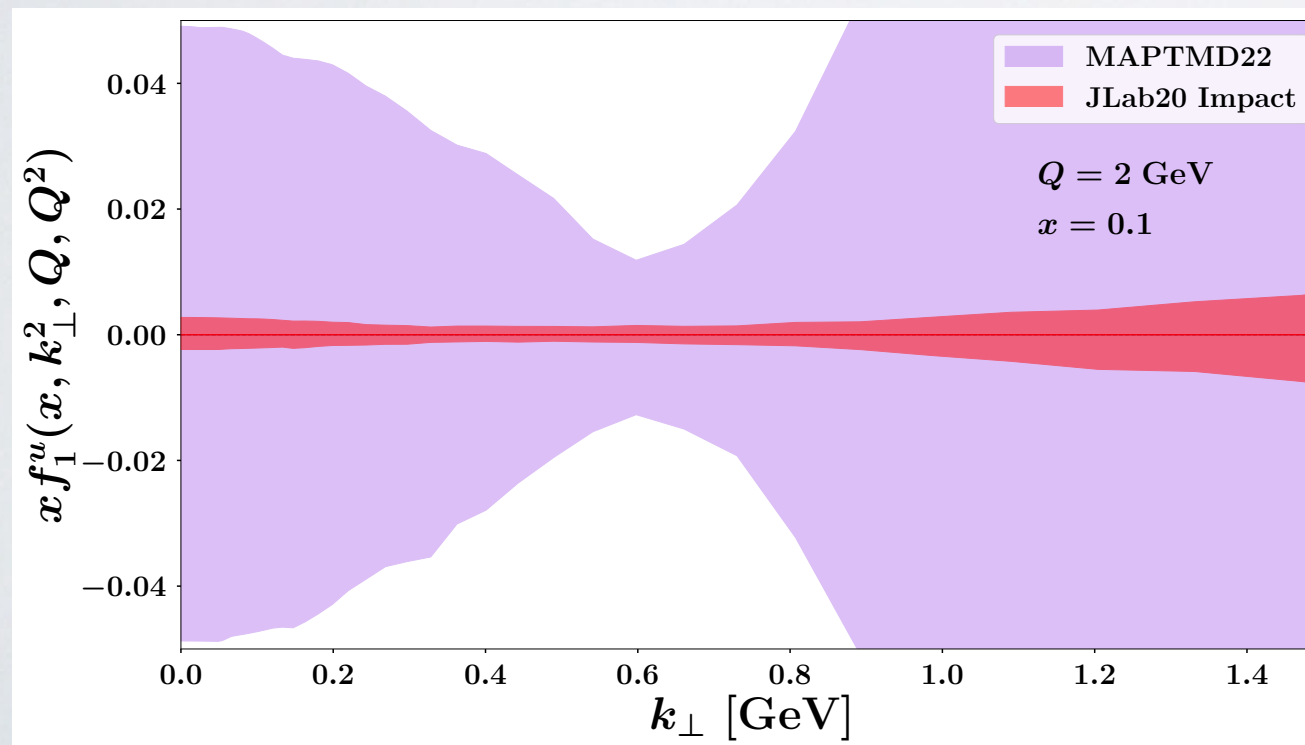
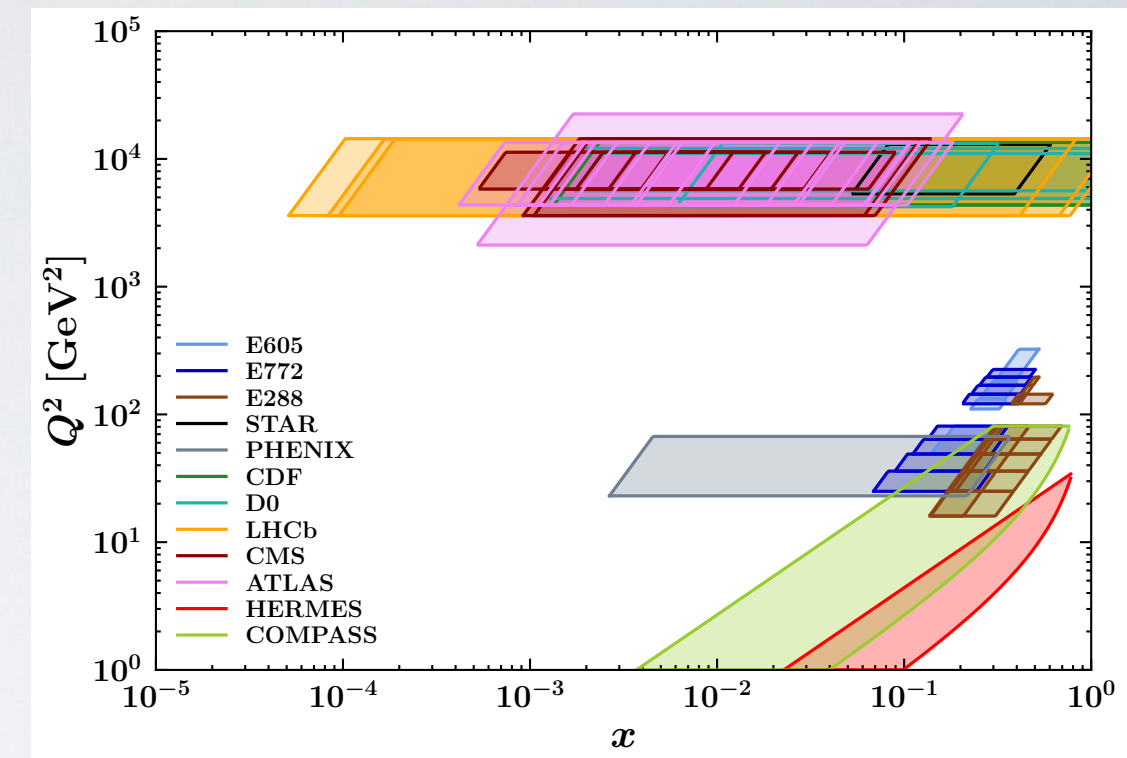
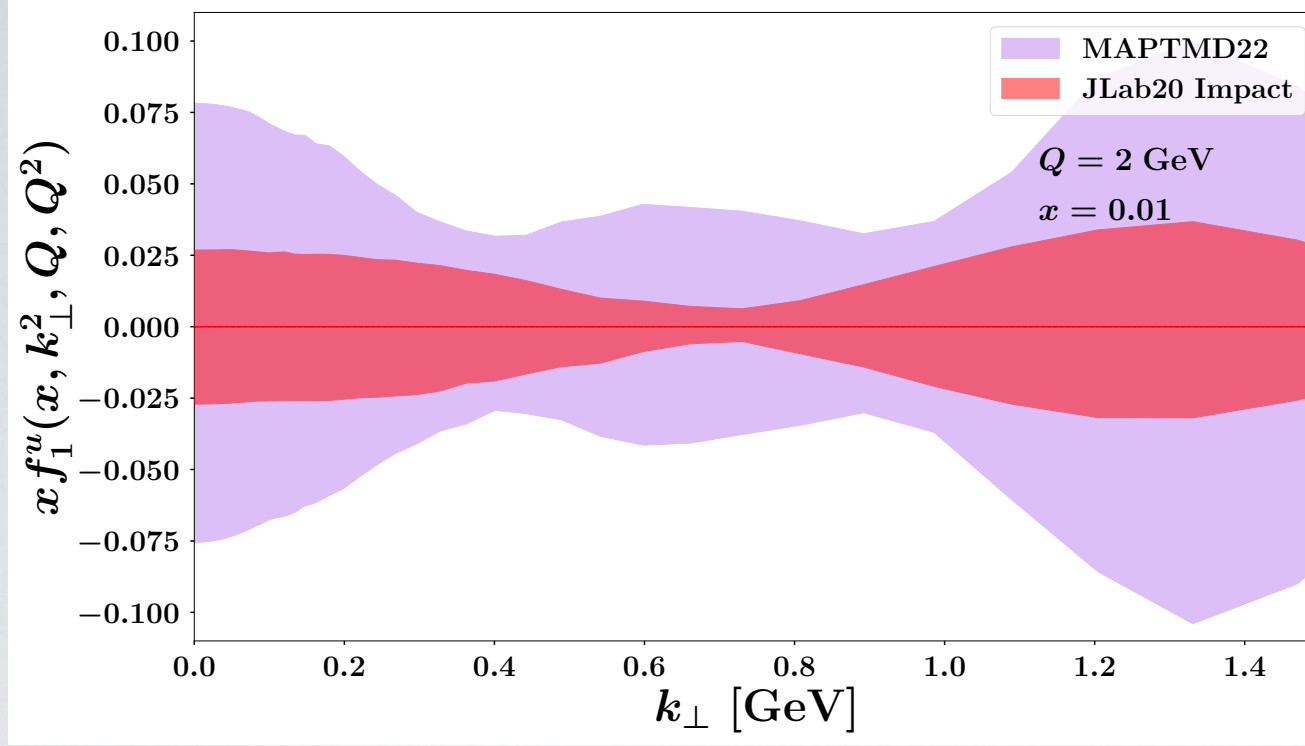
The EIC impact



kinematics 10x100

major improvements at smaller x

The JLab20+ impact



kinematics JLab20

major improvements at valence x

The Nanga Parbat fitting framework

All material available at the Nanga Parbat github site



Nanga Parbat: a TMD fitting framework

Nanga Parbat is a fitting framework aimed at the determination of the non-perturbative component of TMD distributions.

Download

You can obtain NangaParbat directly from the github repository:

<https://github.com/MapCollaboration/NangaParbat>

